Studies on improving ethanol productivity of self-cloning xylose-using Saccharomyces cerevisiae by endogenous genes utilization

福田, 明

Studies on improving ethanol productivity of self-cloning xylose-using *Saccharomyces cerevisiae* by endogenous genes utilization

Akira Fukuda

2019

ABBREVIATIONS

SHF   Separate hydrolysis and fermentation

SSF   Simultaneous saccharification and fermentation

GMO   Genetically modified organism

GRAS   Generally recognized as safe

XR   Xylose reductase

XDH   Xylitol dehydrogenase

XK   Xylulose kinase

XI   Xylose isomerase

ADH   Alcohol dehydrogenase

FBA   Flux balance analysis

MFA   Metabolic flux analysis

DFBA   Dynamic flux balance analysis

DMFA   Dynamic metabolic flux analysis

GC-MS   Gas chromatography mass spectrometry

LC-MS   Liquid chromatography mass spectrometry

ATP   Adenosine triphosphate

ADP   Adenosine diphosphate

AMP   Adenosine monophosphate

NAD^+ Nicotinamide adenine dinucleotide (oxidized)

NADH   Nicotinamide adenine dinucleotide (reduced)

$NADP^+$ Nicotinamide adenine dinucleotide phosphate (oxidized)

NADPH   Nicotinamide adenine dinucleotide phosphate (reduced)

CoA	Coenzyme A
X5P	Xylulose 5-phosphate
Ru5P	Ribulose 5-phosphate
R5P	Ribose 5-phosphate
S7P	Sedoheptulose 7-phosphate
GAP	Glyceraldehyde 3-phosphate
E4P	Erythrose 4-phosphate
F6P	Fructose 6-phosphate
G6P	Glucose 6-phosphate
PGL	6-Phosphogluconolactone
6PG	6-Phosphogluconate
FBP	Fructose 1, 6-bisphosphate
1,3BPG	1,3-Bisphosphoglycerate
3PG	Glycerate 3-phosphate
2PG	Glycerate 2-phosphate
PEP	Phosphoenolpyruvic acid
DHAP	Dihydroxyacetone phosphate
Gly3P	Glycerol 3-phosphate
OXA	Oxaloacetic acid
LC-QqQ-MS	Liquid chromatography/triple-stage quadrupole mass spectrometry
ED	Endpoint deviation

TABLE OF CONTENTS

CHPATER 3

Construction of kinetic model of the ethanol production pathway of self-cloning xylose-using *S. cerevisiae*

CHAPTER 4

Evaluation of *ADH1* overexpression effect toward ethanol productivity in self-cloning xylose-using *S. cerevisiae*

CHAPTER 5

CHPATER 1

Introduction

1.1 Lignocellulosic ethanol production

In recent years, instead of petroleum resources, renewable biomass is being converted to useful substances, and used in energy sources and industrial raw materials around the world. Ethanol produced by fermentation of microorganisms using biomass as a raw material, so-called bioethanol, is expected as an alternative fuel from the viewpoint of suppressing the consumption of petroleum resources and the increase of carbon dioxide in the atmosphere. Bioethanol has two categories. One is first generation bioethanol that made from sugar- or starch- rich food crops such as cereals, sugarcane, sugar beet and corn. The other is the second-generation bioethanol that made from lignocellulose biomass, agricultural residues and organic waste. Brazil and USA are the world's largest ethanol producers, which produce ethanol from sugarcane and corn respectively, and they account for more than 65% of world bioethanol production (Badger, P. C., 2002). However, productions of the first generation bioethanol are not sustainable from competition with food production, including the use of water and land area, and biodiversity (Scheidel, A. and Sorman, A. H., 2012). Therefore the second generation bioethanol production from low cost substrates such as non-edible parts of cellulose-based herbaceous and woody plants as a main fuel that does not compete with food has attracted attention in particular (Chartchalerm, I. N. A. *et al.,* 2007).

The production process of lignocellulosic ethanol consists of the following four processes as shown in Fig. 1-1: (i) Pretreatment, (ii) Saccharification, (iii) Fermentation and (iv) Distillation.
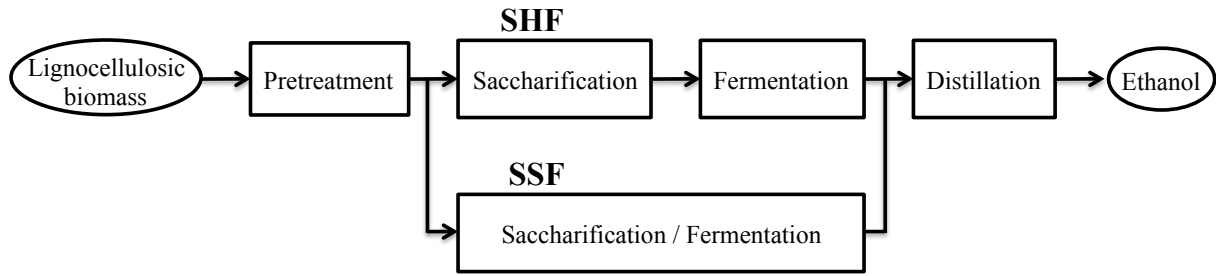
Fig. 1-1 Scheme of lignocellulosic ethanol production.

SHF; Separate hydrolysis and fermentation, SSF; Simultaneous saccharification and

fermentation, Saccharification; enzymatic or acid hydrolysis of cellulose and hemicellulose,

Fermentation; conversion of sugars to ethanol by yeast

Since lignocellulose biomass has a rigid and complex structure, it is not easily

hydrolysed by enzyme or acid. Therefore the purpose of pretreatment step is to change the

structure of the lignocellulose biomass to make cellulose more accessible and to promote the

decomposition by subsequent saccharification. Various techniques are used for pretreatment

such as physical treatment (milling, chipping, shredding, grinding irradiation and pyrolysis),

chemical treatment (dilute acid, concentrated acid and alkali treatment), physicochemical

treatment (steam explosion, ammonia fiber explosion, SO_2 and CO_2 explosion, liquid hot

water, wet oxidation, organosolve, and ionic liquids), and biological treatment (using white,

brown and soft rot fungi, and actiomycetes) (Hsu, T. A. *et al.*, 1980; Saini, A. *et al.*, 2015).

Pretreatment opens up the structure of lignocellulose by three effects: partial break down of

its constituent polymers, weakening of hemicellulose and lignin heteromatrix and reducing

the crystallinity of cellulose (Kumar, P. *et al.*, 2009). When pretreatment is not carried out,

the sugar yield is less than 20 %, but it is possible to increase sugar yield to about 90 % by

pretreatment (Lynd, L. R., 1996).

After pretreatment, it follows that either enzymatic or acidic hydrolysis of cellulose

9

and hemicellulose to monomeric sugars. Finally the sugars are fermented to ethanol, and the produced ethanol is recovered by distillation (Fig. 1-1). Saccharification and fermentation are separately carried out in separate hydrolysis and fermentation (SHF) process. The advantage of this method is that because each reaction can be carried out under optimum conditions, reactivity is high. In addition saccharification is conducted at 50°C, so the risk of contamination with bacteria is low. On the other hand, there is disadvantage that equipment cost is high due to the large number of equipment. Simultaneous saccharification and fermentation (SSF) is a process of simultaneously carrying out saccharification and fermentation in one reactor. Equipment costs can be reduced because the number of equipment is small, but reactivity decreases because enzymatic saccharification is carried out at low temperature, approximately 30°C, in accordance with fermentation.

1.2 Lignocellulose biomass

1.2.1 Compositions of lignocellulose biomass

Lignocellulose biomass has gained attention as a raw material for petroleum replacement products such as bioethanol and bio-plastic (Himmel, M. E. *et al.,* 2007). Lignocellulose biomass is composed of three components; cellulose, hemicellulose and lignin and these are the most abundant and organic resources on the earth. It is said that the ratio of these components differs on biomass species. The composition ratio is generally as follows. Cellulose is about 50%, subsequently hemicellulose is 20-25% and lignin is 25-30% (Eriksson, K. E. *et al.,* 1990). Cellulose and hemicellulose are polysaccharides and used as raw materials for bioethanol and bioplastic. On the other hand, since lignin is aromatic compounds and cannot be used as a raw material for them, it is burned and recovered as a

heat source and is often used as an energy source for maintaining the process.

1.2.2 Properties of cellulose and hemicellulose

Cellulose is the most abundant polysaccharide on earth, whose total amount has been estimated around 7×10^{11} tons (Coughlan, M., 1985) and the structure of cellulose is a linear homopolymer of beta-1, 4-linked glucose residues. Thus when enzymes or other methods decompose cellulose completely, it produces glucose only.

Hemicellulose is the second abundant polysaccharide on earth and can be divided into four groups of structurally different polysaccharide type: xylans, mannans, xyloglucans and mixed linkage beta-glucan (Ebringerova, A. *et al.,* 2005; Ebringerova, A., 2006). Xylan is the most abundant component of hemicellulose for most species of land plants (Joseleau, J. P., *et al.,* 1992). The structure of xylan is heteropolymer consisting of main chain of 1, 4-linked beta-D-xylopyranose unit substituted with mainly acetyl, arabinofuranosyl and glucuronosyl residue. Hemicellulose of hardwoods and herbaceous plants is mainly xylan. While hardwoods and herbaceous plants have weaker lignin structure compared to softwoods hence require less energy and cost to remove it, they are currently considered as raw materials for lignocellulosic ethanol.

1.3 Self-cloning

1.3.1 Differences between "non-self-cloning" and "self-cloning"

There are two kinds of genetic modification technologies classified by the source of genes; non-self-coning and self-cloning (Akada, R., 2002). Non-self-cloning yeast has "foreign" genes or DNA sequences that have altered using genetic engineering techniques

11

such as recombinant DNA technology, it is regarded as a genetically modified organism (GMO) and subjected to controls and limitations when it is used. On the other hand, self-cloning yeast does not contain heterologous genes, and consists only of genes from the yeast itself and closely related species, in general the same species of the same genus. Definitions and treatment of self-cloning yeasts differ by country and region; some countries do not regard self-cloning yeasts as GMOs (Hino, A., 2002). The followings are examples of not treated as GMOs. In Japan, the definition of GMO in the Cartagena domestic law is the same as the text of Cartagena Protocols of living modified organisms resulting from modern biotechnology. Recombinant microorganisms obtained using self-cloning or natural occurrence are exempt from restrictions imposed by the Cartagena domestic law (Kasai, Y. *et al*., 2015). In Australia, the Gene Technology Act 2000 provides the GMO definition and the Gene Technology Regulations 2001 include a list of techniques that are not considered to be gene technology and a list of organisms that are not GMOs (Lusser, M. and Davies, H. V., 2013). Some kinds of organisms with genes introduced from the same species without T-DNA borders and other foreign DNA would not fall under Australian GM-definition (Holme, I. B. *et al*., 2013).

1.3.2 Advantages of self-cloning

Many papers reported the construction of self-cloning yeast and the results of fermentation evaluations (Ishida-Fujii, K. *et al*., 1998; Hirosawa, I. *et al*., 2004; Aritomo, K. *et al*., 2004; Takagi, H. *et al*., 2007; Wang, Z. Y. *et al*., 2007, 2008, 2009; Iijima, K. and Ogata, T., 2010; Dahabieh, M. S. *et al*., 2010; Kusunoki, K. and Ogata, T., 2012; Ogata, T. *et al*., 2013). All the above-mentioned papers relate to the fermented industries like brewing, vinification and sake or wine production, since the commercial application of GMOs is

problematic because of the lack of public acceptance (Schilter, B. *et al*., 2002; Falk, M. *et al*., 2002). The reason why GMOs cannot gain public acceptance is thought to be that due to fear of toxic or allergenic products expressed by foreign genes or bacterial sequences introduced into GMOs (Jonas, D. A. *et al*., 2001). Because of these backgrounds, self-cloning is one solution to obtain public acceptance using genetically modified yeast. In addition, there is another big advantage for the use of self-cloning yeast. As mentioned at 1.3.1 Differences between "non-self-cloning" and "self-cloning", since self-cloning yeast is not recognized as GMOs in Japan, it is unnecessary to contain yeast containment and diffusion prevention measures in Japan. Although the establishment of self-cloning yeast has large restriction in the origin of genes, compared with genetically modified yeast, it has a very significant meaning to ensure profitability of the ethanol production process that the fact containment of yeast and diffusion prevention measures are unnecessary when producing inexpensive substances such as ethanol.

1.4 Xylose fermentation

1.4.1 Microorganisms considered for ethanol fermentation

As described above, because glucose is the most abundant sugar and xylose is the second abundant sugar in softwoods and herbaceous plants, converting not only glucose but also xylose to ethanol is necessary for economically competitive fuel ethanol production from lignocellulose (von Sivers, M. and Zacchi, G., 1995). In nature, there are many bacteria, yeast and filamentous fungi that can ferment xylose to ethanol (Jeffries, T. W., 1983; Toivola, A. *et al.,* 1984; Skoog, K. and Hahn-Hägerdal, B., 1990). The substrate and product ranges of microorganisms most frequently considered for ethanolic fermentation of lignocellulosic

biomass are summarized in Table1-1 (Hahn-Hägerdal, B. *et al.,* 2007). Anaerobic bacteria can ferment all sugars that derived from lignocellulose hydrolysate to ethanol, other solvents and acids (Wiegel, J. and Ljungdahl, L. G., 1986). However, since ethanol-producing bacteria are weak against lignocellulose-derived inhibitors, a detoxification step is required before fermentation (Hahn-Hägerdal, B. *et al.,* 1994). *Escherichia coli* can also ferment all sugars derived from lignocellulose hydrolysate, and it is said that recombinant *E. coli* are the most efficient bacteria for fermentation of detoxified lignocellulose hydrolysate (Ingram, L. O. *et al.,* 1987; Hespell, R. B. *et al.,* 1996; Bothast, R. J. *et al.,* 1999; Dien, B. S. *et al.,* 2003). The characteristic of *Zymomonas mobilis* is to produce ethanol in stoichiometric yield (Swings, J. and DeLey, J., 1977), but its substrate range is limited. Recombinant xylose- and arabinose-fermenting strains have been constructed (Zhang, M. *et al.,* 1995; Deanda, K. *et al.,* 1996; Mohagheghi, A. *et al.,* 2002). However it is still necessary to impart the ability to *Z. mobilis* to metabolize mannose and galactose contained in lignocellulosic biomass. Aerobic filamentous fungi have industrial substrates tolerance and ferment pentose sugars, but the sugars consumption rate and product formation rates are low (Skoog, K and Hahn-Hägerdal, B., 1988; Hahn-Hägerdal, B. *et al.,* 1994). It is known that some species of anaerobic filamentous fungi can produce ethanol, in addition to acids and hydrogen (Wu J. F. and Ljungdahl, L. G., 1986; Boxma *et al.,* 2004; Panagiotou *et al.,* 2006), and they are used in industrial scale fermentation for antibiotics and acids production (Atkinson B. and Mavituna, F, 1991) However, the ethanol tolerance of these organisms are poor.

Table 1-1 Characteristics of various natural microorganisms with regard to industrial ethanol production

Organism	Natural sugar utilization pathway[a]					Major products			Torelance	
	Glc	Man	Gal	Xyl	Ara	Ethanol	Others	Alcohols	Acids	Hydrolysate
Anaerobic bacteria	+	+	+	+	+	+	+	−	−	−
Eshrichia coli	+	+	+	+	+	−	+	−	−	−
Zymomonas mobilis	+	−	−	−	−	+	−	+	−	−
Saccharomyces cerevisae	+	+	+	−	−	+	−	++	++	++
Schefferomyces stipitis	+	+	+	+	+	+	−	−	−	−
Filamentous fungi	+	+	+	+	+	+	−	++	++	++

[a] Sugars are abbreviated as follows: Glc, Glucose; Man, Mannose; Gal, Galactose; Xyl, Xylose; Ara, Arabinose

1.4.2 Metabolic engineering of *Saccharomyces cerevisiae* for xylose fermentation

The yeast *Saccharomyces cerevisiae* is highly effective for the production of ethanol from glucose and possesses tolerance toward high ethanol concentrations and other inhibitory compounds (Almeida, J. R. *et al*., 2007; Lau, M. W. *et al*., 2010). Moreover, it is used for the fermentation industry for a long time, and regarded as being safe. It is classified as GRAS, Generally Recognized As Safe (Fischer, S. *et al.,* 2013). Since *S. cerevisiae* can grow and produce ethanol on xylulose but, not on xylose (Chiang, L. C. e*t al.*, 1981; Richard, P. *et al.*, 2000; Ueng, P. P. *et al.*, 1981; Wang P. Y. and Schneider, H., 1980), many researchers have tried to develop an engineered *S. cerevisiae* that is able to convert xylose to ethanol. Heterologous expression of the xylose reductase (XR) and xylitol dehydrogenase (XDH) genes from natural xylose fermenting yeast such as *Scheffersomyces (Pichia) stipites* are often used to introduce xylose-fermenting ability to *S. cerevisiae* (Kötter, P. and Ciriacy, M., 1993; Ho, N. W. *et al.,* 1998; Karhumaa, K. *et al.,* 2007)*.* Xylose is first reduced to xylitol by XR coding by *XYL1* gene, and then xylitol is oxidized to xylulose by XDH coding by *XYL2*

gene. Xylulose is phosphorylated by xylulokinase (XK) to xylulose 5-phosphate (X5P) and metabolized into ethanol via the pentose phosphate pathway and glycolysis.

Although *S. cerevisiae* does not have xylose-utilizing ability, it possesses aldose reductase and XDH genes that are homologous to the XR and XDH genes, *XYL1* and *XYL2*, from *S. stipitis* (Träff, K. L. *et al.*, 2002; Richard, P. *et al.,* 1999; Toivari, M. H. *et al.,* 2004). Six aldo-keto reductase genes, *GRE3*, *YJR096w*, *YPR1*, *GCY1*, *ARA1* and *YDL124w*, are found in *S. cerevisiae* (Träff, K. L. *et al.*, 2002). Among them, since deletion of the *GRE3* gene reduced xylitol production, *GRE3* gene was thought to be the main xylose-reducing enzyme in *S. cerevisiae* (Träff, K. L. *et al.*, 2002). Three genes, *XYL2*, *SOR1* and *SOR2*, which are similar to XDH gene from *S. stipitis*, are also found in *S. cerevisiae* (Richard, P. *et al.,* 1999; Toivari, M. H. *et al.*, 2004). Cofactor specificity of XR and XDH in *S. cerevisiae* and *S. stipitis* is summarized in Fig. 1-2 (Toivari, M. H. *et al.*, 2004; Kuhn, A. *et al.*, 1995). While XR of *S. cerevisiae* uses only NADPH as cofactor, XR of *S. stipitis* can utilize both NADH and NADPH as cofactors of xylose reduction. XDH uses NAD as cofactor of xylitol dehydrogenation in both yeasts. Thus this leads to xylitol accumulation due to cofactor imbalance. In order to neutralize cofactor imbalance between XR and XDH, it was carried out that modifications of cofactor specificity of both enzymes by many researchers (Bengtsson, O. *et al.*, 2009; Jeppsson, M. *et al.*, 2006; Matsushika, A. et al., 2008; Petschacher, B. and Nidetzky, B., 2008; Runquist, D. *et al.*, 2010; Watanabe, S. et al., 2007; Zeng, Q. K. *et al.*, 2009). This approach reduced xylitol production significantly, but about 15% of the consumed xylose was still secreted as xylitol even in the most successful mutants (Bengtsson, O. *et al.*, 2009; Petschacher, B. and Nidetzky, B., 2008; Runquist, D. *et al.*, 2010).
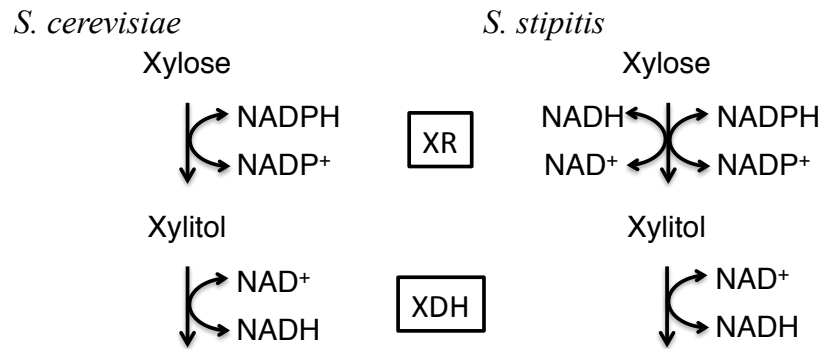
Fig. 1-2 Cofactor specificity of XR and XDH in *S. cerevisiae* and *S. stipitis*

Since *XYL2* gene of *S. cerevisiae* showed the highest homology to *XYL2* gene of *S. stipitis*, the possibility of creating self-cloning xylose-using *S. cerevisiae* with *GRE3* and *XYL2* genes has been demonstrated (Toivari, M. H. *et al.*, 2004). While *XYL2* gene was not induced in the presence of xylose, *SOR1* gene, coding for a sorbitol dehydrogenase that also has XDH activity, was induced (Sarthy, A. V., 1994). And also it is known that *S. cerevisiae* possesses XK activity and *XKS1* gene, that encodes XK (Rodriguez-Pena, J. M. *et al.*, 1998), and *S. stipitis* has *XYL3* gene, that also encodes XK (Jin, Y. *et al.*, 2002). Therefore it is sufficient to create self-cloning xylose-using *S. cerevisiae* by overexpression of three endogenous genes, *GRE3*, *SOR1* and *XKS1*.

Another metabolic pathway of xylose is known in microorganism, especially in bacteria. Many bacteria use a xylose isomerase (XI) enzyme to convert xylose to xylulose directly and it does not need pyridine nucleotide as cofactors. Many researchers tried to express heterologous *xylA* gene, that encodes XI, in *S. cerevisiae*, but it was unsuccessful. While putative *xylA* transcripts were detected in Northern blots, putative XI protein products were not solubilized and not active (Amore, R. et al., 1989; Gárdnyi, M. and Hahn-Hägerdal, B., 2003; Ho, N. *et al.*, 1983; Moes, C. J. et al., 1996; Sarthy, A. V. *et al.*, 1987; Walfridsson, M. *et al.*, 1996). For this reason, the XR-XDH pathway has long been used to impart xylose

utilization ability to *S. cerevisiae.* However, the anaerobic fungus *Piromyces* sp. Strain E2 that metabolized xylose using the XI pathway was discovered (Harhangi, H. R. *et al.*, 2003), and the XI from this organism was functionally expressed in *S. cerevisiae* (Kuyper, M. *et al.*, 2003; Kuyper, M. *et al.*, 2004). When the performance of XI and XR-XDH pathways were compared in same strains on minimal medium with xylose as a sole carbon source, the strain with XI pathway showed 30 % higher yield and the xylitol production was less (Karhumaa, K. et al., 2007). However, the strain with XR-XDH pathway showed higher xylose consumption rate and specific ethanol productivity.

1.5 Metabolic pathway simulations

It has become a key activity to estimate the flow of metabolism within the cell in biotechnological applications such as biopharmaceutical industries, food industry, and chemicals production, which include fuels, in order to improve productivity of microorganisms. Metabolic pathway simulation is one of the most successful and useful approaches for improving the productivity of industrially relevant microorganisms during their cultivation (Bailey, J. E., 1991; Stephanopoulos, G. and Vallino, J. J., 1991; Vallino, J. J. and Stephanopoulos, G., 1993; Kuriya, Y. *et al*., 2011). Flux balance analysis (FBA) and metabolic flux analysis (MFA) are two of most frequently used methods (Chen, X. *et al.*, 2011). FBA is *in silico* simulation that uses a genome-scale stoichiometry and measured extracellular fluxes, and MFA is *in vivo* analysis that measures fluxes by using isotope experimental data along with simplified model mainly such as central carbon stoichiometry and measured extracellular fluxes (Martin, H. G. *et al.*, 2015).

FBA is an analysis method of metabolic flux that covers the entire targeted metabolic pathway based only on stoichiometry, while dynamic analysis of metabolism and

relation between metabolite concentration and reaction rate cannot be dealt with (Kauffman, K. J. *et al.*, 2003; Palsson, B. Ø., 2006; Orth, J. D. *et al.*, 2010). That is, when predicting metabolic flux in FBA, it is placed the assumption that metabolism is in steady state. It means a state in which intermediates and metabolic flux in cells are constant without being changed over the time. This is an unrealistic assumption for a batch culture with time change, a nonsteady state, while it is considered to be a realistic assumption for continuous culture where steady state without time change is obtained. Furthermore in FBA, the metabolic pathway is described by algebraic equations, but the solution is calculated under the assumption that the cell regulates its metabolism so as to maximize the cell growth under a given environment.

MFA is a systematic and general approach to assess the roles of individual steps in a extensive metabolic pathway network. In particular, MFA is an experimental-based method of obtaining data on internal metabolites and metabolic fluxes by labeling experiments using isotopes (Stephanopoulos, G. *et al.*, 1998; Sauer, U. *et al.*, 1999; Wiechert, W., 2001; Nanchen, A. *et al.*, 2007; Zamboni, N. *et al.*, 2009). Microorganisms are cultured on ^{13}C labeled substrates and analytical chemical techniques such as GC-MS and LC-MS obtain the labeling of metabolic end products. Internal fluxes are estimated based on the measurements of labeled metabolite data and external fluxes. The resulting metabolic flux maps quantitatively show flow through metabolism. However, MFA also includes the assumption that metabolism is steady state, so in order to assess the metabolic fluxes of the reactions that include a nonstationary state, it is necessary that dynamic analysis taking time change into account. Therefore, although MFA was extended to Dynamic metabolic flux analysis (DMFA) taking time change into consideration, it still contains an assumption that intracellular metabolite concentration is constant (Antoniewicz, M. R., 2013). Hence it is

difficult to adapt to cases where metabolic intermediates change rapidly. In addition, FBA is also expanded to Dynamic flux balance analysis (DFBA) based on the same way of thinking (Mahadevan, R. *et al* ., 2002).

1.6 Aim of this study

This study aimed to construct recombinant xylose-using *S. cerevisiae* strains by endogenous xylose-assimilating genes utilization (self-cloning). In addition, in order to improve the ethanol productivity of self-cloning *S. cerevisiae*, a kinetic model of ethanol production pathway from xylose was constructed and a metabolic bottleneck reaction was estimated by sensitivity analysis. Furthermore, according to the estimation of the bottleneck reaction in the ethanol production pathway was eliminated by gene modification. The gene modification effect was validated and examined by fermentation evaluations.

CHAPTER 2

Construction of xylose-using *S. cerevisiae* by endogenous genes utilization (self-cloning)

2.1 Introduction

        Saccharomyces cerevisiae is traditionally used in various industries, especially for ethanol production, because *S. cerevisiae* has high tolerance toward ethanol and other inhibitory compounds (Almeida, J. R. *et al.,* 2007; Lau, M. W. *et al.,* 2010). And also, it has been studied for many years as a eukaryotic model organism, and accumulated gene information and tools for various genetic modifications are available. As mentioned in Chapter 1, ethanol production from xylose as well as glucose is also necessary to reduce ethanol production costs and to establish ethanol production economically. In order to impart xylose utilization ability to *S. cerevisiae*, it is common to use XR and XDH derived from naturally xylose-fermenting yeast *Scheffersomyces (Pichia) stipitis* (Kötter, P. and Ciriacy, M., 1993; Ho, N. W. *et al.,* 1998; Karhumaa, K. *et al.,* 2007). However, when genes derived from another microorganism are introduced, it corresponds to genetically modified organisms (GMOs). When it falls under the GMOs, measures to prevent the diffusion of yeasts are required, and the equipment cost for diffusion prevention is high. Thus, the manufacturing cost of ethanol plant becomes also high, and it is reflected in the ethanol cost. Although *S. cerevisiae* cannot utilize xylose naturally, it is known that it possesses genes, aldose reductase (*GRE3*) and sorbitol dehydrogenase (*SOR1*), that are homologous to the xylose-assimilating genes of *S. stipitis* (Träff, K. L. *et al.*, 2002; Richard, P. *et al.,* 1999; Toivari, M. H. *et al.,* 2004).

        In this chapter, therefore, to realize ethanol production using self-cloning yeast, xylose-using *S. cerevisiae* by endogenous genes utilization, *GRE3* and *SOR1*, was constructed and it was compared that the ethanol fermentation performance of endogenous genes utilized *S. cerevisiae* and engineered *S. cerevisiae* with XR (*XYL1*) and XDH (*XYL2*) genes from *S. stipitis*.

2.2 Materials and methods

2.2.1 Plasmid and strain construction

Xylose-using *Saccharomyces cerevisiae* by endogenous genes utilization was constructed as follows. The industrial Sake yeast *S. cerevisiae* Kyokai No.7 (K7) was used for host strain. *GRE3*, *SOR1*, *XK* gene (*XKS1*), and a phosphoglycerate kinase gene (*PGK1*) promoter and a terminator were amplified from the genomic DNA of *S. cerevisiae* CEN. PK.2-1C. Xylose reductase (*SsXYL1*) and Xylitol dehydrogenase (*SsXYL2*) from *Scheffersomyces stipitis* were amplified from the genomic DNA of *S. stipitis* NBRC 1687.

For the construction of the xylose-using gene expression cassette, the *GRE3*, *SOR1* and *XKS1* genes were cloned into the *Sal*I site located between the *PGK1* promoter and terminator introduced into pUC18 (Takara, Shiga, Japan). The *GRE3*, *SOR1* and *XKS1* with the *PGK1* promoter and terminator were digested with *Eco*RI and *Sph*I. Digested fragments were introduced in tandem into pUC18 by blunt-end ligation to create pUC-XYL.

For the preparation of K7-SsXYL, XKS1 with a PGK1 promoter and a terminator was ligated into pUC18 to yield pUC18-XKS1. Then, *SsXYL2* with a *PGK1* promoter and a terminator was blunt-ligated into the *Bam* HI site of pUC-XKS1 to yield pUC-SsXYL2-XKS1. Finally, *SsXYL1* with a *PGK1* promoter and a terminator was blunt-ligated into the *Sma* I site of pUC-SsXYL2-XKS1 to yield pUC-SsXYL.

The pUC-XYL and the pUC-SsXYL were digested with *Pvu*II and ligated into pAUR135 (Takara) which was digested with *Sma*I to yield pAUR-XYL and pAUR-SsXYL. pAUR-XYL and pAUR-SsXYL were digested with *Stu*I and transformed into K7 to produce K7-A-XYL and K7-A-SsXYL respectively. Yeast transformation was carried out by the lithium acetate method (Giets, D. *et al.*, 1992). For selection of transformants, 0.5 mg/L

aureobasidin A (Takara) was added to YPD agar plates. Synthetic complete (SC) medium containing 6.7 g/L yeast nitrogen base was used for yeast transformants selection. *Escherichia coli* JM109 was used for cloning of plasmids and grown at 37°C with shaking at 140 rpm in LB medium (yeast extract 5 g/L, tryptone 10 g/L, NaCl 5g/L).

2.2.2 Culture conditions

For precultivation of yeast cells, YP medium (yeast extract 10 g/L, peptone 20 g/L) with glucose 20 g/L was used. Yeast cells were harvested by centrifugation, washed twice with sterile distilled water to remove traces of glucose and ethanol, then suspended in an appropriate amount of the water. Batch fermentations were carried out in 200-mL baffled shaken flasks (with a filtered silicone plug to avoid ethanol evaporation), at 30°C with shaking at 140 rpm in CBS medium (ammonium sulfate 7.5 g/L, magnesium sulfate heptahydrate 0.75 g/L, potassium dihydrogenphosphate 3.5 g/L, potassium hydrogen phthalate 10.2 g/L; pH 5.0). Each flask contained 70 g/L glucose and 50 g/L xylose as the carbon sources and the initial concentration was 2×10^8 cells/mL. The flask fermentation was carried out in duplicate. The sampling frequency was 0, 2, 4, 6, 24, 30, 48, 54, 72 h and the sampling volumes were 0.6 mL.

2.2.3 Extracellular metabolites analysis

Concentrations of xylose, ethanol, glycerol, xylitol, and acetate in culture supernatants were determined with a high-performance liquid chromatography system (Shimadzu, Kyoto, Japan) equipped with a SUGAR SP0810 column (Shodex, Tokyo, Japan) using water as the mobile phase at a flow rate of 0.8 mL/min and 80°C.

2.3 Results

Flask-scale cultures of strains K7-A-XYL, integrated *GRE3, SOR1* and *XKS1* from *S. cerevisiae*, and K7-A-SsXYL, *XYL1* and *XYL2* from *S. stipitis* and *XKS1* from *S. cerevisiae*, were grown in 200-mL baffled shaken flasks containing CBS medium with initial glucose concentration of 70 g/L and xylose concentration of 50 g/L (Fig. 2-1 and Fig. 2-2). All the glucose was converted to ethanol within 6 h in both strains. While regarding the consumption of xylose, both strains showed different profiles. Although K7-A-XYL consumed xylose at a rate of 1.5 g/L·h and exhausted all the xylose within 48 h, K7-A-SsXYL converted xylose to ethanol at a rate of 0.73 g/L·h and only about 50 % of the xylose was consumed even after 72 h of fermentation. As a result K7-A-XYL produced more ethanol compared to K7-A-SsXYL (K7-A-XYL 37.6 g/L, K7-A-SsXYL 32.0 g/L). Furthermore although both strains did not accumulate much xylitol, less than 1.0 g/L, the glycerol and acetic acid production of both strains were significantly different. K7-A-SsXYL produced 8.1 g/L glycerol and 5.3 g/L acetate, while K7-A-XYL produced 17.2 g/L glycerol and 3.9 g/L acetate respectively.
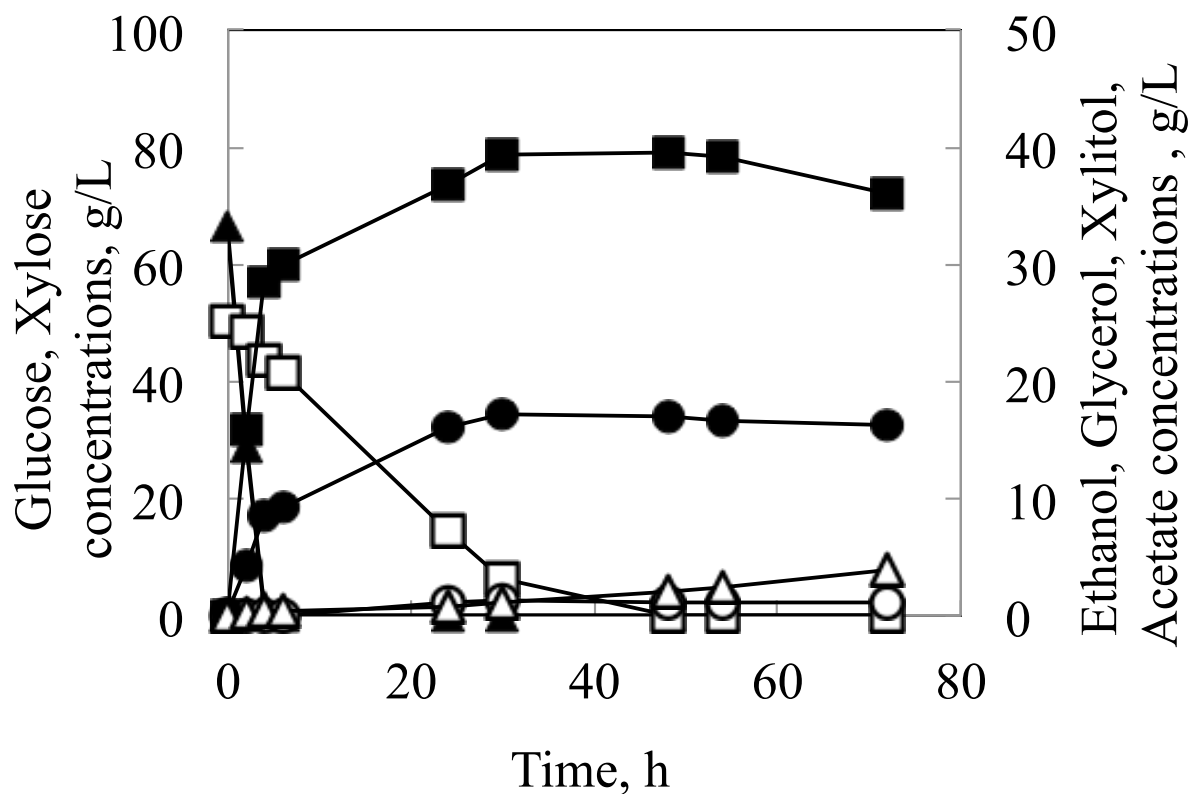
Fig. 2-1 Fermentation profiles of flask cultures of strains K7-A-XYL in CBS medium containing 70 g/L glucose and 50 g/L xylose as the carbon sources. Results were based on two replications. Deviation was below 10 % of the average.

Glucose, closed triangles; Xylose, open squares; Ethanol, closed squares; Xylitol, open circles; Glycerol, closed circles; Acetate, open triangles.
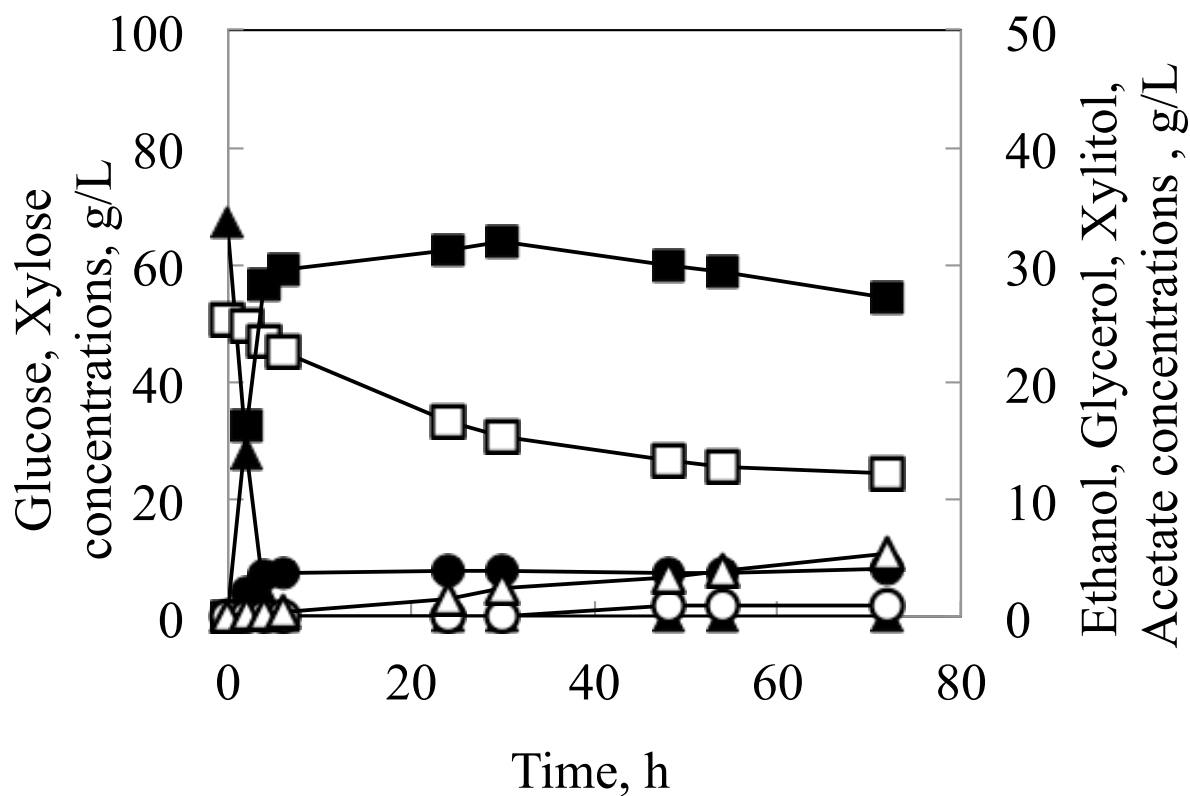
Fig. 2-2 Fermentation profiles of flask cultures of strains K7-A-SsXYL in CBS medium containing 70 g/L glucose and 50 g/L xylose as the carbon sources. Results were based on two replications. Deviation was below 10 % of the average.

Glucose, closed triangles; Xylose, open squares; Ethanol, closed squares; Xylitol, open circles; Glycerol, closed circles; Acetate, open triangles.

2.4 Discussion

Two xylose-using *S. cerevisiae* were constructed. One was endogenous genes utilized *S. cerevisiae* (K7-A-XYL)*,* which possessed *GRE3* and *SOR1* genes. The other was engineered *S. cerevisiae* (K7-A-SsXYL) with *XYL1* and *XYL2* genes from *S. stipitis*. Comparing the ethanol production amount of both strains, it is strongly suggested that K7-A-XYL showed higher ethanol productivity, and that sufficient xylose utilizing ability could be given even by utilization of the endogenous genes. This suggests that ethanol production from lignocellulose biomass, which contains much xylose, may be realized.

Ethanol production rate of K7-A-SsXYL was slow and it seemed that it stopped xylose consumption after 48 h. K7-A-SsXYL produced a large amount of acetic acid; 5.31 g/L in 72 h. This may be one reason of the slow ethanol production and suspension of xylose utilization, since it is known that acetic acid concentration at 0.05-0.1 % w/v begins to stress the *S. cerevisiae* as seen by reduced growth rates and decreased rates of ethanol production as the concentration of acetic acid in the media raised (Narendranath, N. V. *et al.*, 2001). And also it is reported that acetic acid concentration at 0.5 % w/v inhibits xylose consumption (Limtong, S., *et al.*, 2000).

In order to convert xylitol to xylulose by the reaction of SOR1 and XYL2, the supply of NAD^+ as a cofactor is considered to be essential as shown in chapter 1. XYL1 from *S. stipitis* can utilize both NADH and NADPD as cofactors of xylose reduction, whereas GRE3 uses only NADPH (Toivari, M. H. *et al.*, 2004; Kuhn, A. *et al.*, 1995). Therefore it was considered that K7-A-SsXYL has more advantage than K7-A-XYL in terms of xylitol accumulation and smooth metabolic flow from xylose to ethanol, since the cycles of NAD^+ and NADH rotate between XYL1 and XYL2. Unexpectedly, there was no difference in the production of xylitol in both strains, and the xylitol production amount was very small, less

28

than 1.0 g/L. The reason that low xylitol production in K7-A-XYL may be presumably due to that sufficient NAD^+ regeneration has occurred by adequate oxygen supply in this culture condition. Since NAD^+ regeneration is closely related to the dissolved oxygen in the culture medium, it seems to be important to control the culture conditions with a focus on dissolved oxygen concentration.

CHAPTER 3

Construction of kinetic model of the ethanol production pathway of self-cloning xylose-using *S. cerevisiae*

3.1 Introduction

Xylose-using *S. cerevisiae* (K7-A-XYL) by endogenous *GRE3* and *SOR1* genes utilization was constructed in Chapter 2. The xylose-using *S. cerevisiae* showed better ethanol producing performance than genetically modified *S. cerevisiae* (K7-A-SsXYL) with *XYL1* and *XYL2* genes from *S. stipitis* in this culture conditions. The ethanol yield (g ethanol/ g sugars) of strain K7-A-XYL was 0.34. Ethanolic fermentation of starch and sugar generally reaches 0.45-48 g ethanol/ g sugars, equivalent to 90-95% of the theoretical yield (Hahn-Hägerdal, B. *et al.*, 2007). Therefore further enhancement of the ethanol productivity of self-cloning yeast is necessary. Cost analysis of the ethanol fermentation from lignocellulose biomass showed that approximately one-third of the manufacturing cost is raw material cost (von Sivers, M. and Zacchi, G., 1996; Galbe, M. and Zacchi, G., 2002; Wingren, A. *et al.*, 2003). Thus conversion of all sugars to ethanol and increasing ethanol productivity are important for the cost effectiveness of the process (Carroll, A. and Somerville, C., 2009; Stephanopoulos, G., 2007).

Metabolic pathway simulation is one of the most successful and useful approaches for improving the productivity of industrially relevant microorganisms during their cultivation as descried in Chapter 1. Based on predictions by simulation, it is expected that gene manipulation candidates for improving ethanol productivity can be efficiently extracted. In addition extraction of candidate genes by simulation is particularly effective for assessing the influence of combining multiple genetic modifications. Although the metabolic pathway simulations on xylose-using pathway have been performed on genetically modified yeasts before (Wahlbom, C. F. *et al.*, 2001; Pitkansen J.P. *et al.*, 2003; Sonderegger, M. *et al.*, 2004; Grotkjaer, T. *et al.*, 2005; Parachin, *N. S. et al.*, 2011; Matsushika, A. *et al.,* 2013; Wasylenko, T. M. and Stephanopoulos, G., 2015), such analysis has not been conducted so far on

self-cloning yeasts. Genetically modified yeasts and self-cloning yeasts have different genes used to metabolize xylose, and because of different coenzyme specificities, their metabolic behaviors are considered to be different. And also the time change of metabolites was not considered in the conventional metabolic pathway simulation as detailed in Chapter 1.

The definition of self-cloning is that it does not contain heterologous genes, and consists only of genes from the organism itself and closely related species. According to this definition, since K7-A-XYL constructed in Chapter 2 contains pARU135 (Takara, Shiga, Japan) vector sequences, the yeast is not a self-cloning *S. cerevisiae*. Therefore, the method of preparing the strains needs to be changed, and sequences constituted only from *S. cerevisiae* should be used to impart xylose utilization capability without containing vector-derived sequences.

Ethanol yield from starch and glucose is nearly close to the theoretical value, and it remains little improvement in margin. On the other hand, since the ethanol yield from xylose is still low, it needs to be more improvement. Thus the improvement of ethanol yield from xylose is the target in this study. In this chapter, the culture supernatant and intracellular metabolites of self-cloning xylose-using *S. cerevisiae*, which does not contain vector sequences, were analyzed in xylose culture and a kinetic model of the ethanol production pathway from xylose was constructed. Then, sensitivity analysis was carried out to identify a metabolic bottleneck reaction and manipulated a gene corresponding to the bottleneck reaction.

3.2 Materials and methods

3.2.1 Plasmid and strain construction

The strain used for the experimental data collection of the kinetic model constructions was K7-XYL. K7-XYL was constructed as follows. The industrial Sake yeast *S. cerevisiae* K7 was used for host strain. Construction of the xylose assimilating gene expression cassette, XR, XDH and XKS with a *PGK1* promoter and a terminator was described previously (Konishi, J. *et al*., 2015). The expression cassette with *Eco*RI and *Hin*dIII restriction sites was introduced into the multiple cloning site of pUC18 (Takara, Shiga, Japan) to create pUC-XYL. *XYL2* was amplified from the genomic DNA of strain K7 with a *Sma*I restriction site and introduced into *Sma*I-digested pUC18 to create pUC-XYL2. pUC-XYL and pUC-XYL2 were digested with *Eco*RI and *Hin*dIII, and *Apa*I respectively. The fragments were blunted and ligated to create pUC-XYL2-XYL-XYL2. pUC-XYL2-XYL-XYL2 was digested with *Sma*I and transformed into K7 to produce strain K7-XYL. Yeast transformation was carried out by the lithium acetate method (Giets, D. *et al*., 1992). Synthetic complete (SC) medium containing 6.7 g/L yeast nitrogen base was used for yeast transformants selection. *Escherichia coli* JM109 was used for cloning of plasmids and grown at 37°C with shaking at 140 rpm in LB medium (yeast extract 5 g/L, tryptone 10 g/L, NaCl 5g/L).

3.2.2 Culture conditions

The strain used for the experimental data collection of the kinetic model constructions was K7-XYL described in 3.2.1 Plasmid and strain construction.

For precultivation of yeast cells, YP medium (yeast extract 10 g/L, peptone 20 g/L) with glucose 20 g/L was used. Batch fermentations were carried out in 500-mL baffled shaken flasks, with a filtered silicone plug to avoid ethanol evaporation, at 30°C with shaking at 140 rpm in YP medium (pH 5.0). Each flask contained 50 g/L xylose as the carbon source and the initial concentration was 2×10^8 cells/mL. The flask fermentation was carried out in duplicate. The sampling frequency was 0, 1, 2, 3, 6, 9, 24, 48 h and the sampling volumes were 1.6 mL.

3.2.3 Extracellular metabolites analysis

Concentrations of xylose, ethanol, glycerol, xylitol, and acetate in culture supernatants were determined with a high-performance liquid chromatography system (Shimadzu, Kyoto, Japan) equipped with a SUGAR SP0810 column (Shodex, Tokyo, Japan) using water as the mobile phase at a flow rate of 0.8 mL/min and 80°C. Cell density was measured by optical density measurement at 600 nm (OD600) using a UV1800 spectrophotometer (Shimadzu). Cell growth was calculated using a predetermined correlation with OD600.

3.2.4 Intracellular metabolites analysis

Intracellular metabolites were quantitated using liquid chromatography/triple-stage quadrupole mass spectrometry (LC-QqQ-MS). Metabolite analysis with LC-QqQ-MS was performed as previously described (Kiyonari, S. *et al.*, 2015), and samples were prepared as follows. For quenching, 1 mL cell culture was injected into a 15-mL Falcon tube containing 5 mL pure methanol precooled to −20°C and mixed by inversion. Subsequently, samples were centrifuged at 15000 × *g* at −9°C for 2 min, and the supernatant was discarded. The pellets were washed with 3 mL precooled water and centrifuged at 15000 × *g* at −9°C for 2 min.

Samples were stored at −80°C until metabolite extraction. For metabolite extraction, the pellets were resuspended in 1 mL 100% methanol containing 6 μM (+)-10-camphor sulfonic acid (Tokyo Chemical Industry, Tokyo, Japan) as an internal standard and transferred to a 1.5-mL tube that contained 2 mm zirconia beads. The cell suspension was disrupted using a bead cell disrupter MS-100R (TOMY, Tokyo, Japan) at 3000 rpm and −9°C for 5 min. Then samples were centrifuged at 15000 × g at −9°C for 5 min, and supernatants were collected in a fresh 15-mL Falcon tube on ice. The pellets were resuspended in 1 mL 50% (v/v) methanol and disrupted again. Samples were centrifuged, and supernatants were added to the 15-mL Falcon tube containing the methanol extract already recovered. The collected supernatants were mixed with chloroform and water at a ratio of 1:1.5:1 and centrifuged at 15000 × g at −9°C for 5 min. The aqueous phase of the extract was dried under vacuum (CVE-2000, EYELA, Tokyo and DTU-20, ULVAC, Kanagawa) and stored at −80°C until further use.

3.2.5 Model development

A mathematical model of ethanol production from xylose using xylose-assimilating *S. cerevisiae* was constructed by an ordinary differential equation system with reference to previously reported models (Teusink, B. *et al.*, 2000; Hynne, F. *et al.*, 2001; Rizzi, M. *et al.*, 1997). The range of the target metabolic pathway was shown in Fig. 3-1. The metabolic model includes the central carbon metabolism system, pentose phosphate pathway, xylose metabolism pathway, and glycerol, ethanol and acetic acid production pathways. Regarding the pathway that generates biomass, this study assumed a system in which xylose entrapped (Xylose$_{cyt}$ in Fig.3-1) flows into biomass (R43 in Fig. 3-1). The mathematical model consists of two compartments: extracellular (culture fluid) and intracellular (cytoplasm). The intracellular metabolic reactions were described based on each enzyme reaction mechanism

(Cleland, W. W., 1963). The rate equations of reaction number (R1-R43) in mathematical model shown in Fig. 3-1 were described in Table 3-1. Sugar uptake was described by a Michaelis-Menten type equation based on the difference in concentration inside and outside the cell (Bertilsson, M. *et al.*, 2008; Teusink, B. *et al.*, 1998). Substance transport between the two compartments was described via linear equations. Concentration change in each compartment because of the transport of substances inside and outside the cell was converted based on the yeast-specific cell volume 2.0 mL/g-dry cell weight (van Urk, H. *et al.*, 1988). Mass balance of mathematical model shown in Fig. 3-1 was described in Table 3-2. Among the coenzymes included in the model, ATP, ADP, AMP, NAD^+, NADH, $NADP^+$ and NADPH concentrations were interpolated from experimental time course data and used for simulation in Table 3-3 and Fig. 3-2. Quinone, quinol, CoA, phosphoric acid and CO_2 were assumed to be constant regardless of time in Table 3-2.

First, the kinetic parameter values for the mathematical model were investigated in enzyme reaction databases such as BRENDA (Schomburg, I. *et al.*, 2013), and as many kinetic parameter values as possible were acquired in Table 3-4. Next, other parameters whose values were unknown were estimated using a real-valued genetic algorithm (Akimoto, Y. *et al,*, 2009) and manual operation to reproduce the experimental data obtained in flask culture with an initial xylose concentration of 50 g/L. Simulations were carried out with the Gear method (Gear, G. W., 1971). The initial values of dependent variables were listed in Table 3-5.

Forty-three reactions and forty-six metabolites were included in the mathematical model shown in Fig. 3-1. An original program developed in C language carried out the simulation. This model included allosteric regulations in 6-phosphofructokinase and pyruvate

36

kinase based on previous works (Teusink, B. *et al.*, 2000; Rizzi, M. *et al.*, 1997). Additionally cell growth rate equation had a term for growth shutdown to avoid excess growth in simulation. For coenzymes, the time-course data of the coenzyme concentrations obtained by measurements were interpolated and expressed as the function of time t. As for the rest, constraints such as competitive inhibition by substrate(s) and/or product(s) and equilibrium constant were included based on enzyme kinetics and reactions.

3.2.6 Sensitivity analysis

Sensitivity analysis is a method for assessing the validity of a developed model and clarifying which pathway(s) have the most impact, in the present case on ethanol productivity. The amount of ethanol production at 48 h was assessed in this study because all the xylose was consumed by 48 h.

The endpoint deviation (ED) of ethanol described below was assessed to reveal which reaction pathway(s) impact ethanol production. In this calculation, a 100% increase was assigned to each kinetic parameter in rate equations in the model; each kinetic parameter was tested individually in this way.

$$ED = 100 \times ([Ethanol]_{change} - [Ethanol]_{control})/[Ethanol]_{control}$$

Where $[Ethanol]_{change}$ was the ethanol concentration at 48 h given a 100% increase in the kinetic parameter in the rate equation, and $[Ethanol]_{control}$ was the ethanol concentration without any change. The higher the absolute value of ED, the more a kinetic parameter affects the ethanol production. Various genetic manipulation strategies were developed based on the outcomes of this analysis.

Fig. 3-1 Metabolic pathway of ethanol production from xylose

Table 3-1 Rate equations of reaction number (R1 – R43) in mathematical model shown in Fig. 3-1

Reaction No.	Rate equations
R1: Xylose uptake	V_1 = V_Xylose_uptalose_uptake = Vmax_XU × (Xylose_ex – Xylose_cyt) / (Km_Xylose + Xylose_ex + Xylose_cyt +α× Xylose_ex × Xylose_cyt / Km_Xylose) (1)
R2: NADPH–dependent xylose reductase (Aldose reductase: Xylose → Xylitol)	V_2 = V_XR = Vf_XR / (Ki_NADPH × Km_Xylose) × (NADPH_cyt × Xylose_cyt – Xylitol_cyt × NADP_cyt / Keq_NADPH) / (1.0 + Km_NADPH × Xylose_cyt / (Ki_NADPH × Km_Xylose + Km_NADP × Xylitol_cyt / (Km_Xylitol × Ki_NADP) + NADPH_cyt / Ki_NADPH + NADP_cyt / Ki_NADP + NADPH_cyt × Xylose_cyt / (Ki_NADPH × Km_Xylose) + Km_NADP × NADPH_cyt × Xylitol_cyt /(Ki_NADPH × Km_Xylitol × Ki_NADP) + Km_NADPH × Xylose_cyt × NADP_cyt / (Ki_NADPH × Km_Xylose × Ki_NADP) + Xylitol_cyt × NADP_cyt / (Km_Xylitol × Ki_NADP) + NADPH_cyt × Xylose_cyt × Xylitol_cyt / (Ki_NADPH × Km_Xylose × Ki_Xylitol) + Xylose_cyt × Xylitol_cyt × NADP_cyt / (Ki_Xylose × Km_Xylitol × Ki_NADP)) (2)
R3: Xylitol secretion from intracellular space (cytosol) to extracellular space	V_3 = V_Xylit_sec = Vsec_Xylit × Xylitol_cyt (3)
R4: Xylitol uptake from extracellular space to intracellular space (cytosol)	V_4 = V_Xylit_up = Vup_Xylit × Xylitol_ex (4)
R5: NAD$^+$–dependent xylitol dehydrogenase (Sorbitol dehydrogenase: Xylitol → Xylulose)	V_5 = V_XDH = Vf_XDH × Vr × (NAD × Xylitol_cyt – Xylulose × NADH / Keq) / (Ki_NAD × Km_Xylitol × Vr + Km_Xylitol × Vr × NAD + Km_NAD × Vr × Xylitol_cyt + Vr × NAD × Xylitol_cyt + Km_NADH ×

Vf_XDH × Xylulose / Keq + Km_Xylulose × Vf_XDH × NADH / Keq + Vf_XDH × Xylulose × NADH / Keq + Km_NADH × Vf_XDH × NAD × Xylulose / (Ki_NAD × Keq) + Km_NAD × Vr × Xylitol_cyt × NADH / Ki_NADH + Vr × NAD × Xylitol_cyt × Xylulose / Ki_Xylulose + Vf_XDH × Xylitol_cyt × Xylulose × NADH / (Ki_Xylitol × Keq)) (5)

R6: Xylulokinase (Xylulose + ATP ↔ X5P + ADP)

V_6 = V_XK = Vf_XK × ATP_cyt × Xylulose / (Km_Xylulose × Km_ATP × (1 + Xylulose / Km_Xylulose) × (1 + ATP_cyt / Km_ATP)) (6)

R7: Ribulose-5-phosphate epimerase

V_7 = V_RPE = (Vf_RPE / Km_X5P × X5P – Vr_RPE / Km_Ru5P × Ru5P) / (1 + X5P / Km_X5P + Ru5P / Km_Ru5P) (7)

R8: Ribulose-5-phosphate isomerase

V_8 = V_RPI = (Vf_RPI / Km_Ru5P × Ru5P – Vr / Km_R5P × R5P) / (1 + Ru5P / Km_Ru5P + R5P / Km_R5P) (8)

R9: Transketolase 1 (X5P + R5P ↔ GAP + S7P)

Keq calculation:

Keq = Vf_TKL1 × Vf_TKL1 / (Vr_TKL1 × Vr_TKL1) × Km_GAP × Km_S7P / (Km_R5P × Km_X5P) (9)

V_9 = V_TKL1 = Vf_TKL1 × Vr_TKL1 × (X5P × R5P – GAP × S7P / Keq_TKL1) / (Km_R5P × Vr_TKL1 × X5P + Km_X5P × Vr_TKL1 × R5P + Vr_TKL1 × X5P × R5P + Km_S7P × Vf_TKL1 × GAP / Keq + Km_GAP × Vf_TKL1 × S7P / Keq + Vf_TKL1 × GAP × S7P / Keq + Vf_TKL1 × X5P × GAP / (Ki_X5P × Keq) + Km_X5P × Vr × R5P × S7P / Ki_S7P) (10)

R10: Transaldolase (S7P + GAP ↔ E4P + F6P)

Keq calculation:

Keq = Vf_TAL × Vf_TAL / (Vr × Vr) × Km_E4P × Km_F6P / (Km_GAP × Km_S7P) (11)

V_{10} = V_TAL = Vf_TAL × Vr × (S7P × GAP − E4P × F6P / Keq) / (Km_GAP × Vr × S7P + Km_S7P × Vr × GAP + Vr × S7P × GAP + Km_F6P × Vf_TAL × E4P / Keq + Km_E4P × Vf_TAL × F6P / Keq + Vf_TAL × E4P × F6P / Keq + Km_F6P × Vf_TAL × S7P × E4P / (Ki_S7P × Keq) + Km_S7P × Vr × GAP × F6P / Ki_F6P)　　　　　(12)

R11: Transketolase 2 (X5P + E4P ↔ GAP + F6P)

Keq calculation:

Keq_TKL2 = Vf_TKL2 × Vf_TKL2 / (Vr_TKL2 × Vr_TKL2) × Km_GAP × Km_F6P / (Km_E4P × Km_X5P)　　　　　(13)

V_{11} = V_TKL2 = Vf_TKL2 × Vr_TKL2 × (X5P × E4P − GAP × F6P / Keq_TKL2) / (Km_E4P × Vr_TKL2 × X5P + Km_X5P × Vr × E4P + Vr_TKL2 × X5P × E4P + Km_F6P × Vf_TKL2 × GAP / Keq_TKL2 + Km_GAP × Vf_TKL2 × F6P / Keq_TKL2 + Vf_TKL2 × GAP × F6P / Keq_TKL2 + Km_F6P × Vf_TKL2 × X5P × GAP / (Ki_X5P × Keq_TKL2) + Km_X5P × Vr_TKL2 × E4P × F6P / Ki_F6P)　　　　　(14)

R12: Transketolase 3 (S7P + E4P ↔ R5P + F6P)

Keq calculation:

Keq = Vf_TKL3 × Vf_TKL3 / (Vr × Vr) × Km_R5P × Km_F6P / (Km_E4P × Km_S7P)　　　　　(15)

V_{12} = V_TKL3 = Vf_TKL3 × Vr × (S7P × E4P − R5P × F6P / Keq) / (Km_E4P × Vr × S7P + Km_S7P × Vr × E4P + Vr × S7P × E4P + Km_F6P × Vf_TKL3 × R5P / Keq + Km_R5P × Vf_TKL3 × F6P / Keq + Vf_TKL3 × R5P × F6P / Keq + Km_F6P × Vf_TKL3 × S7P × R5P / (Ki_S7P × Keq) + Km_S7P × Vr × E4P × F6P / Ki_F6P)　　　　　(16)

R13: Glucose phosphate isomerase (F6P ↔ G6P)

V_{13} = V_GPI = (Vf_GPI / Km_F6P × F6P − Vr_GPI / Km_G6P × G6P) / (1.0 + F6P / Km_F6P + G6P / Km_G6P)　　　　　(17)

R14: Glucose 6–phosphate dehydrogenase

Vr calculation:

(G6P + NADP$^+$ ↔ PGL + NADPH)

Vr_G6PDH = Vf_G6PDH × Ki_NADP × Km_G6P × Ki_6PGL × Km_NADPH / (Km_NADP × Ki_G6P × Km_6PGL × Ki_NADPH)　　(18)

Keq calculation:

Keq_G6PDH = Vf_G6PDH × Km_6PGL × Ki_NADPH / (Vr_G6PDH × Ki_NADP × Km_G6P)　　(19)

V_{14} = V_G6PDH = Vf_G6PDH × Vr_G6PDH × (NADP_cyt × G6P − PGL × NADPH_cyt / Keq_G6PDH) / (Ki_NADP × Km_G6P × Vr_G6PDH + Km_G6P × Vr_G6PDH × NADP_cyt + Km_NADP × Vr_G6PDH × G6P + Vr_G6PDH × NADP_cyt × G6P + Km_NADPH × Vf_G6PDH × PGL / Keq_G6PDH + Km_6PGL × Vf_G6PDH × NADPH_cyt / Keq_G6PDH + Vf_G6PDH × PGL × NADPH_cyt / Keq_G6PDH + Km_NADPH × Vf_G6PDH × NADP_cyt × PGL / (Ki_NADP × Keq_G6PDH) + Km_NADP × Vr_G6PDH × G6P × NADPH_cyt / Ki_NADPH + Vr_G6PDH × NADP_cyt × G6P × PGL / Ki_6PGL + Vf_G6PDH × G6P × PGL × NADPH_cyt / (Ki_G6P × Keq_G6PDH))　　(20)

R15: 6–Phosphogluconolactonase (PGL + H$_2$O → 6PG)

V_{15} = V_6PGL = Vmax_6PGL × PGL / (Km_6PGL + PGL)　　(21)

R16: Phosphogluconate dehydrogenase

(6PG + NADP$^+$ ↔ Ru5P + NADPH + CO$_2$)
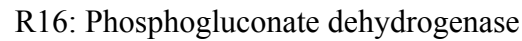
Vr calculation:

Vr_6PGDH = Vf_6PGDH × Ki_6PG × Km_CO2 / (Km_6PG × Ki_CO2)　　(22)

Keq calculation:

Keq_6PGDH =Ki_NADPH × Ki_Ru5P × Ki_CO2 / (Ki_NADP × Ki_6PG)　　(23)

V_{16} = V_6PGDH = Vf_6PGDH × Vr_6PGDH × (NADP_cyt × 6PG − CO2 × X5P × NADPH_cyt / Keq_6PGDH) / (Ki_NADP × Km_6PG × Vr_6PGDH + Km_6PG × Vr_6PGDH × NADP_cyt + Km_NADP ×

Vr_6PGDH × 6PG + Vr_6PGDH × NADP_cyt × 6PG + Ki_NADPH × Km_Ru5P × Vf_6PGDH × CO2 / Keq_6PGDH + Ki_Ru5P × Km_CO2 × Vf_6PGDH × NADPH_cyt / Keq_6PGDH + Km_NADPH × Vf_6PGDH × CO2 × X5P / Keq_6PGDH + Km_Ru5P × Vf_6PGDH × CO2 × NADPH_cyt / Keq_6PGDH + Km_CO2 × Vf_6PGDH × X5P × NADPH_cyt / Keq_6PGDH + Vf_6PGDH × CO2 × X5P × NADPH_cyt / Keq_6PGDH + Ki_NADPH × Km_Ru5P × Vf_6PGDH × NADP_cyt × CO2 / (Ki_NADP × Keq_6PGDH) + Km_NADP × Vr_6PGDH × 6PG × NADPH_cyt / Ki_NADPH + Ki_NADPH × Km_Ru5P × Vf_6PGDH × NADP_cyt × 6PG × CO2 / (Ki_NADP × Ki_6PG) + Km_NADPH × Ki_CO2 × Vf_6PGDH × NADP_cyt × 6PG × X5P / (Ki_NADP × Ki_6PG × Keq_6PGDH) + Km_NADP × Vr_6PGDH × 6PG × X5P × NADPH_cyt / (Ki_NADPH × Ki_Ru5P) + Km_NADPH × Vf_6PGDH × NADP_cyt × CO2 × X5P / (Ki_NADP × Keq_6PGDH) + Km_NADPH × Vf_6PGDH × NADP_cyt × 6PG × CO2 × X5P / (Ki_NADP × Ki_6PG × Keq_6PGDH) + Km_NADP × Vr_6PGDH × 6PG × CO2 × X5P × NADPH_cyt / (Ki_NADPH × Ki_Ru5P × Ki_CO2))   (24)

R17: 6–Phosphofructokinase (F6P + ATP → FBP + ADP)

V_{17} = V_PFK = Vmax_PFK × ATP_cyt × F6P / ((ATP_cyt + Km_ATP × (1 + ADP_cyt / Ki_ADP)) × (F6P + Km_F6P × (1 + ATP_cyt / Ki_ATP + ADP_cyt / KmB_ADP + AMP_cyt / KmB_AMP) / (1 + ADP_cyt / KmA_ADP + AMP_cyt / KmA_AMP)) × (1 + L_pfk / (1.0 + F6P × (1 + ADP_cyt / KmA_ADP + AMP_cyt / KmA_AMP) / (Km_F6P × (1 + ATP_cyt / Ki_ATP + ADP_cyt / KmB_ADP + AMP_cyt / KmB_AMP)))$^{n\_pfk}$))   (25)

R18: FBP–aldolase (FBP ↔ GAP + DHAP)

Vr calculation:

$$Vr\_ALDo = 5.0 \times Vf\_ALDo \tag{26}$$

$$V_{18} = V\_Aldo = Vf\_ALDo \times (FBP - GAP \times DHAP / Keq\_ALDo) / (Km\_FBP + FBP + GAP \times Km\_DHAP \times Vf\_ALDo / (Keq\_ALDo \times Vr\_ALDo) + DHAP \times Km\_GAP \times Vf\_ALDo / (Keq\_ALDo \times Vr\_ALDo) + FBP \times GAP / Ki\_GAP + GAP \times DHAP \times Vf\_ALDo / (Keq\_ALDo \times Vr\_ALDo)) \tag{27}$$

R19: Triose phosphate isomerase (DHAP ↔ GAP)

Vr calculation:

$$Vr\_TPI = 22.0 \times Vf\_TPI \times Km\_GAP / Km\_DHAP \tag{28}$$

$$V_{19} = V\_TPI = (Vf\_TPI / Km\_DHAP \times DHAP - Vr\_TPI / Km\_GAP \times GAP) / (1 + DHAP / Km\_DHAP + GAP / Km\_GAP) \tag{29}$$

R20: Glyceraldehyde 3–phosphate dehydrogenase

$(GAP + NAD^+ + P_i \leftrightarrow 1,3–BPG + NADH)$

Vr calculation based on Vf:

$$Vr\_GAPDH = Vf\_GAPDH \times Ki\_Pi \times Km\_13BPG / (Km\_Pi \times Ki\_13BPG) \tag{30}$$

Keq calculation:

$$Keq\_GAPDH = Ki\_13BPG \times Ki\_NADH / (Ki\_NAD \times Ki\_GAP \times Ki\_Pi) \tag{31}$$

$$V_{20} = V\_GAPDH = Vf\_GAPDH \times Vr\_GAPDH \times (NAD\_cyt \times GAP \times Pi\_cyt - 13BPG \times NADH\_cyt / Keq\_GAPDH) / (Ki\_NAD \times Ki\_GAP \times Km\_Pi \times Vr\_GAPDH + Ki\_GAP \times Km\_Pi \times Vr\_GAPDH \times NAD\_cyt + Ki\_NAD \times Km\_GAP \times Vr\_GAPDH \times Pi\_cyt + Km\_Pi \times Vr\_GAPDH \times NAD\_cyt \times GAP + Km\_GAP \times Vr\_GAPDH \times NAD\_cyt \times Pi\_cyt + Km\_NAD \times Vr\_GAPDH \times GAP \times Pi\_cyt + Vr\_GAPDH \times NAD\_cyt \times GAP \times Pi\_cyt + Km\_13BPG \times Vf\_GAPDH \times NADH\_cyt / Keq\_GAPDH + Km\_NADH \times Vf\_GAPDH \times 13BPG / Keq\_GAPDH + Vf\_GAPDH \times 13BPG \times NADH\_cyt / Keq\_GAPDH + Km\_NADH \times Vf\_GAPDH \times$$

NAD_cyt × GAP / (Ki_NAD × Keq_GAPDH) + Ki_NAD × Km_GAP × Vr_GAPDH × Pi_cyt × NADH_cyt / Ki_NADH + Km_NADH × Vf_GAPDH × NAD_cyt × GAP × 13BPG / (Ki_NAD × Ki_GAP × Keq_GAPDH) + Km_NAD × Vr_GAPDH × GAP × Pi_cyt × NADH_cyt / Ki_NADH + Km_NAD × Ki_Pi × Vr_GAPDH × GAP × 13BPG × NADH_cyt / (Ki_13BPG × Ki_NADH) + Ki_NAD × Km_GAP × Vr_GAPDH × Pi_cyt × 13BPG × NADH_cyt / (Ki_13BPG × Ki_NADH) + Km_NADH × Vf_GAPDH × NAD_cyt × GAP × Pi_cyt × 13BPG / (Ki_NAD × Ki_GAP × Ki_Pi × Keq_GAPDH) + Km_NAD × Vr_GAPDH × GAP × Pi_cyt × 13BPG × NADH_cyt / (Ki_13BPG × Ki_NADH))

(32)

R21: Phosphoglycerate kinase
(1,3–BPG + ADP ↔ 3PG + ATP)

Keq calculation:

Keq_PGK = Vf_PGK× Km_3PG × Ki_ATP / (Vr_PGK × Ki_ADP × Km_BPG

(33)

V_{21} = V_PGK = Vf_PGK × Vr_PGK × (ADP_cyt × BPG – ATP_cyt × 3PG / Keq_PGK) / (Ki_ADP × Km_BPG × Vr_PGK + Km_BPG × Vr_PGK × ADP_cyt + Km_ADP × Vr_PGK × BPG + Vr_PGK × ADP_cyt × BPG + Km_3PG × Vf_PGK × ATP_cyt / Keq_PGK + Km_ATP × Vf_PGK × 3PG / Keq_PGK + Vf_PGK × ATP_cyt × 3PG / Keq_PGK)

(34)

R22: Phosphoglycerate mutase (3PG ↔ 2PG)

V_{22} = V_PGM = Vmax_PGM × (3PG – 2PG / Keq_PGM) / (Km_3PG × (1 + 2PG / Ki_2PG) + 3PG)

(35)

R23: Enolase (2PG ↔ PEP + H_2O)

V_{23} = V_ENO = (Vf_ENO / Km_2PG × 2PG – Vr_ENO / Km_PEP × PEP) / (1 + 2PG / Km_2PG + PEP / Km_PEP)

(36)

R24: Pyruvate kinase (PEP + ADP → PYR + ATP)

V_{24} = V_PYK = Vmax_PYK × PEP × (PEP / Ki_PEP + 1.0)$^{(n\_pyk - 1.0)}$ × ADP_cyt / (Km_PEP × (L_pyk × ((1.0 + ATP_cyt / Ki_ATP) / (FBP /

R25: Pyruvate decarboxylase
($Pyr_{cyt} \rightarrow Acetaldehyde_{cyt} + CO_2$)

R26 (R26-1, R26-2): Alcohol dehydrogenase
($Acetaldehyde_{cyt} + NAD(P)H \leftrightarrow Ethanol_{cyt} + NAD(P)^+$)

R26-1: Cytosolic NADH–dependent alcohol dehydrogenase 1
($Acetaldehyde_{cyt} + NADH \leftrightarrow Ethanol_{cyt} + NAD^+$)

$$Ka\_FBP + AMP\_cyt / Ka\_AMP + 1.0))^{n\_pyk} + (PEP / Ki\_PEP + 1.0)^{n\_pyk}) \times (ADP\_cyt + Km\_ADP)) \tag{37}$$

$$V_{25} = V\_PDC = Vmax\_PDC \times Pyr\_cyt \times Pyr\_cyt / (A + B \times Pyr\_cyt + Pyr\_cyt \times Pyr\_cyt \times (1.0 + Pyr\_cyt / Ki\_Pyr)) \tag{38}$$

$$V_{26} = V\_ADH\_cyt = V\_ADH1 + V\_ADH1\_NADPH \tag{39}$$

Vr calculation:

$$Vr\_ADH1 = Vf\_ADH1 \times Ki\_Ethanol \times Km\_NAD \times Ki\_NADH \times Km\_Aldehyde / (Km\_NADH \times Ki\_Aldehyde \times Km\_Ethanol \times Ki\_NAD) \tag{40}$$

Keq calculation:

$$Keq\_ADH1 = Vf\_ADH1 \times Km\_Ethanol \times Ki\_NAD / (Vr \times Ki\_NADH \times Km\_Aldehyde) \tag{41}$$

If concentration of extracellular xylose ($Xylose_{ex}$) is lower than 10^{-3} M then

$$Vf\_ADH1 = theta\_NADH \times Vf\_ADH1 \tag{42}$$

$$Vr\_ADH1 = theta\_NADH \times Vr\_ADH1 \tag{43}$$

$V\_ADH1 = Vf\_ADH1 \times Vr\_ADH1 \times (NADH \times Acetaldehyde - Ethanol\_cyt \times NAD / Keq\_ADH1) / (Ki\_NADH \times Km\_Aldehyde \times Vr + Km\_Aldehyde \times Vr\_ADH1 \times NADH + Km\_NADH \times Vr\_ADH1 \times Acetaldehyde + Vr\_ADH1 \times NADH \times Acetaldehyde + Km\_NAD \times Vf\_ADH1 \times Ethanol\_cyt / Keq\_ADH1 + Km\_Ethanol \times Vf\_ADH1 \times NAD / Keq\_ADH1 + Vf\_ADH1 \times Ethanol\_cyt \times NAD / Keq\_ADH1 + Km\_NAD \times Vf\_ADH1 \times NADH \times Ethanol\_cyt / (Ki\_NADH \times Keq\_ADH1) + Km\_NADH \times Vr\_ADH1 \times Acetaldehyde \times NAD / Ki\_NAD + Vr\_ADH1 \times NADH \times Acetaldehyde \times Ethanol\_cyt / Ki\_Ethanol + Vf\_ADH1 \times$

Acetaldehyde × Ethanol_cyt × NAD / (Ki_Aldehyde × Keq_ADH1))

$$(44)$$

R26-2: NADPH–dependent alcohol dehydrogenase 1
(Acetaldehyde$_{cyt}$ + NADPH ↔ Ethanol$_{cyt}$ + NADP$^+$)

Vr calculation:

Vr_ADH1_NADPH = Vf_ADH1_NADPH × Ki_Ethanol × Km_NADP × Ki_NADPH × Km_Aldehyde / (Km_NADPH × Ki_Aldehyde × Km_Ethanol × Ki_NADP)

$$(45)$$

Keq calculation:

Keq_ADH1_NADPH = Vf_ADH1_NADPH × Km_Ethanol × Ki_NADP / (Vr × Ki_NADPH × Km_Aldehyde)

$$(46)$$

If concentration of extracellular xylose (Xylose$_{ex}$) is lower than 10^{-3} M then

Vf_ADH1_NADPH = theta_NADPH × Vf_ADH1_NADPH

$$(47)$$

Vr_ADH1_NADPH = theta_NADPH × Vr_ADH1_NADPH

$$(48)$$

V_ADH1_NADPH = Vf_ADH1_NADPH × Vr_ADH1_NADPH × (NADPH × Acetaldehyde – Ethanol_cyt × NADP / Keq_ADH1_NADPH) / (Ki_NADPH × Km_Aldehyde × Vr_ADH1_NADPH + Km_Aldehyde × Vr_ADH1_NADPH × NADPH + Km_NADPH × Vr_ADH1_NADPH × Acetaldehyde + Vr_ADH1_NADPH × NADPH × Acetaldehyde + Km_NADP × Vf_ADH1_NADPH × Ethanol_cyt / Keq_ADH1_NADPH + Km_Ethanol × Vf_ADH1_NADPH × NADP / Keq_ADH1_NADPH + Vf_ADH1_NADPH × Ethanol_cyt × NADP / Keq_ADH1_NADPH + Km_NADP × Vf_ADH1_NADPH × NADPH × Ethanol_cyt / (Ki_NADPH × Keq_ADH1_NADPH) + Km_NADPH × Vr_ADH1_NADPH × Acetaldehyde × NADP / Ki_NADP + Vr_ADH1_NADPH × NADPH ×

Acetaldehyde × Ethanol_cyt / Ki_Ethanol + Vf_ADH1_NADPH × Acetaldehyde × Ethanol_cyt × NADP / (Ki_Aldehyde × Keq_ADH1_NADPH))　　　　　　　　　　　　　　　　(49)

R27: Ethanol secretion (EtOH$_{cyt}$ → EtOH$_{ex}$)

V_{27} = V_EtOH_sec = Vsec_EtOH × EtOH_cyt　　　　　　(50)

R28: Ethanol uptake (EtOH$_{ex}$ → EtOH$_{cyt}$)

V_{28} = V_EtOH_up = Vup_EtOH × EtOH_ex　　　　　　(51)

R29: Glycerol 3–phosphate dehydrogenase
(DHAP + NADH ↔ Gly3P + NAD^{+})

Vr calculation:

Vr = Vf_G3PDH × Ki_Gly3P × Km_NAD / (Keq × Ki_NADH × Km_DHAP)　　　　　　　　　　　　　　　　　(52)

V_{29} = V_G3PDH = Vf_G3PDH × Vr × (NADH_cyt × DHAP – Gly3P × NAD_cyt / Keq) / (Vr × Ki_NADH × Km_DHAP + Vr × Km_DHAP × NADH_cyt + Vr × Km_NADH × DHAP + Vr × NADH_cyt × DHAP + Vf_G3PDH × Km_NAD × Gly3P / Keq + Vf_G3PDH × Km_Gly3P × NAD_cyt / Keq + Vf_G3PDH × Gly3P × NAD_cyt / Keq + Vr × Ki_NADH × Km_DHAP × Pi_cyt / Ki_Pi + Vr × Km_DHAP × NADH_cyt × Pi_cyt / Kii_Pi + Vr × Km_NADH × DHAP × NAD_cyt / Kii_NAD + Vf_G3PDH × Km_Gly3P × Pi_cyt × NAD_cyt / (Kii2_Pi × Keq))　　　　　　　(53)

R30: Mitochondrial glycerol–3–phosphate dehydrogenase
(Gly3P + Quinone ↔ DHAP + Quinol)

Keq calculation:

Keq_GUT2 = Vf_GUT2 × Vf_GUT2 × Km_QH2 × Km_DHAP / (Vr × Vr × Km_Q × Km_Gly3P)　　　　　　　　　　(54)

V_{30} = V_GUT2 = Vf_GUT2 × Vr × (Quinone × G3P – Quinol × DHAP / Keq_GUT2) / (Km_Gly3P × Vr × Quinone + Km_Q × Vr × G3P + Vr × Quinone × G3P + Km_DHAP × Vf_GUT2 × Quinol / Keq_GUT2 + Km_QH2 × Vf_GUT2 × DHAP / Keq_GUT2 + Vf_GUT2 × Quinol × DHAP / Keq_GUT2 + Km_DHAP × Vf_GUT2 × Quinone × Quinol / (Ki_Q × Keq_GUT2) + Km_Q × Vr × G3P × DHAP / Ki_DHAP)　　　　(55)

R31: Glycerol–3–phosphate phosphatase
(Gly3P + H₂O → Glycerol_cyt + Pi)

V_{31} = V_GPP = Vmax_GPP × Gly3P / (Km_Gly3P + Gly3P)　　　(56)

R32: Glycerol kinase
(Glycerol_cyt + ATP → Gly3P + ADP)

V_{32} = V_GUT1 = Vmax_GUT1 × Glycerol_cyt × ATP_cyt / (Ki_Glycerol × Km_ATP + Km_ATP × Glycerol_cyt + Km_Glycerol × ATP_cyt + Glycerol_cyt × ATP_cyt)　　　(57)
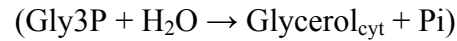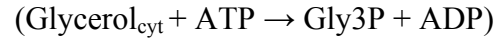
R33: Glycerol passive diffusion
(Glycerol_cyt ↔ Glycerol_ex)

V_{33} = V_Glycerol_PD = Vmax_Glycerol_PD × (Glycerol_cyt – Glycerol_ex)　　　(58)

R34: Glycerol/H⁺ symport
(Glycerol_ex + H⁺ → Glycerol_cyt + H⁺)

V_{34} = V_H_Glycerol_Symport = Vmax_Glycerol_SP × Glycerol_ex / (Kt + Glycerol_ex)　　　(59)
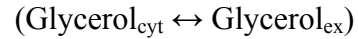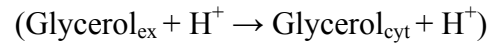
R35 (R35-1, R35-2):
Cytosolic NAD(P)⁺–dependent acetaldehyde dehydrogenase
(Acetaldehyde_cyt + NAD(P)⁺ → Acetate_cyt + NAD(P)H)

V_{35} = V_ALDH_cyt = V_ALDH_NADP_cyt + V_ALDH_NAD_cyt　　　(60)

R35-1: Cytosolic NADP⁺–dependent acetaldehyde dehydrogenase (Acetaldehyde_cyt + NADP⁺ → Acetate_cyt + NADPH)

Vr–calculation:
Vr = Vf_ALDH × Ki_Acetate × Km_NADPH × Ki_NADP × Km_Aldehyde / (Km_NADP × Ki_Aldehyde × Km_Acetate × Ki_NADPH)　　　(61)

Keq–calculation:
Keq = Vf_ALDH × Km_Acetate × Ki_NADPH / (Vr × Ki_NADP × Km_Aldehyde)　　　(62)

V_ALDH_NADP_cyt = Vf_ALDH × NADP_cyt × Acetaldehyde_cyt / (Ki_NADP × Km_Aldehyde + Km_Aldehyde × NADP_cyt + Km_NADP × Acetaldehyde_cyt + NADP_cyt × Acetaldehyde_cyt)　　　(63)

R35-2: Cytosolic NAD⁺–dependent acetaldehyde dehydrogenase
(Acetaldehyde_cyt + NAD⁺ → Acetate_cyt + NADH)

Vr calculation:
Vr = Vf_ALDH_NAD × Ki_Acetate × Km_NADH × Ki_NAD × Km_Aldehyde / (Km_NAD × Ki_Aldehyde × Km_Acetate × Ki_NADH)

Keq calculation:

$$\text{Keq} = \text{Vf\_ALDH\_NAD} \times \text{Km\_Acetate} \times \text{Ki\_NADH} / (\text{Vr} \times \text{Ki\_NAD} \times \text{Km\_Aldehyde})$$ (65)

$$\text{V\_ALDH\_NAD\_cyt} = \text{Vf\_ALDH\_NAD} \times (\text{NAD\_cyt} \times \text{Acetaldehyde\_cyt}) / (\text{Ki\_NAD} \times \text{Km\_Aldehyde} + \text{Km\_Aldehyde} \times \text{NAD\_cyt} + \text{Km\_NAD} \times \text{Acetaldehyde\_cyt} + \text{NAD\_cyt} \times \text{Acetaldehyde\_cyt})$$ (66)

R36: Cytosolic acetic acid secretion ($\text{Acetatep}_{cyt} \to \text{Acetatep}_{ex}$) $V_{36} = \text{V\_Ac\_sec} = \text{Vsec\_Ace} \times \text{Acetate\_cyt}$ (67)

R37: Extracellular acetic acid uptake ($\text{Acetatep}_{ex} \to \text{Acetatep}_{cyt}$) $V_{37} = \text{V\_Ac\_up} = \text{Vup\_Ace} \times \text{Acetate\_ex}$ (68)

R38: Acetyl–CoA synthetase

($\text{Acetate}_{cyt} + \text{ATP} + \text{CoA} \to \text{AceCoA}_{cyt} + \text{AMP}$)

$$V_{38} = \text{V\_ACS} = \text{Vf\_Acs1} \times \text{ATP\_cyt} \times \text{Acetate\_cyt} \times \text{CoA\_cyt} / (\text{Ki\_ATP} \times \text{Km\_Acetate} \times \text{CoA\_cyt} + \text{Km\_Acetate} \times \text{ATP\_cyt} \times \text{CoA\_cyt} + \text{Km\_CoA} \times \text{ATP\_cyt} \times \text{Acetate\_cyt} + \text{Km\_ATP} \times \text{Acetate\_cyt} \times \text{CoA\_cyt} + \text{ATP\_cyt} \times \text{Acetate\_cyt} \times \text{CoA\_cyt}) / (1 + \text{Acetyl\_CoA\_cyt} / \text{Kii\_AceCoA})$$ (69)

R39: Pyruvate transport between cytosol and mitochondrial matrix ($\text{Pyr}_{cyt} \to \text{Pyr}_{mit}$) $V_{39} = \text{V\_PYR\_TRP\_CM} = \text{Vm\_pyr\_T} \times \text{Pyr\_cyt}$ (70)

R40: Oxaloacetate transport between cytosol and mitochondrial matrix ($\text{OXA}_{cyt} \to \text{OXA}_{mit}$) $V_{40} = \text{V\_OXA\_TRP\_CM} = \text{Vm\_OXA\_trp\_cm} \times \text{OXA\_cyt}$ (71)

R41: Pyruvate carboxylase

($\text{Pyr}_{cyt} + \text{ATP} + CO_2 \leftrightarrow \text{OXA}_{cyt} + \text{ADP}$)

Ki–OAA calculation:

$$\text{Ki\_OAA} = \text{Vf\_PYC} \times \text{Ki\_Pyr} \times \text{Km\_OAA} / (\text{Vr} \times \text{Km\_Pyr})$$ (72)

Keq–calculation:

$$\text{Keq} = \text{Ki\_OAA} \times \text{Ki\_Pi} \times \text{Ki\_ADP} / (\text{Ki\_ATP} \times \text{Ki\_CO2} \times \text{Ki\_Pyr})$$ (73)

$$V_{41} = \text{V\_PYC} = \text{Vf\_PYC} \times \text{Vr} \times (\text{ATP\_cyt} \times \text{CO2} \times \text{PYR\_cyt} - \text{Pi} \times$$

$$
\begin{aligned}
&OAA\_cyt \times ADP\_cyt \;/\; Keq) \;/\; (Ki\_ATP \times Ki\_CO2 \times Km\_Pyr \times Vr + \\
&Ki\_CO2 \times Km\_Pyr \times Vr \times ATP\_cyt + Ki\_ATP \times Km\_CO2 \times Vr \times PYR\_cyt \\
&+ Km\_Pyr \times Vr \times ATP\_cyt \times CO2 + Km\_CO2 \times Vr \times ATP\_cyt \times PYR\_cyt \\
&+ Km\_ATP \times Vr \times CO2 \times PYR\_cyt + Vr \times ATP\_cyt \times CO2 \times PYR\_cyt + \\
&Ki\_ADP \times Km\_Pi \times Vf\_PYC \times Pi \;/\; Keq + Ki\_Pi \times Km\_OAA \times Vf\_PYC \times \\
&ADP\_cyt \;/\; Keq + Km\_ADP \times Vf\_PYC \times Pi \times OAA\_cyt \;/\; Keq + Km\_Pi \times \\
&Vf\_PYC \times Pi \times ADP\_cyt \;/\; Keq + Km\_OAA \times Vf\_PYC \times OAA\_cyt \times \\
&ADP\_cyt \;/\; Keq + Vf\_PYC \times Pi \times OAA\_cyt \times ADP\_cyt \;/\; Keq + Km\_Pi \times \\
&Ki\_ADP \times Vf\_PYC \times ATP\_cyt \times Pi \;/\; (Ki\_ATP \times Keq) + Ki\_ATP \times \\
&Km\_CO2 \times Vr \times PYR\_cyt \times ADP\_cyt \;/\; Ki\_ADP + Km\_Pi \times Ki\_ADP \times \\
&Vf\_PYC \times ATP\_cyt \times CO2 \times Pi \;/\; (Ki\_ATP \times Ki\_CO2 \times Keq) + Km\_ADP \times \\
&Vf\_PYC \times ATP\_cyt \times Pi \times OAA\_cyt \;/\; (Ki\_ATP \times Keq) + Km\_ATP \times Vr \times \\
&CO2 \times PYR\_cyt \times ADP\_cyt \;/\; Ki\_ADP + Ki\_ATP \times Km\_CO2 \times Vr \times \\
&PYR\_cyt \times OAA\_cyt \times ADP\_cyt \;/\; (Ki\_Pi \times Ki\_ADP) + Ki\_ADP \times Km\_Pi \\
&\times Vf\_PYC \times ATP\_cyt \times CO2 \times PYR\_cyt \times Pi \;/\; (Ki\_ATP \times Ki\_CO2 \times \\
&Ki\_Pyr \times Keq) + Ki\_OAA \times Km\_ADP \times Vf\_PYC \times ATP\_cyt \times CO2 \times \\
&PYR\_cyt \times OAA\_cyt \;/\; (Ki\_ATP \times Ki\_CO2 \times Ki\_Pyr \times Keq) + Km\_ADP \times \\
&Vf\_PYC \times ATP\_cyt \times CO2 \times Pi \times OAA\_cyt \;/\; (Ki\_ATP \times Ki\_CO2 \times Keq) + \\
&Km\_ATP \times Vr \times CO2 \times PYR\_cyt \times OAA\_cyt \times ADP\_cyt \;/\; (Ki\_Pi \times \\
&Ki\_ADP) + Km\_ATP \times Ki\_Pyr \times Vr \times CO2 \times Pi \times OAA\_cyt \times ADP\_cyt \;/\; \\
&(Ki\_OAA \times Ki\_Pi \times Ki\_ADP) + Ki\_ATP \times Km\_CO2 \times Vr \times PYR\_cyt \times Pi \\
&\times OAA\_cyt \times ADP\_cyt \;/\; (Ki\_OAA \times Ki\_Pi \times Ki\_ADP) + Km\_ADP \times \\
&Vf\_PYC \times ATP\_cyt \times CO2 \times PYR\_cyt \times Pi \times OAA\_cyt \;/\; (Ki\_ATP \times \\
&Ki\_CO2 \times Ki\_Pyr \times Keq) + Km\_ATP \times Vr \times CO2 \times PYR\_cyt \times Pi \times \\
&OAA\_cyt \times ADP\_cyt \;/\; (Ki\_OAA \times Ki\_Pi \times Ki\_ADP))
\end{aligned}
\tag{74}
$$

R42: Phosphoenolpyruvate carboxykinase ($OXA_{cyt} + ATP \leftrightarrow PEP + ADP + CO_2$)	Keq–calculation:
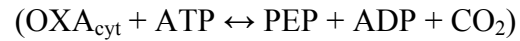
$$\text{Keq\_PCK} = \text{Vf\_PCK} \times \text{Km\_CO2} \times \text{Km\_PEP} \times \text{Ki\_ADP} / (\text{Vr} \times \text{Ki\_ATP} \times \text{Km\_OAA}) \tag{75}$$

$$V_{42} = \text{V\_PCK} = \text{Vf\_PCK} \times \text{Vr} \times (\text{ATP\_cyt} \times \text{OAA\_cyt} - \text{CO2\_cyt} \times \text{PEP\_cyt} \times \text{ADP\_cyt} / \text{Keq\_PCK}) / (\text{Vr} \times \text{Ki\_ATP} \times \text{Km\_OAA} + \text{Vr} \times \text{Km\_OAA} \times \text{ATP\_cyt} + \text{Vr} \times \text{Km\_ATP} \times \text{OAA\_cyt} + \text{Vr} \times \text{ATP\_cyt} \times \text{OAA\_cyt} + \text{Vf\_PCK} \times \text{Km\_PEP} \times \text{Km\_ADP} / \text{Keq\_PCK} \times \text{CO2\_cyt} + \text{Vf\_PCK} \times \text{Km\_CO2} \times \text{Km\_ADP} / \text{Keq\_PCK} \times \text{PEP\_cyt} + \text{Vf\_PCK} \times \text{Km\_CO2} \times \text{Km\_PEP} / \text{Keq\_PCK} \times \text{ADP\_cyt} + \text{Vf\_PCK} \times \text{Km\_CO2} / \text{Keq\_PCK} \times \text{PEP\_cyt} \times \text{ADP\_cyt} + \text{Vf\_PCK} \times \text{Km\_PEP} / \text{Keq\_PCK} \times \text{CO2\_cyt} \times \text{ADP\_cyt} + \text{Vf\_PCK} \times \text{Km\_ADP} / \text{Keq\_PCK} \times \text{CO2\_cyt} \times \text{PEP\_cyt} + \text{Vf\_PCK} / \text{Keq\_PCK} \times \text{CO2\_cyt} \times \text{PEP\_cyt} \times \text{ADP\_cyt} + \text{Vr} \times \text{Km\_OAA} / \text{Kii\_ADP} \times \text{ATP\_cyt} \times \text{ADP\_cyt} + \text{Vr} \times \text{Km\_ATP} / \text{Kii\_PEP} \times \text{OAA\_cyt} \times \text{PEP\_cyt}) / (1 + \text{Xylex} / \text{Kii\_Xyl}) \tag{76}$$

R43: Cell growth on xylose (biomass synthesis)	

$$V_{43} = \text{V\_Growth} = \text{mmax} \times \text{Xylose\_cyt} / (\text{Ks\_Xylose} + \text{Xylose\_cyt} \times (1.0 + \text{Xylose\_cyt} / \text{Kis\_Xylose})) / (1.0 + (\text{Biomass} / (\text{Xinit\_biomass} + \text{Xmax\_biomass}))^{\text{n\_growth}}) \tag{77}$$

Metabolic reactions were described by Michaelis–Menten type equations (based on enzyme kinetics). Transport reactions of acetate, ethanol, oxaloacetate and pyruvate via cell and mitochondrial membranes were described by first order kinetics for model simplification. Transport reaction of xylose was described by Haldane type equation based on facilitated diffusion with carrier (Teusink, B. et al., 1998). On the other hand, transport reaction of glycerol was described by Michaelis-Menten type equation and first order kinetics. In this reaction, Michaelis-Menten type equation and first order kinetics corresponded to facilitated dissusion and passive diffusion, respectively. Ri (i = 1, 2, …,

43) represents reaction number in metabolic pathway of Fig. 3-1. "V_" represent velocity of each reaction. Vmax, Keq, Km, Ki (Kii), n, represent maximum velocities, equiblium constants, Michaelis constants, inhibition constants, power exponents, respectively. Vf and Vr represent velocities of forward and reverse reactions, respectively. Descriptions in rate equations, "in (cyt)", "ex", mean compartments of those metabolites, "intracellular space (cytosol)" and "extracellular space", respectively. "_up", "_sec" show uptake and secretion of the metabolite, respectively. α in R1 represents interactive constant that depends on the relative mobility of the substrate bound and unbound (free) carrier (Teusink, B. et al., 1998).

Table 3-2 Mass balance of mathematical model shown in Fig. 3-1.

Reaction names	Mass balance	
Extracellular Xylose (Xylose$_{ex}$ in Fig.3-1)	$\frac{d[Xylose_{ex}]}{dt} = -V_1 \times \frac{V_c}{V_e} \times [Biomass]$	(78)
Intracellular (cytosolic) Xylose (Xylose$_{cyt}$ in Fig.3-1)	$\frac{d[Xylose_{cyt}]}{dt} = V_1 - V_2 - \mu[Xylose_{cyt}]$	(79)
Intracellular (cytosolic) Xylitol (Xylitol$_{cyt}$ in Fig. 3-1)	$\frac{d[Xylitol_{cyt}]}{dt} = V_2 + V_3 - V_4 - V_5 - \mu[Xylitol_{cyt}]$	(80)
Extracellular Xylitol (Xylitol$_{ex}$ in Fig.3-1)	$\frac{d[Xylitol_{ex}]}{dt} = (V_4 - V_3) \times \frac{V_c}{V_e} \times [Biomass]$	(81)
Xylulose	$\frac{d[Xylulose_{cyt}]}{dt} = V_5 - V_6 - \mu[Xylulose_{cyt}]$	(82)
X5P	$\frac{d[X5P]}{dt} = V_6 - V_7 - V_9 - V_{11} - \mu[X5P]$	(83)
Ru5P	$\frac{d[Ru5P]}{dt} = V_7 - V_8 + V_{16} - \mu[Ru5P]$	(84)
R5P	$\frac{d[R5P]}{dt} = V_8 - V_9 + V_{12} - \mu[R5P]$	(85)
S7P	$\frac{d[S7P]}{dt} = V_9 - V_{10} - V_{12} - \mu[S7P]$	(86)
GAP	$\frac{d[GAP]}{dt} = V_9 - V_{10} + V_{11} + V_{18} + V_{19} - V_{20} - \mu[GAP]$	(87)

E4P	$$\frac{d[E4P]}{dt} = V_{10} - V_{11} - V_{12} - \mu[E4P]$$	(88)
F6P	$$\frac{d[F6P]}{dt} = V_{10} + V_{11} + V_{12} - V_{13} - V_{17} - \mu[F6P]$$	(89)
G6P	$$\frac{d[G6P]}{dt} = V_{13} - V_{14} - \mu[G6P]$$	(90)
PGL	$$\frac{d[PGL]}{dt} = V_{14} - V_{15} - \mu[PGL]$$	(91)
6PG	$$\frac{d[6PG]}{dt} = V_{15} - V_{16} - \mu[6PG]$$	(92)
FBP	$$\frac{d[FBP]}{dt} = V_{17} - V_{18} - \mu[FBP]$$	(93)
DHAP	$$\frac{d[DHAP]}{dt} = V_{18} - V_{19} - V_{29} + V_{30} - \mu[DHAP]$$	(94)
Gly3P	$$\frac{d[Gly3P]}{dt} = V_{29} - V_{30} - V_{31} + V_{32} - \mu[Gly3P]$$	(95)
Glycerol$_{cyt}$	$$\frac{d[Glycerol_{cyt}]}{dt} = V_{31} - V_{32} - V_{33} + V_{34} - \mu[Glycerol_{cyt}]$$	(96)
Glycerol$_{ex}$	$$\frac{d[Glycerol_{ex}]}{dt} = (V_{33} - V_{34}) \times \frac{V_c}{V_e} \times [Biomass]$$	(97)
1,3BPG	$$\frac{d[1,3BPG]}{dt} = V_{20} - V_{21} - \mu[1,3BPG]$$	(98)
3PG	$$\frac{d[3PG]}{dt} = V_{21} - V_{22} - \mu[3PG]$$	(99)

2PG	$\dfrac{d[2PG]}{dt} = V_{22} - V_{23} - \mu[2PG]$	(100)
PEP	$\dfrac{d[PEP]}{dt} = V_{23} - V_{24} + V_{42} - \mu[PEP]$	(101)
Pyruvate$_{cyt}$ (Pyruvate in Fig. 3-1)	$\dfrac{d[Pyruvate_{cyt}]}{dt} = V_{24} - V_{25} - V_{41} - V_{39} - \mu[Pyruvate_{cyt}]$	(102)
Acetaldehyde$_{cyt}$ (Acetaldehyde in Fig. 3-1)	$\dfrac{d[Acetaldehyde_{cyt}]}{dt} = V_{25} - V_{26} - V_{35} - \mu[Acetaldehyde_{cyt}]$	(103)
Ethanol$_{cyt}$	$\dfrac{d[\text{Ethanol}_{cyt}]}{dt} = V_{26} - V_{27} + V_{28} - \mu[\text{Ethanol}_{cyt}]$	(104)
Ethanol$_{ex}$	$\dfrac{d[\text{Ethanol}_{ex}]}{dt} = (V_{27} - V_{28}) \times \dfrac{V_c}{V_e} \times [Biomass]$	(105)
Acetate$_{cyt}$	$\dfrac{d[Acetate_{cyt}]}{dt} = V_{35} - V_{36} + V_{37} - V_{38} - \mu[Acetate_{cyt}]$	(106)
Acetate$_{ex}$	$\dfrac{d[Acetate_{ex}]}{dt} = (V_{36} - V_{37}) \times \dfrac{V_c}{V_e} \times [Biomass]$	(107)
Oxaloacetate$_{cyt}$ (OXA in Fig. 3-1)	$\dfrac{d[OXA_{cyt}]}{dt} = V_{41} - V_{40} - V_{42} - \mu[OXA_{cyt}]$	(108)
AceCoA$_{cyt}$ (Glyoxylate cycle in Fig. 3-1)	$\dfrac{d[AceCoA_{cyt}]}{dt} = V_{38} - \mu[AceCoA_{cyt}]$	(109)
Biomass	$\dfrac{d[Biomass]}{dt} = \mu[Biomass] \times \dfrac{V_c}{V_e}$	(110)
CO$_2$	$\dfrac{d[CO_2]}{dt} = 0.0$	(111)

P$_i$	$\dfrac{d[P_i]}{dt} = 0.0$	(112)
CoA	$\dfrac{d[CoA]}{dt} = 0.0$	(113)
Quinone	$\dfrac{d[Quinone]}{dt} = 0.0$	(114)
Quinol	$\dfrac{d[Quinol]}{dt} = 0.0$	(115)

The numerical subscripts of terms V_i in these equations correspond to the number of the reaction (R_i) in the metabolic map in Fig. 3-1.

V_e and V_c indicate the volume in the medium and intracellularly, respectively; these values are 1.0 (L) and 2.0 (mL/g–dry cell weight),

respectively. μ indicates specific growth rate, so the terms multiplied by μ except for the metabolite concentration balance equation for biomass

indicate dilution by bacterial growth. "cyt" and "ex" represent compartments of those metabolites, "intracellular space (cytosol)" and

"extracellular space", respectively. Metabolites without subscripts, "cyt" or "ex", mean metabolites only in cytosol.

Table 3-3 Interpolation equations of coenzymes in mathematical model shown in Fig. 3-1.

Coenzymes	Interpolation equations
$NADP^+$	If time (t) is lower than 9.0 h, then $NADP^+ = 4.29835 \times 10^{-7} \times t^3 - 7.79247 \times 10^{-6} \times t^2 + 4.29455 \times 10^{-5} \times t + 3.78263 \times 10^{-5}$ (116) else $NADP^+ = -9.5525 \times 10^{-10} \times t^3 + 1.47437 \times 10^{-7} \times t^2 - 7.32887 \times 10^{-6} \times t + 1.61209 \times 10^{-4}$ (117)
NADPH	If time (t) is less than 4.0 h, then $NADPH = -3.59419 \times 10^{-7} \times t^3 + 1.91439 \times 10^{-6} \times t^2 - 2.72624e \times 10^{-6} \times t + 7.21520 \times 10^{-6}$ (118) else $NADPH = 1.72959 \times 10^{-11} \times t^3 + 2.40540 \times 10^{-10} \times t^2 - 1.59976 \times 10^{-9} \times t + 3.93911 \times 10^{-6}$ (119)
NAD^+	$NAD^+ = -5.5 \times 10^{-4} \times t^{1.5} / (2^{1.5} + t^{1.5}) + 9.71509 \times 10^{-4}$ (120)
NADH	If time (t) is less than 9.0 h, then $NADH = 5.05145 \times 10^{-8} \times t^4 - 3.8665 \times 10^{-7} \times t^3 - 2.23803 \times 10^{-6} \times t^2 + 2.39081 \times 10^{-5} \times t + 1.31745 \times 10^{-5}$ (121) else $NADH = 9.66248 \times 10^{-5} \times e^{-5.01492e-2 \times (t - 9.0)}$ (122)
ATP	If time (t) is less than 9.0 h, then $ATP = -4.98325 \times 10^{-7} \times t^5 + 1.36036 \times 10^{-5} \times t^4 - 1.32756 \times 10^{-4} \times t^3 + 5.58578 \times 10^{-4} \times t^2 - 1.16281 \times 10^{-3} \times t + 4.83734 \times 10^{-3}$ (123) else $ATP = -3.81894 \times 10^{-9} \times t^3 + 3.95288 \times 10^{-7} \times t^2 - 3.73556 \times 10^{-5} \times t + 2.96677 \times 10^{-3}$ (124)
ADP	If time (t) is less than 6.0 h, then

$$ADP = -1.13309 \times 10^{-6} \times t^4 + 2.16624 \times 10^{-5} \times t^3 - 1.31499 \times 10^{-4} \times t^2 +$$
$$2.59245 \times 10^{-4} \times t + 2.98180 \times 10^{-4} \tag{125}$$

else if time (t) is less than 9.0 h, then

$$ADP = -4.55324 \times 10^{-7} \times t^2 + 1.00529 \times 10^{-5} \times t + 2.87751 \times 10^{-4} \tag{126}$$

else $ADP = -6.34321 \times 10^{-9} \times t^3 + 7.40566 \times 10^{-7} \times t^2 - 2.38739 \times 10^{-5} \times$
$$t + 5.00849 \times 10^{-4} \tag{127}$$

AMP

If time (t) is less than 6.0 h, then

$$AMP = 6.3433 \times 10^{-6} \times t^3 - 7.79674 \times 10^{-5} \times t^2 + 2.61211 \times 10^{-4} \times t +$$
$$8.23724 \times 10^{-5} \tag{128}$$

else $AMP = -1.24967 \times 10^{-9} \times t^4 + 1.81254 \times 10^{-7} \times t^3 - 8.32678 \times 10^{-6} \times t^2 +$
$$1.36346 \times 10^{-4} \times t - 3.42878 \times 10^{-4} \tag{129}$$

Values for coenzymes were expressed as functions of time (t) by interpolating measurement data. The variables were sequentially

calculated based on these interpolation equations and used for simulation.
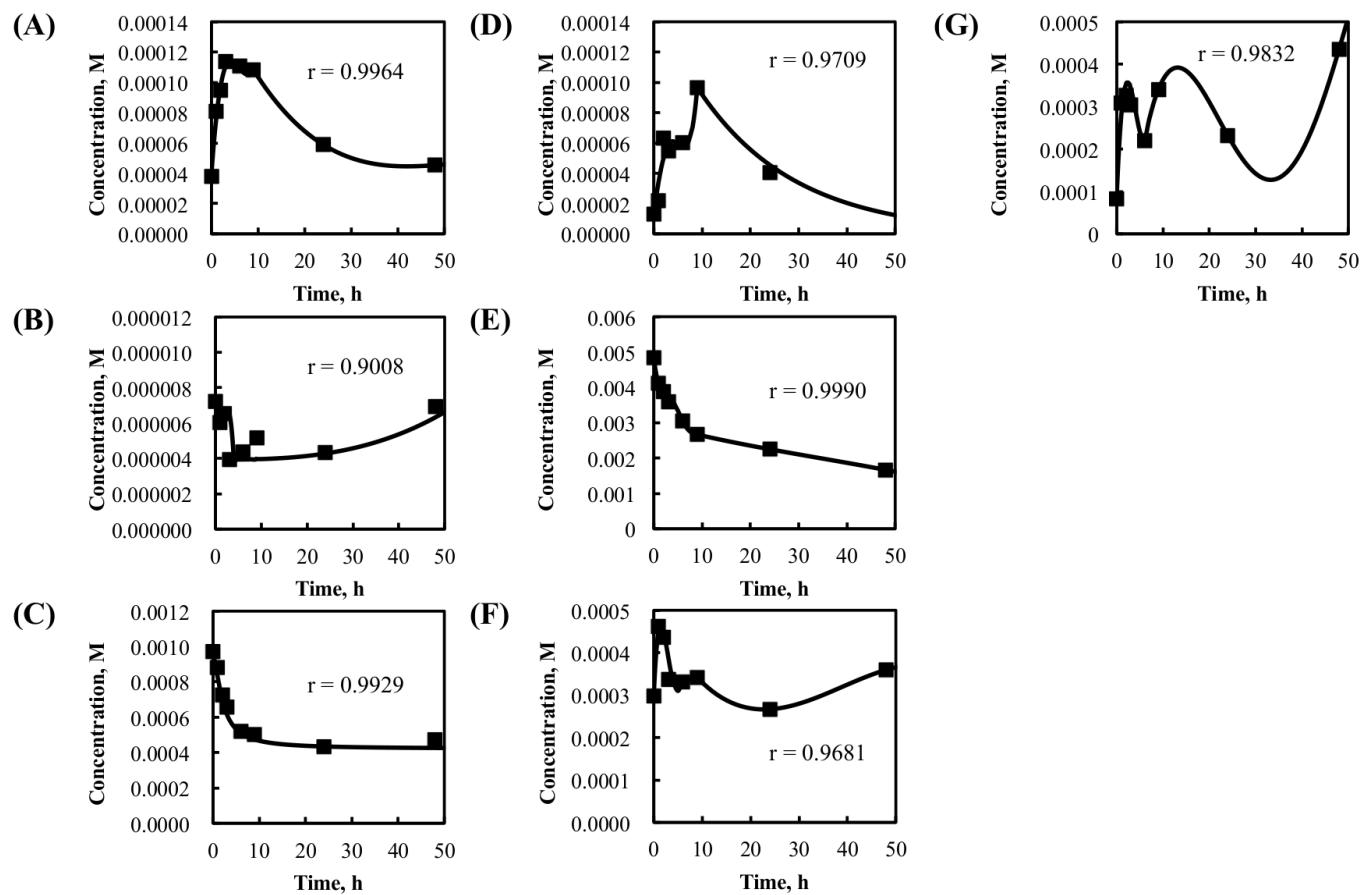
Fig. 3-2 Experimentally obtained time-courses of coenzymes. Symbols show the sampling points of measurement, and curves are interpolated curves based on sampling points. A; NADP, B; NADPH, C; NAD, D; NADH, E; ATP, F; ADP, G; AMP. r in graphs represents correlation coefficients.

Table 3-4 List of kinetic parameters in the constructed model

Reaction No.[*]	Name	Value	Unit	Source
R0	Time_para	1	-	Fixed
R1	Vmax-XU	0.76	M/h	Estimated
	Km-Xylose_ex	0.05	M	Arbitrary
	Alpha	1	-	Arbitrary
R2	Vf-XR	6	M/h	Estimated
	Keq-NADPH	575	-	(Eliasson, A. *et al.*, 2001)
	Keq-NADH	550	-	(Eliasson, A. *et al.*, 2001)
	Ki-NADPH	6.60E-06	M	(Eliasson, A. *et al.*, 2001)
	Km-Xylose	6.77E-02	M	(Eliasson, A. *et al.*, 2001)
	Km-NADPH	3.20E-06	M	(Eliasson, A. *et al.*, 2001)
	Km-NADP+	7.09E-06	M	(Eliasson, A. *et al.*, 2001)
	Km-Xylitol	2.03E+00	M	(Eliasson, A. *et al.*, 2001)
	Ki-NADP+	6.90E-03	M	(Eliasson, A. *et al.*, 2001)
	Ki-Xylitol	4.61E-01	M	(Eliasson, A. *et al.*, 2001)
	Ki-Xylose	5.98E+00	M	(Eliasson, A. *et al.*, 2001)
R3	Vsec-XylitT	0.2	h-1	Estimated
R4	Vup-XylitT	0.2	h-1	Estimated
R5	V1-XDH	0.45	M/h	Estimated
	V2	0.62	M/h	Estimated
	Keq	70	-	Estimated
	Ki-NAD+	4.35E-04	M	(Eliasson, A. *et al.*, 2001)
	Km-Xylitol	1.86E-02	M	(Eliasson, A. *et al.*, 2001)
	Km-NAD+	1.82E-04	M	(Eliasson, A. *et al.*, 2001)
	Km-NADH	8.00E-06	M	(Eliasson, A. *et al.*, 2001)
	Km-Xylulose	9.60E-03	M	(Eliasson, A. *et al.*, 2001)
	Ki-NADH	1.00E-03	M	Estimated
	Ki-Xylulose	2.43E-01	M	(Eliasson, A. *et al.*, 2001)
R6	Vmax-XK	0.5	M/h	Estimated
	Km-Xylulose	3.10E-04	M	(Richard, P. *et al.*, 2000)
	Km-ATP	2.80E-04	M	(Eliasson, A. *et al.*, 2001)
R7	Vf-RPE	3.1	M/h	Estimated
	Vr	8.5	M/h	Estimated
	Km-X5P	1.50E-03	M	Arbitrary
	Km-Ru5P	1.50E-03	M	(Bär, J. *et al.,* 1996)
R8	Vf-RPI	1.5	M/h	Estimated
	Vr	2	M/h	Estimated
	Km-Ru5P	1.00E-03	M	Arbitrary
	Km-R5P	7.40E-04	M	(Noltmann, E.A., 1972)
R9	V1-TK1	0.2	M/h	Estimated
	V2	2	M/h	Estimated
	Keq	Calc	-	Calculated
	Km-R5P	6.00E-05	M	(Yurshev, V.A. *et al.*, 2007)
	Km-X5P	2.10E-05	M	(Sevostyanova, I.A. *et al.*, 2009)

	Km-S7P	4.00E-03	M	(Sprenger, G.A. *et al.*, 1995)
	Km-GAP	4.90E-03	M	(Schenk, G. *et al.*, 1998)
	Ki-X5P	1.00E-02	M	Estimated
	Ki-S7P	1.00E-02	M	Estimated
R10	V1-TA	1.6	M/h	Estimated
	V2	1.2	M/h	Estimated
	Keq	Calc	-	Calculated
	Km-GAP	2.20E-04	M	(Tsolas, O. *et al.*, 1972)
	Km-S7P	1.80E-04	M	(Tsolas, O. *et al.*, 1972)
	Km-F6P	3.20E-04	M	(Tsolas, O. *et al.*, 1972)
	Km-E4P	1.80E-05	M	(Tsolas, O. *et al.*, 1972)
	Ki-S7P	1.00E-03	M	Estimated
	Ki-F6P	1.00E-03	M	Estimated
R11	V1-TK2	0.18	M/h	Estimated
	V2	12	M/h	Estimated
	Keq	Calc	-	Calculated
	Km-E4P	9.00E-05	M	(Schenk, G. *et al.*, 1998).
	Km-X5P	2.10E-05	M	(Sevostyanova, I.A. *et al.*, 2009)
	Km-F6P	1.80E-03	M	(Racker, E., 1961)
	Km-GAP	4.90E-03	M	(Schenk, G. *et al.*, 1998).
	Ki-X5P	1.00E-02	M	Estimated
	Ki-F6P	1.00E-02	M	Estimated
R12	Vf-TK3	0.1	M/h	Estimated
	Vr	0.5	M/h	Estimated
	Keq	Calc	-	Calculated
	Km-E4P	9.00E-05	M	(Schenk, G. *et al.*, 1998).
	Km-S7P	4.00E-03	M	(Sprenger, G.A. *et al.*, 1995)
	Km-F6P	1.80E-03	M	(Racker, E., 1961)
	Km-R5P	6.00E-05	M	(Yurshev, V.A. *et al.*, 2007)
	Ki-S7P	1.00E-03	M	Estimated
	Ki-F6P	1.00E-03	M	Estimated
R13	Vf-GPI	0.7	M/h	Estimated
	Vr	0.265	M/h	Estimated
	Km-F6P	1.50E-04	M	(Noltmann, E.A., 1972).
	Km-G6P	8.00E-04	M	(Noltmann, E.A., 1972).
R14	Vf-G6PDH	0.3	M/h	Estimated
	Vr	Calc	M/h	Calculated
	Keq	Calc	-	Calculated
	Ki-NADP+	2.30E-05	M	Arbitrary
	Km-G6P	2.00E-05	M	Arbitrary
	Km-NADP+	2.00E-06	M	Arbitrary
	Km-NADPH	5.00E-05	M	Arbitrary
	Km-6PGL	7.00E-05	M	Arbitrary
	Ki-NADPH	1.50E-05	M	Arbitrary
	Ki-6PGL	2.00E-06	M	Arbitrary
	Ki-G6P	5.00E-05	M	Arbitrary
R15	Vmax-6PGL	1.2	M/h	Estimated

	Km-6PGL	1.00E-04	M	Arbitrary
R16	Vf-6PGDH	3	M/h	Estimated
	Vr	Calc	M/h	Calculated
	Keq	Calc	M	Calculated
	Ki-NADP+	3.40E-05	M	Arbitrary
	Km-6PG	6.80E-05	M	(Rendina, A.R. *et al.*, 1984).
	Km-NADP+	3.30E-05	M	(Rendina, A.R. *et al.*, 1984).
	Ki-NADPH	3.50E-04	M	Arbitrary
	Km-Ru5P	1.00E-03	M	(Berdis, A.J. *et al.,* 1993)
	Ki-Ru5P	5.00E-03	M	Arbitrary
	Km-CO2	5.00E-02	M	(Berdis, A.J. *et al.,* 1993)
	6PGDH_Km-NADPH	5.00E-04	M	Arbitrary
	Ki-6PG	6.20E-05	M	Arbitrary
	Ki-CO2	1.00E-01	M	Arbitrary
R17	Vmax-PFK	26	M/h	Estimated
	Km-ATP	3.10E-05	M	(Hofmann, E. *et al.,* 1998)
	Ki-ADP	2.50E-04	M	(Rizzi, M. *et al*., 1997)
	Km-F6P	2.00E-04	M	(Hofmann, E. *et al.,* 1998)
	Ki-PEP	3.50E-03	M	Estimated
	KmB-ADP	5.00E-04	M	Estimated
	KmB-AMP	2.00E-04	M	Estimated
	KmA-ADP	2.00E-04	M	(Hofmann, E. *et al.,* 1982)
	KmA-AMP	1.50E-05	M	(Hofmann, E. *et al.,* 1982)
	L-pfk	4357	-	(Rizzi, M. *et al*., 1997)
	n-pfk	8	-	(Hofmann, E. *et al.,* 1982)
R18	Vf-ALDo	400	M/h	Estimated
	Vr	Calc	M/h	Calculated
	Keq	5.90E-04	M	Estimated
	Km-FBP	3.00E-04	M	(Teusink, B. *et al.*, 2000)
	Km-DHAP	2.40E-03	M	(Teusink, B. *et al.*, 2000)
	Km-GAP	2.00E-03	M	(Teusink, B. *et al.*, 2000)
	Ki-GAP	1.00E-02	M	(Teusink, B. *et al.*, 2000)
R19	Vf-TPI	180	M/h	Estimated
	Vr	Calc	M/h	Calculated
	Km-DHAP	1.23E-03	M	(Krietsch, W.K.G., 1975).
	Km-GAP	1.27E-03	M	(Krietsch, W.K.G., 1975).
R20	Vf-GAPDH	7.5	M/h	Estimated
	Vr	Calc	M/h	Calculated
	Keq	Calc	M-1	Calculated
	Ki-NAD+	5.00E-04	M	Arbitrary
	Ki-GAP	1.00E-04	M	Arbitrary
	Km-Pi	1.50E-03	M	(Byers, L.D., 1982).
	KmGAP	6.00E-04	M	(Byers, L.D., 1982).
	Km-NAD+	1.00E-04	M	(Byers, L.D., 1982).
	Km-13BPG	1.00E-05	M	(Hynne, F. *et al.,* 2001)
	Km-NADH	5.00E-05	M	Arbitrary
	Ki-NADH	1.20E-04	M	Arbitrary
	Ki-Pi	4.30E-03	M	Arbitrary

	Ki-13BPG	1.00E-05	M	Arbitrary
R21	Vf-PGK	3.8	M/h	Estimated
	Vr	0.245	M/h	Estimated
	Keq	Calc	-	Calculated
	Ki-ADP	2.20E-04	M	(Larsson-Raźnikiewicz, M. *et al.*, 1971)
	Km-BPG	3.00E-06	M	(Teusink, B. *et al.*, 2000)
	Km-ADP	2.00E-04	M	(Teusink, B. *et al.*, 2000)
	Km-3PG	5.30E-04	M	(Teusink, B. *et al.*, 2000)
	Km-ATP	3.00E-04	M	(Teusink, B. *et al.*, 2000)
	Ki-ATP	7.00E-04	M	Arbitrary
R22	Vmax-PGM	6.5	M/h	Estimated
	Keq	0.19	-	(Teusink, B. *et al.*, 2000)
	Km-3PG	6.50E-04	M	(21)
	Ki-2PG	4.10E-05	M	(21)
R23	Vf-ENO	2	M/h	Estimated
	Vr	0.11056	M/h	Estimated
	Km-2PG	4.00E-05	M	(Teusink, B. *et al.*, 2000)
	Km-PEP	5.00E-04	M	(Teusink, B. *et al.*, 2000)
R24	Vmax-PYK	1500	M/h	Estimated
	Ki-PEP	6.00E-04	M	(Rizzi, M. *et al*., 1997)
	n-pk	4	-	(Rizzi, M. *et al*., 1997)
	Km-PEP	6.00E-04	M	(Rizzi, M. *et al*., 1997)
	L-pk	100	-	(Rizzi, M. *et al*., 1997)
	Ki-ATP	2.00E-03	M	(Rizzi, M. *et al*., 1997)
	Ka-FBP	3.90E-03	M	(Rizzi, M. *et al*., 1997)
	Ka-AMP	2.00E-04	M	(Chassagnole, C. *et al.*, 2002)
	Km-ADP	6.00E-04	M	(Rizzi, M. *et al*., 1997)
	pYK_Ka-xylose	5.00E-03	M	Arbitrary
	n	1	-	Arbitrary
R25	Vmax-PDC	20	M/h	Estimated
	A	2.73E-06	M2	(Sergienko, E.A *et al.*, 2001).
	B	1.37E-03	M	(Sergienko, E.A *et al.*, 2001).
	Ki-Pyr	2.64E-01	M	(Sergienko, E.A *et al.*, 2001).
R26	Vf-ADH	150	M/h	Estimated
	Vr	Calc	M/h	Calculated
	Keq	Calc	-	Calculated
	Ki-NADH	3.10E-05	M	Estimated
	Km-Aldehyde	1.11E-03	M	(Leskovac, V. *et al.*, 2002)
	Km-NADH	1.10E-04	M	(Leskovac, V. *et al.*, 2002)
	Km-NAD+	1.70E-04	M	(Leskovac, V. *et al.*, 2002)
	Km-Ethanol	1.70E-02	M	(Leskovac, V. *et al.*, 2002)
	Ki-NAD+	9.20E-04	M	Estimated
	Ki-Ethanol	9.00E-02	M	Estimated

	Ki-Aldehyde	1.10E-03	M	Estimated
	theta_NADH	1.00E+00	-	Arbitrary
	Vf-ADH-NADPH	0.5	M/h	Estimated
	Vr	Calc	M/h	Calculated
	Keq	Calc	-	Calculated
	Ki-NADPH	3.10E-05	M	Estimated
	Km-Aldehyde	1.11E-03	M	(Leskovac, V. *et al.*, 2002)
	Km-NADPH	1.10E-05	M	(Larroy, C. *et al.,* 2002)
	Km-NADP+	1.70E-05	M	Estimated
	Km-Ethanol	1.70E-02	M	(Leskovac, V. *et al.*, 2002)
	Ki-NADP+	9.20E-05	M	Estimated
	Ki-Ethanol	9.00E-02	M	Estimated
	theta_NADPH	1.00E-03	-	Arbitrary
	Ki-Aldehyde	1.10E-03	M	Estimated
R27	Vt-EtOH-T-Sec	100	M/h	Arbitrary
R28	Vt-EtOH-T-Syn	100	M/h	Arbitrary
R29	Vf-G3PDH	2	M/h	Estimated
	Vr	Calc	M/h	Calculated
	Keq	35000	-	Estimated
	Ki-NADH	3.40E-05	M	Arbitrary
	Km-DHAP	1.60E-03	M	Arbitrary
	Km-NADH	1.30E-04	M	Arbitrary
	Km-G3P	0.115	M	Arbitrary
	Km-NAD+	3.00E-04	M	Arbitrary
	Ki-Pi	7.30E-04	M	Arbitrary
	Kii-Pi	7.30E-04	M	Arbitrary
	Kii2-Pi	7.30E-04	M	Arbitrary
	Kii-NAD+	1.30E-04	M	Arbitrary
	Ki-G3P	0.05	M	Arbitrary
R30	Vf-GUT2	5	M/h	Estimated
	Vr	2.00E-01	M/h	Estimated
	Keq	Calc	-	Calculated
	Km-G3P	3.40E-02	M	(Pahlman, I.L. *et al.*, 2002)
	Km-Q	1.10E-04	M	Arbitrary
	Km-DHAP	5.00E-03	M	Arbitrary
	Km-QH2	6.00E-04	M	Arbitrary
	Ki-Q	3.00E-05	M	Arbitrary
	Ki-DHAP	1.00E-04	M	Arbitrary
R31	Vmax-GPP	15	M/h	Estimated
	Km-G3P	3.50E-03	M	(Norbeck, J. *et al.,* 1996)
R32	Vmax-GUT1	0.14	M/h	Estimated
	Ki-Glycerol	6.00E-02	M	Arbitrary
	Km-ATP	4.00E-05	M	Arbitrary
	Km-Glycerol	2.01E-02	M	Arbitrary
R33	Vmax-Glycer-PD	0.2	M/h	Estimated
R34	Vmax-Glycer-SP	1.00E-05	M/h	Estimated
	Kt	5.00E-02	M	Arbitrary
R35	Vf-ALDH	80	M/h	Estimated

	Vr	Calc	M/h	Calculated
	Keq	Calc	-	Calculated
	Ki-NADP+	7.43E-05	M	Arbitrary
	Km-Aldehyde	3.50E-05	M	(Seegmiller, J.E., 1953)
	Km-NADP+	1.40E-05	M	(Seegmiller, J.E., 1953)
	Km-NADPH	3.00E-06	M	Arbitrary
	Km-Acetate	1.00E-04	M	Arbitrary
	Ki-NADPH	1.20E-05	M	Arbitrary
	Ki-Acetate	1.00E-03	M	Arbitrary
	Ki-Aldehyde	2.00E-04	M	Arbitrary
	Vf-ALDH_NADH	0.05	M/h	Estimated
	Vr	Calc	M/h	Calculated
	Keq	Calc	-	Calculated
	Ki-NAD+	4.30E-04	M	Arbitrary
	Km-Aldehyde	1.00E-05	M	(Wang, X. *et al.*, 1998)
	Km-NAD+	1.10E-03	M	(Wang, X. *et al.*, 1998)
	Km-NADH	3.00E-05	M	Arbitrary
	Km-Acetate	1.00E-04	M	Arbitrary
	Ki-NADH	1.20E-04	M	Arbitrary
	Ki-Acetate	1.00E-03	M	Arbitrary
	Ki-Aldehyde	4.00E-04	M	Arbitrary
R36	Vsec-Ace	50	h-1	Estimated
R37	Vup-Ace	35	h-1	Estimated
R38	Vf-Acs2	0.2	M/h	Estimated
	Ki-ATP	1.20E-03	M	Arbitrary
	Km-Acetate	8.80E-03	M	(van den Berg, M.A. *et al.*, 1996)
	Km-CoA	3.50E-05	M	(Frenkel, E.P. *et al.,* 1981)
	Km-ATP	1.60E-04	M	(Guranowski, A. *et al.,* 1994)
	Kii-Xylose_ex2	1	M	Arbitrary
	n-Acs2-Xyl2	10	-	Arbitrary
R39	Vm-pyr-T	5	h-1	Estimated
R40	Vm-oaa-T	6.5	h-1	Estimated
R41	V1-PYC	169	M/h	Estimated
	V2	11.1	M/h	Estimated
	Keq	Calc	-	Calculated
	Ki-ATP	1.50E-05	M	Arbitrary
	Ki-CO2	5.60E-05	M	Arbitrary
	Km-Pyr	5.00E-04	M	(Branson, J.P. *et al*., 2002)
	Km-CO2	1.36E-03	M	(Branson, J.P. *et al*., 2002)
	Km-ATP	5.60E-05	M	(Branson, J.P. *et al*., 2002)
	Ki-ADP	8.90E-04	M	Arbitrary
	Km-Pi	1.25E-03	M	Arbitrary
	Ki-Pi	1.00E-03	M	Arbitrary
	Km-OAA	1.30E-05	M	Arbitrary
	Km-ADP	4.50E-04	M	Arbitrary
	Ki-Pyr	2.50E-04	M	Arbitrary

	Ki-OAA	Calc	M	Calculated
R42	Vf-PCK	1.50E-02	M/h	Estimated
	Vr	0.5	M/h	Estimated
	Keq	Calc	M	Calculated
	Ki-ATP	1.50E-06	M	Arbitrary
	Km-OAA	1.30E-04	M	(Perez, E. *et al.*, 2010)
	Km-ATP	3.00E-05	M	(Perez, E. *et al.*, 2010)
	Km-PEP	3.07E-04	M	(Cristina Ravanal, M. *et al.*, 2004)
	Km-ADP	3.40E-05	M	(Cristina Ravanal, M. *et al.*, 2004)
	Km-CO2	1.70E-02	M	(Sepulveda, C. *et al.*, 2010)
	Kii-ADP	2.00E-05	M	Arbitrary
	Kii-PEP	4.00E-05	M	Arbitrary
	Ki-ADP	1.00E-05	M	Arbitrary
	Kii-Xyl	0.001	M	Arbitrary
R43	mmax	0.45	h-1	Estimated
	Ks-Xylose	0.06	M	Estimated
	Kis-Xylose	100	M	Estimated
	Xinit-biomass	12.10198	g/L	From experiment
	Xmax-biomass	12.5	g/L	Arbitrary
	n-growth	30	-	Arbitrary

*Ri (i = 1, 2, …, 43) represent reactions in Fig. 3-1 except for R0 (time).

Table 3-5 Initial values of dependent variables

Name	Initial value	Unit
Time	0	h
Xylose_ex	0.365338373	M
Xylose_cyt	1.00E-10	M
Xylitol_cyt	1.00E-10	M
Xylitol_ex	1.00E-10	M
Xylulose	1.00E-10	M
X5P	6.69E-04	M
Ru5P	1.79E-04	M
R5P	1.10E-04	M
S7P	6.82E-04	M
GAP	5.34E-05	M
E4P	1.00E-10	M
F6P	2.27E-04	M
G6P	6.99E-04	M
PGL	1.00E-10	M
6PG	3.26E-06	M
FBP	2.41E-04	M
DHAP	4.42E-04	M
13BPG	1.00E-04	M
3PG	2.15E-03	M
2PG	2.15E-03	M
PEP	2.75E-04	M
PYR_cyt	5.20E-04	M
Acetaldehyde_cyt	0	M
EtOH_cyt	0	M
EtOH_ex	0	M
G3P	0	M
Glycerol-cy	0	M
Glycerol-ex	0	M
Acetate_cyt	0	M
Acetate_ex	0	M
AceCoA_cyt	7.64E-05	M
OAA_cyt	6.75E-04	M
NADP+_cyt	3.78E-05	M
NADPH_cyt	7.22E-06	M
NAD+_cyt	9.72E-04	M
NADH_cyt	1.32E-05	M
ATP_cyt	4.84E-03	M
ADP_cyt	2.98E-04	M
AMP_cyt	8.24E-05	M
Quinone_	1.00E-04	M
Quinol	5.00E-05	M
Pi	6.00E-03	M
PPi	0	M

CO2	1.00E-05	M
CoA_cyt	3.27E-05	M
Biomass	12.10198	g/L

3.3 Results

3.3.1 Development of the kinetic simulation model of the ethanol production pathway

Batch cultures of strain K7-XYL were carried out in 500-mL baffled shaken flasks containing YP medium and an initial xylose concentration of 50 g/L to obtain experimental data in preparation for the development of the kinetic simulation model of ethanol production. The experimental time course data and simulation results for xylose, ethanol, glycerol, xylitol, acetate and cell growth are shown in Fig. 3-3 and Fig. 3-4. The xylose was depleted after 48 h and the ethanol concentration reached 12.6 g/L at 24 h. Cell growth increased from 12.1 g-dry cell/L to 23.9 g-dry cell/L approximately twice as much as in 48 h.

The simulation was conducted using an original program developed in the language C. The metabolic concentration data and the initial metabolic state were determined based on the data acquired in this study as shown in Table 3-5. The simulation results of the model were evaluated by comparison with the time course of the experimental results in Fig. 3-3 and the correlation coefficient between the experimental values and the simulation values. The correlation coefficients for each metabolite were calculated and shown in Table 3-6. It was judged that the simulation results were coincident with the experimental data, so sensitivity analysis using this mathematical model was conducted.

3.3.2 Estimated bottleneck reactions in the ethanol production pathway from xylose

The sensitivity analysis results and genetic manipulation strategies were shown in Table 3-7. Those exhibiting a sensitivity of 10% or more and expected to have high improvement effects were extracted. The factor in this simulation that had the biggest effect on ethanol production was upregulation of XDH (R5 in Fig. 3-1). The simulation suggested

70

that upregulation of XDH would improve xylitol use and result in higher ethanol production.

The second ranked reaction that had an impact on ethanol production was downregulation of xylose uptake (R1 in Fig. 3-1). The simulation suggested that downregulation of xylose uptake would result in higher ethanol production.

The third ranked enzyme reaction that had an impact on ethanol production was that upregulation of alcohol dehydrogenase (ADH) (R26 in Fig. 3-1). The simulation suggested upregulation of ADH would improve the metabolism of acetaldehyde to ethanol and result in higher ethanol production.

The fourth ranked enzyme reaction that had an impact on ethanol production was downregulation of acetaldehyde dehydrogenase (ALDH) (R35 in Fig. 3-1). The simulation suggested downregulation of ALDH would reduce the metabolism of acetaldehyde to acetate and result in higher ethanol production.

The fifth ranked reaction that had an impact on ethanol production was downregulation of glycerol 3–phosphate dehydrogenase (G3PDH) (R29 in Fig. 3-1). The simulation suggested downregulation of G3PDH would reduce the metabolism of glycerol 3–phosphate to dihydroxyacetone phosphate, which is metabolized to glycerol and result in higher ethanol production.

The sixth ranked reaction that had an impact on ethanol production was downregulation of passive diffusion of ethanol from extracellular to intracellular (cytosol) (R28 in Fig. 3-1). The simulation suggested downregulation of passive diffusion of ethanol result in higher ethanol production.
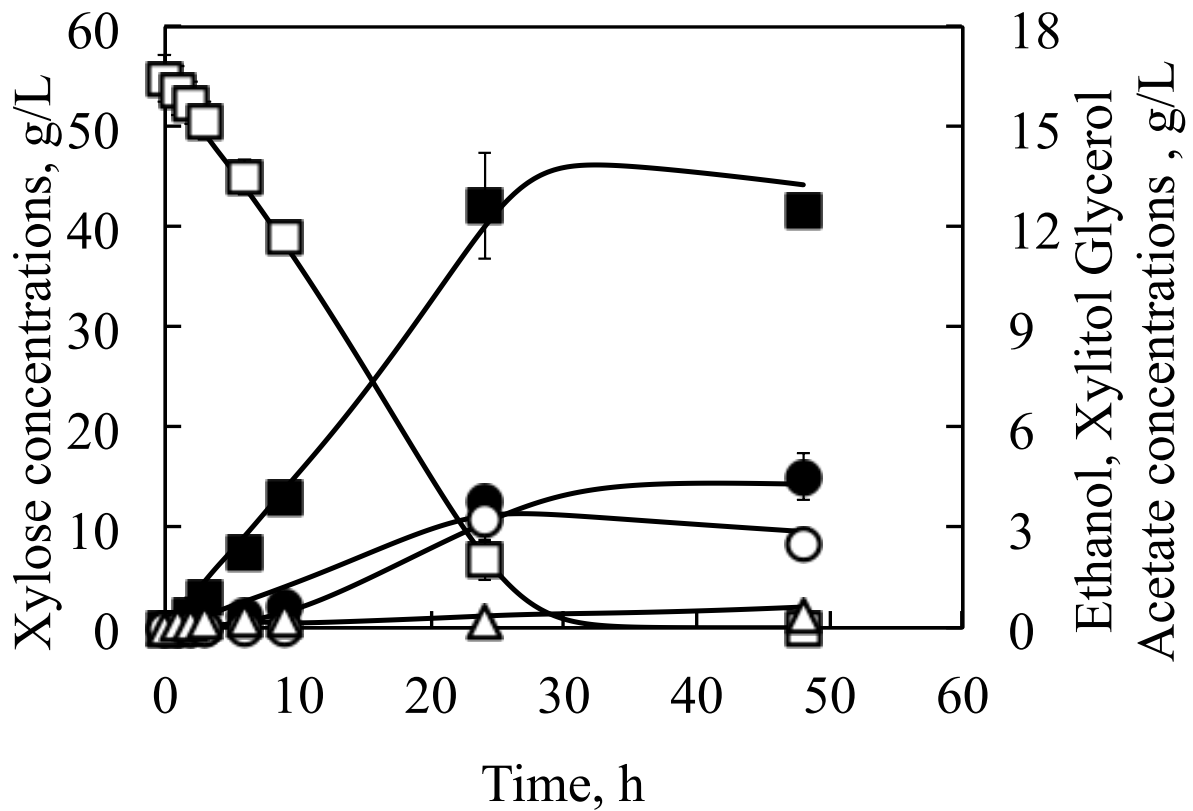
Fig. 3-3 Experimental time course data and simulation results (Xylose, Ethanol, Xylitol,

Glycerol and Acetate) with initial xylose concentration 50 g/L

The symbols show experimental data and the lines indicate simulation results. Experimental

results were based on two replications. Data points represent the average of two experiments

and error bars indicate standard deviation.

Xylose, open squares; Ethanol, closed squares; Xylitol, open circles; Glycerol, closed circles;

Acetate, open triangles.
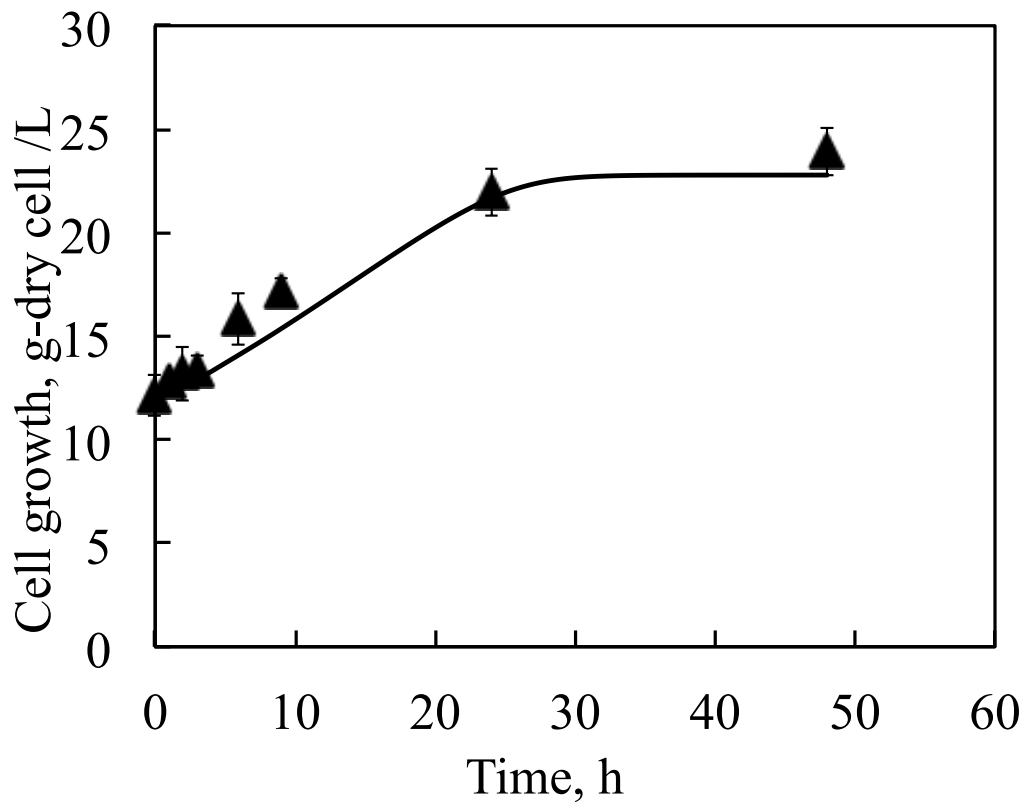
Fig. 3-4 Experimental time course data and simulation results (Biomass) with initial xylose

concentration 50 g/L

The symbols show experimental data and the lines indicate simulation results. Experimental

results were based on two replications. Data points represent the average of two experiments

and error bars indicate standard deviation.

Biomass, closed triangles.

Table 3-6 Correlation coefficients between experimental data and simulation results for each

metabolite

Metabolite	Correlation coefficients
Xylose	0.999
Xylitol	0.953
Glycerol	0.997
Ethanol	0.999
Acetate	0.927
Biomass	0.991
Overall	0.978

Table 3-7 Top six-ranked manipulation strategies for higher production of ethanol.

Rank	Reaction step [a]	Strategy	Enzyme [b]	Sensitivity, % [c]	Reaction
1	R5	Up	XDH	16.4	$Xylitol_{cyt} + NAD^+$ $\Leftrightarrow Xylulose + NADH$
2	R1	Down	Xylose uptake	13.3	$Xylose_{ex} \rightarrow Xylose_{cyt}$
3	R26	Up	ADH	13.2	$Acetaldehyde + NAD(P)H$ $\rightarrow Ethanol_{cyt} + NAD(P)^+$
4	R35	Down	ALDH	13.1	$Acetaldehyde + NAD(P)^+$ $\rightarrow Acetate_{cyt} + NAD(P)H$
5	R29	Down	G3PDH	12.2	Dihydroxyacetone phosphate $+ NADH$ $\rightarrow$ Glycerol 3-phosphate $+ NAD^+$
6	R28	Down	Passive diffusion	11.2	$Ethanol_{ex} \rightarrow Ethanol_{cyt}$

[a] Reaction step corresponds to numbering in Fig. 3-1.

[b] Enzymes are abbreviated as follows: XDH, Xylose dehydrogenase; ADH, Alcohol dehydrogenase; ALDH, Acetaldehyde dehydrogenase; G3PDH, Glycerol 3–phosphate dehydrogenase.

[c] Sensitivity indicates the endpoint deviation (ED) of ethanol at 48 h, when a 100% increase to each respective kinetic parameter in the rate equations in the model was applied.

3.4 Discussions

It was analyzed that an ethanol production pathway of *S. cerevisiae* involving the endogenous xylose-assimilating genes *GRE3* and *SOR1* (i.e., a self-cloning xylose-using *S. cerevisiae*) by construction of a kinetic simulation model of the ethanol producing pathway and undertaking sensitivity analysis in that model. Then metabolic bottlenecks in the pathway were estimated

As shown in Table 3-7, the simulation predicted that upregulation of XDH (R5 in Fig. 3-1) would improve xylitol use and result in higher ethanol production. Accumulation of xylitol is one of the biggest problems from the beginning of constructing xylose-using *S. cerevisiae* and has not been solved yet (Kötter, P. and Ciriacy, M., 1993; Ho, N. W., Chen, X. and Brainard, A. P., 1998; van Vleet, J.H. and Jeffries, T. W., 2009; Kim, S. R.. *et al.*, 2012; Moysés, D. N. *et al.*, 2016; Jo, J. H. *et al.*, 2017), although the limiting step was identified; XR preferentially uses NADPH as a cofactor, XDH exclusively uses NAD^+ (Hahn-Hägerdal, B. *et al.*, 2007). In order to add xylose-assimilating ability to the yeast, it was activated that XR (R2 in Fig. 3-1), XDH (R5 in Fig. 3-1) and XKS (R6 in Fig. 3-1) with a *PGK1* promoter and terminator in this study. Since the *PGK1* promoter is one of the strongest promoters in *S. cerevisiae* (Partow, S. *et al.*, 2010), it was thought that further upregulation of XDH would be difficult.

The second ranked reaction that had an impact on ethanol production in the simulation was downregulation of xylose uptake (R1 in Fig. 3-1). A xylose-specific transporter is not found in *S. cerevisiae*, and it is believed that non-specific hexose transporters transport xylose with low transport rate (Lee, W. J. *et al*., 2002; Saloheimo, A. *et al.*, 2007). Thus, downregulation of xylose uptake is not feasible within the constraints of this experiments (self-cloning xylose-using *S. cerevisiae*). In addition, the slow xylose uptake of *S.*

cerevisiae has been mentioned as problem from the past (van Vleet, J.H. and Jeffries, T. W., 2009; Moysés, D. N. *et al.*, 2016). Considering the previous study, downregulation of xylose uptake is not considered to be a reasonable modification. The reason why such an irrational result was obtained may be due to the structure of the model. Since the xylose taken into cells (Xylose$_{cyt}$ in Fig. 3-1) was a substrate for biomass synthesis in this model, so it determined the amount of xylose used for ethanol production that the metabolic balance between cell growth (R43 in Fig. 3-1) and xylose reduction (R2 in Fig. 3-1). Hence in order to decrease cell growth, it was thought that downregulation of xylose uptake was listed in manipulation strategies for higher production of ethanol.

The third ranked enzyme reaction that had an impact on ethanol production in the simulation was upregulation of ADH (R26 in Fig. 1). The simulation suggested that if ADH were upregulated twofold, the ethanol productivity would increase by about 13%. This manipulation strategy is feasible and logically congruous.

The fourth and fifth ranked enzyme reaction that had an impact on ethanol production in the simulation was upregulation of ALDH (R35 in Fig. 1) and downregulation of G3PDH (R29 in Fig. 3-1). These manipulation strategies are also feasible and logically congruous.

The sixth ranked reaction that had an impact on ethanol production was downregulation of passive diffusion of ethanol from extracellular to intracellular (cytosol) (R28 in Fig. 3-1). The simulation suggested downregulation of passive diffusion of ethanol result in higher ethanol production. Although this manipulation strategy is also considered to be logically congruous, feasibility is low because it is difficult to control passive diffusion of ethanol by genetic manipulation.

77

CHAPTER 4

Evaluation of *ADH1* overexpression effect on ethanol productivity in self-cloning xylose-using *S. cerevisiae*

4.1 Introduction

There are two approaches to improve the ethanol productivity of self-cloning xylose-using *S. cerevisiae.* One is fermentation engineering technique such as optimization of medium (carbon sources, nitrogen sources and trace metals) and culture conditions (pH, temperature, dissolved oxygen concentration and pressure). The other is genetic engineering technique such as overexpression of genes in the main product generation pathway, and suppression or disruption of genes in the byproduct producing pathway. Although both approaches are thought to be effective, in ethanol production from cellulosic biomass, there is not much room for improving ethanol productivity from the viewpoint of fermentation. This is because the medium is limited to biomass hydrolysate, and additives are not added to keep costs down. Consequently, it is more important to develop yeast with improved ethanol productivity by genetic engineering.

On one hand, since it takes time to perform one genetic manipulation, to repeat manipulating genes without any information is time-consuming process. It is considered that the ethanol productivity of yeast can be increased efficiently by selecting genes to be manipulated based on computer simulation as shown in Chapter 3. Six gene manipulation strategies were presented in Chapter 3: upregulation of XDH (R5 in Fig. 3-1), downregulation of xylose uptake (R1 in Fig. 3-1), upregulation of ADH (R26 in Fig. 3-1) downregulation of ALDH (R35 in Fig. 3-1), downregulation of G3PDH (R29 in Fig. 3-1) and downregulation of passive diffusion of ethanol (R28 in Fig. 3-1). Upregulation of ADH, downregulation of ALDH, and downregulation of G3PDH are thought to be logically correct and can be implemented within the constraints of self-cloning. In this chapter, the overexpression of *ADH1* that encodes ADH, which has highest sensitivity among them and is

expected to improve ethanol productivity was investigated in both flask culture and 5-L scale jar fermenter culture.

4.2 Materials and methods

4.2.1 Plasmid and strain construction

The K7-XYL was used as a host strain for overexpression of *ADH1* gene. Construction of the *ADH1* overexpression vector was as follows. A *PGK1* promoter and terminator, and *ADH1* were respectively amplified from the genomic DNA of the industrial Sake yeast *S. cerevisiae* K7. The three fragments were ligated and introduced into the *Sma*I site of pAUR135 (Takara, Shiga, Japan) to create pAUR135-ADH1. pAUR135-ADH1 was digested with *Stu*I and transformed into K7-XYL to produce strain K7-XYL-ADH1. Yeast transformation was carried out by the lithium acetate method (Giets, D. *et al*., 1992). For selection of transformants, 0.5 mg/L aureobasidin A (Takara) was added to YPD agar plates. Synthetic complete (SC) medium containing 6.7 g/L yeast nitrogen base was used for yeast transformants selection. *Escherichia coli* JM109 was used for cloning of plasmids and grown at 37°C with shaking at 140 rpm in LB medium (yeast extract 5 g/L, tryptone 10 g/L, NaCl 5g/L).

4.2.2 Conditions for flask culture

For precultivation of yeast cells, YP medium (yeast extract 10 g/L, peptone 20 g/L) with glucose 20 g/L was used. Batch fermentations were carried out in 500-mL baffled shaken flasks, with a filtered silicone plug to avoid ethanol evaporation, at 30°C with shaking at 140 rpm in YP medium (pH 5.0). Each flask contained the indicated amount of sugars as

the carbon source(s) (xylose 50 g/L, or glucose 80 g/L and xylose 50 g/L). The initial cell concentration was 2×10^8 cells/mL for flask fermentation. The sampling frequencies were 0, 6, 24, 30, 48, 72 h for xylose culture and 0, 6, 24, 30, 48, 72, 96 h for glucose and xylose culture. The sampling volumes were 0.6 mL.

4.2.3 Conditions for 5-L jar culture

For precultivation of yeast cells, YP medium with glucose 20 g/L was used. A 5-L scale jar fermenter (ABLE, Tokyo, Japan) with 3 L working volume was also used for batch fermentation to control the dissolved oxygen concentration at 0.2 ppm. It was used that YP medium containing 80 g/L glucose and 50 g/L xylose and this is a typical compositions of biomass hydrolysate. The temperature was maintained at 30°C, and the pH value were controlled at 5.0 through addition of 5 M NaOH. The culture was sparged with air at 0.016 vvm. The initial cell concentration was 1×10^7 cells/mL for jar fermentation. The sampling frequency was 0, 2, 4, 6, 8, 22, 24, 28, 30, 48 h and the sampling volumes were 0.6 mL.

4.2.4 Extracellular metabolite analysis

Concentrations of glucose, xylose, ethanol, glycerol, xylitol, and acetate in culture supernatants were determined with a high-performance liquid chromatography system (Shimadzu, Kyoto, Japan) equipped with a SUGAR SP0810 column (Shodex, Tokyo, Japan) using water as the mobile phase at a flow rate of 0.8 mL/min and 80°C.

4.3 Results

4.3.1 Effect of *ADH1* overexpression in xylose and glucose/xylose mixed medium in flask

Initially, flask-scale cultures of strains K7-XYL and K7-XYL-ADH1 were grown in 500-mL baffled shaken flasks containing YP medium with an initial xylose concentration of 50 g/L (Fig. 4-1 and Fig. 4-2). Although K7-XYL-ADH1 converted xylose to ethanol slightly slower than K7-XYL (K7-XYL 1.31 g/L/h, K7-XYL-ADH1 1.08 g/L/h), the ethanol productivity of strain K7-XYL-ADH1 was higher than that of K7-XYL (K7-XYL 12.5 g/L, K7-XYL-ADH1 13.8 g/L). Glycerol production by K7-XYL-ADH1 increased by 0.73 g/L, and xylitol production of K7-XYL-ADH1 decreased by 4.01 g/L relative to strain K7-XYL respectively. The productivity of xylitol in Fig. 3-3 was about half of that in Fig. 4-1, because the amount of liquid in the flask used to generate the data in Fig. 3-3 became less than that in the flask used for Fig. 4-1, so conditions in Fig. 3-3 were more aerobic and accumulation of xylitol was suppressed. This was because, in order to obtain data for model construction, the sampling frequency in Fig. 3-3 was higher than that in Fig. 4-1. Furthermore, for the collection of intracellular metabolite data, the sampling amount in Fig. 3-3 was large. It was difficult to reproduce reduction of liquid volume by sampling in the simulation. The ethanol yield from the initial sugars was 46.5% for strain K7-XYL and 51.1% for K7-XYL-ADH1, which indicated that overexpression of *ADH1* increased the ethanol yield in xylose medium.

Second, the effect of *ADH1* overexpression in medium containing a mixture of glucose and xylose was evaluated. It was known that xylose-using K7 consumes glucose first, and then ferments xylose after depletion of glucose (Konishi, J. *et al*., 2015). Since K7-XYL does not simultaneously consume glucose and xylose, it was expected that the effect of *ADH1* overexpression would be observed in glucose and xylose mixed medium during the

82

xylose consumption phase. Fig. 4-3 and Fig. 4-4 show culture parameters for flask scale cultures of K7-XYL and K7-XYL-ADH1 with YP medium containing glucose (initial concentration 80 g/L) and xylose (initial concentration 50 g/L), representing the typical sugar composition of cellulosic biomass hydrolysate. Both strains rapidly fermented glucose to ethanol and then fermented xylose. As observed in xylose medium, the xylose consumption rate of K7-XYL-ADH1 was slower than that of K7-XYL. However, the ethanol productivity of K7-XYL-ADH1 was almost the same as that of K7-XYL in the glucose and xylose mixed-medium (K7-XYL 46.3 g/L, K7-XYL-ADH1 45.9 g/L). These data indicated that, unlike in xylose medium, overexpression of *ADH1* did not increase the ethanol yield in glucose and xylose mixed medium in flask-scale culture.
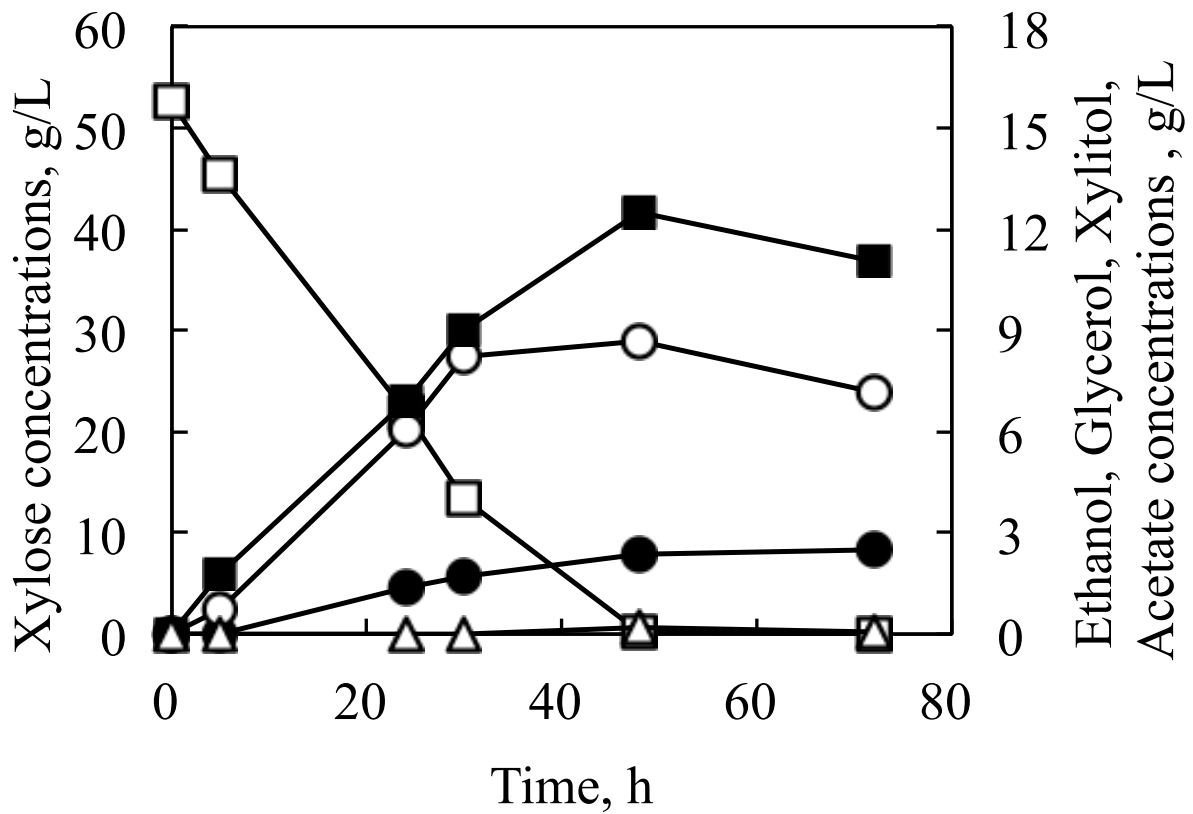
Fig. 4-1 Fermentation profiles of flask cultures of strains K7-XYL in YP medium containing

50 g/L xylose as the carbon sources.

Results were based on two replications. Data points represent the average of two experiments

and error bars indicate standard deviation.

Xylose, open squares; Ethanol, closed squares; Xylitol, open circles; Glycerol, closed circles;

Acetate, open triangles.
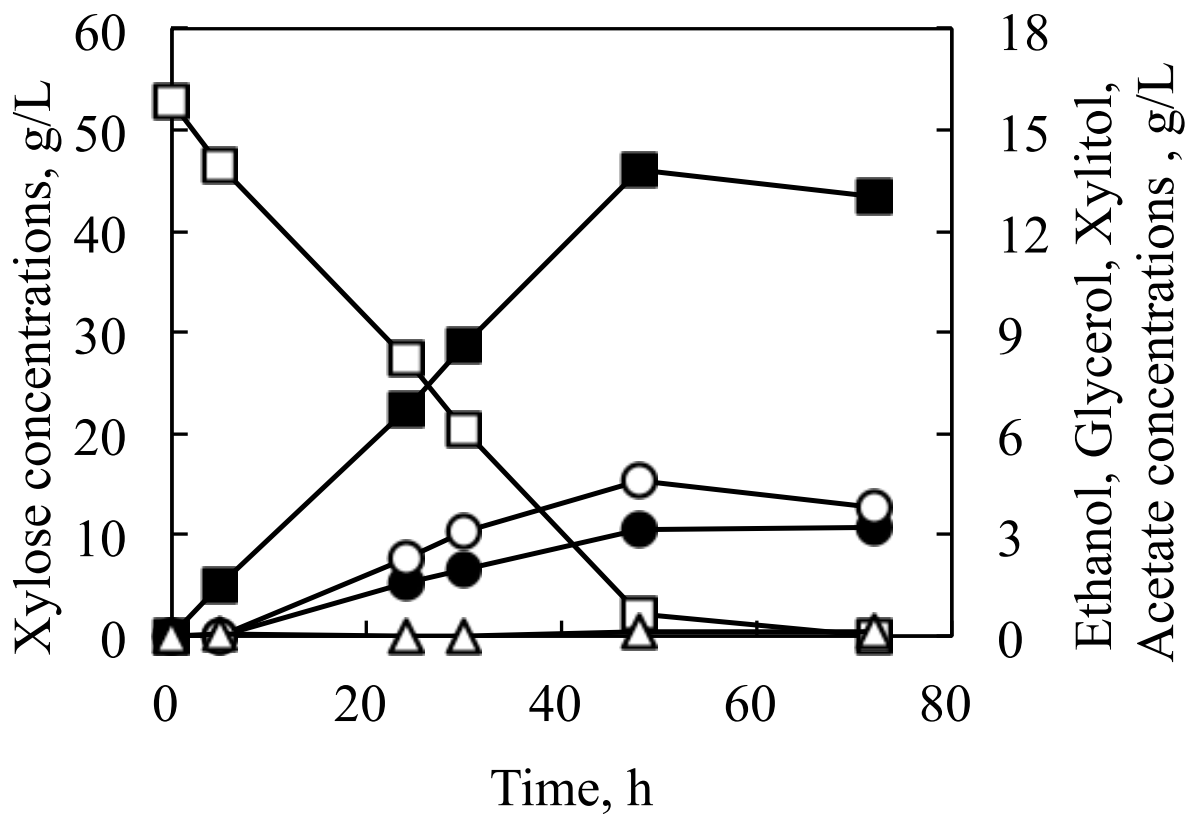
Fig. 4-2 Fermentation profiles of flask cultures of strains K7-XYL-ADH1 in YP medium

containing 50 g/L xylose as the carbon sources.

Results were based on two replications. Data points represent the average of two experiments

and error bars indicate standard deviation.

Xylose, open squares; Ethanol, closed squares; Xylitol, open circles; Glycerol, closed circles;

Acetate, open triangles.

Fig. 4-3 Fermentation profiles of flask cultures of strains K7-XYL in YP medium containing 80 g/L glucose plus 50 g/L xylose as the carbon sources.

Results were based on two replications. Data points represent the average of two experiments and error bars indicate standard deviation.

Glucose, closed triangles; Xylose, open squares; Ethanol, closed squares; Xylitol, open circles; Glycerol, closed circles; Acetate, open triangles.

Fig. 4-4 Fermentation profiles of flask cultures of strains K7-XYL-ADH1 in YP medium containing 80 g/L glucose plus 50 g/L xylose as the carbon sources.

Results were based on two replications. Data points represent the average of two experiments and error bars indicate standard deviation.

Glucose, closed triangles; Xylose, open squares; Ethanol, closed squares; Xylitol, open circles; Glycerol, closed circles; Acetate, open triangles.

4.3.2 Effect of *ADH1* overexpression in 5-L jar culture

In flasks, although an effect of *ADH1* overexpression was observed when xylose was the sole carbon source, the effect was not confirmed in mixed glucose/xylose mix medium. It was presumed that the internal redox balance of the cells changed due to the presence of the glucose and this led to there being no effect of *ADH1* overexpression. To modify the internal redox balances, 5-L jar fermenter cultures of K7-XYL and K7-XYL-ADH1 were grown with dissolved oxygen concentration 0.2 ppm. Fig. 4-5 and Fig. 4-6 showed the culture parameters. Both strains converted 80 g/L glucose and 50 g/L xylose within 48 h. Although the initial cell concentration in the 5-L jar fermenter culture was 20-times lower than that in flask-scale cultures, xylose consumption in the 5-L jar fermenter was faster than that in flask-scale culture. The ethanol productivity of strain K7-XYL-ADH1 was higher than that of K7-XYL (K7-XYL 44.9 g/L, K7-XYL-ADH1 49.2 g/L). The ethanol yield from the initial sugars was 66.9% for K7-XYL, and 73.3% for K7-XYL-ADH1.
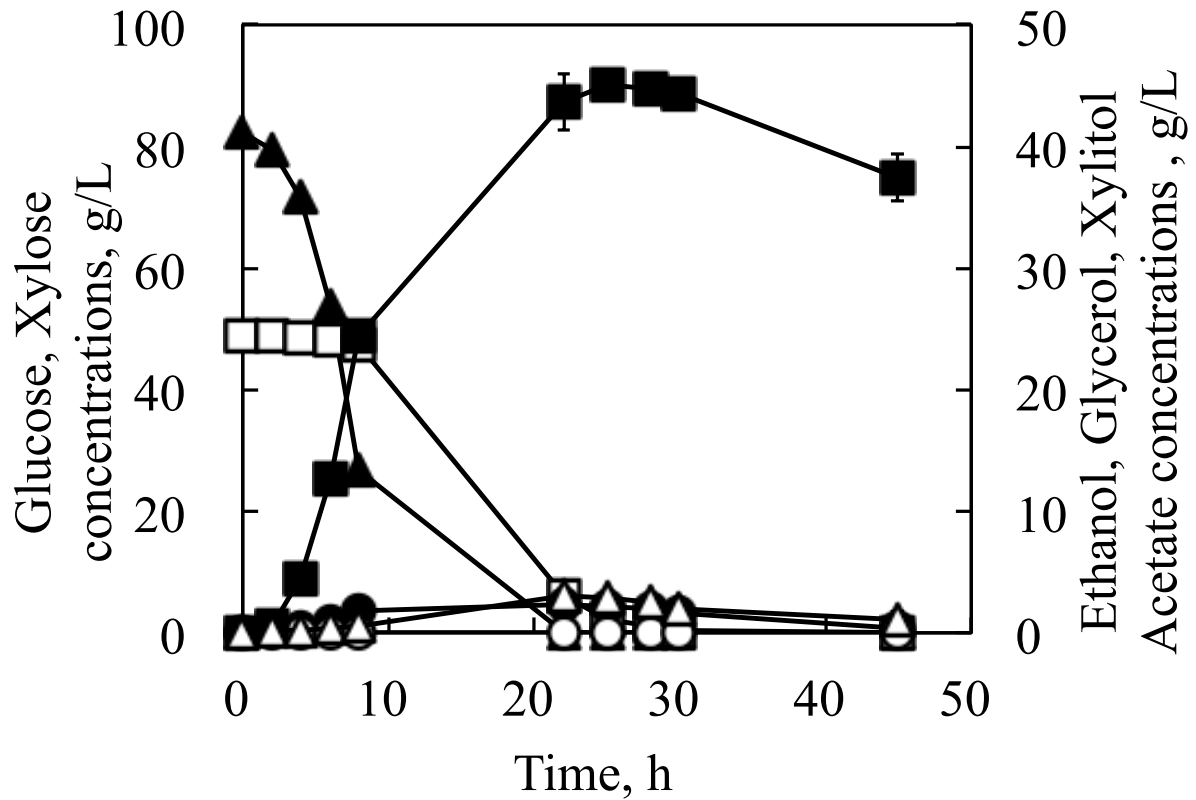
Fig. 4-5 Fermentation profiles of 5-L jar fermenter cultures of strains K7-XYL in YP medium

containing 80 g/L glucose plus 50 g/L xylose as carbon sources.

Results were based on two replications. Data points represent the average of two experiments

and error bars indicate standard deviation.

Glucose, closed triangles; Xylose, open squares; Ethanol, closed squares; Xylitol, open

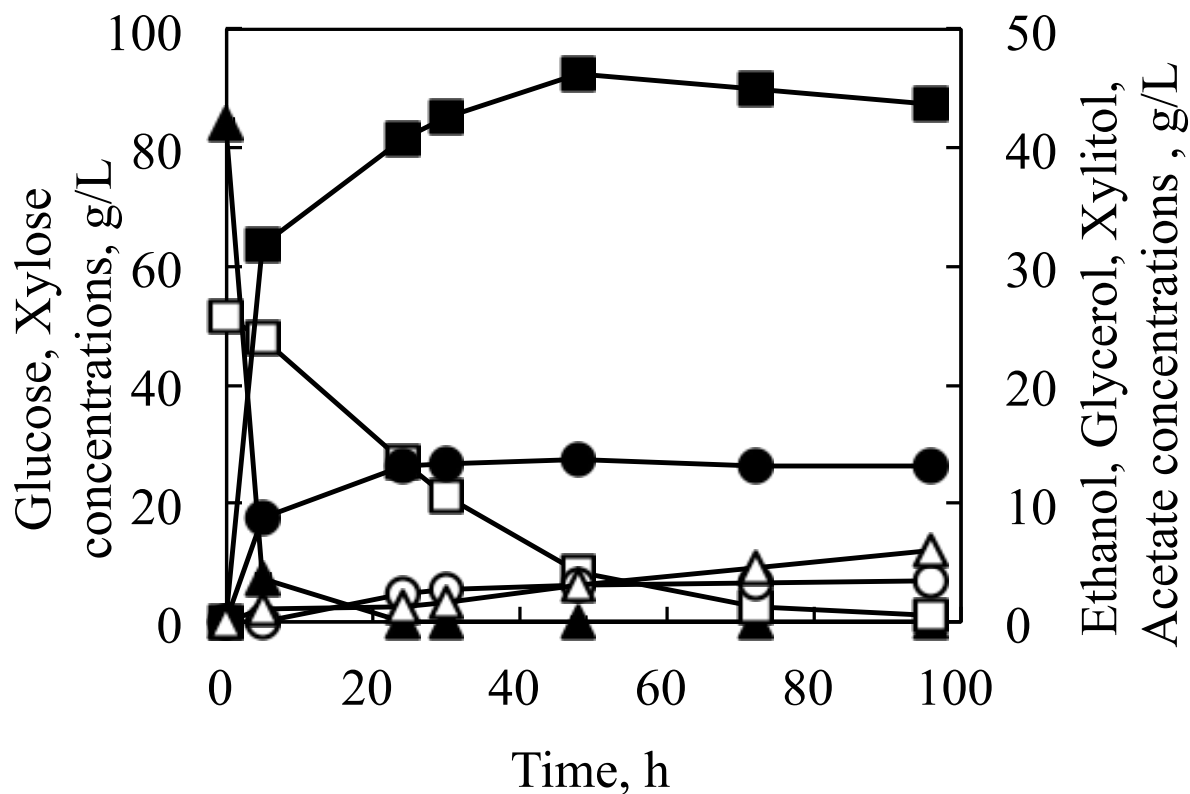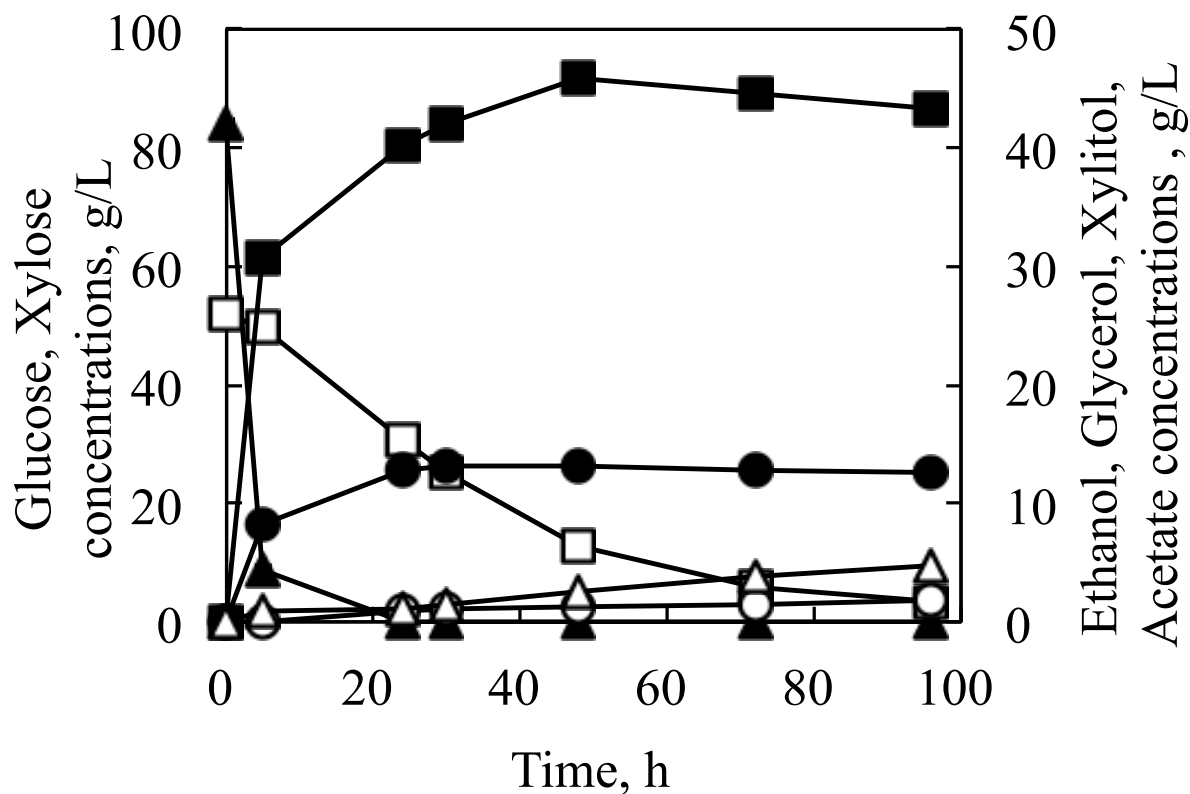circles; Glycerol, closed circles; Acetate, open triangles.

Fig. 4-6 Fermentation profiles of 5-L jar fermenter cultures of strains K7-XYL-ADH1 in YP

medium containing 80 g/L glucose plus 50 g/L xylose as carbon sources.

Results were based on two replications. Data points represent the average of two experiments

and error bars indicate standard deviation.

Glucose, closed triangles; Xylose, open squares; Ethanol, closed squares; Xylitol, open

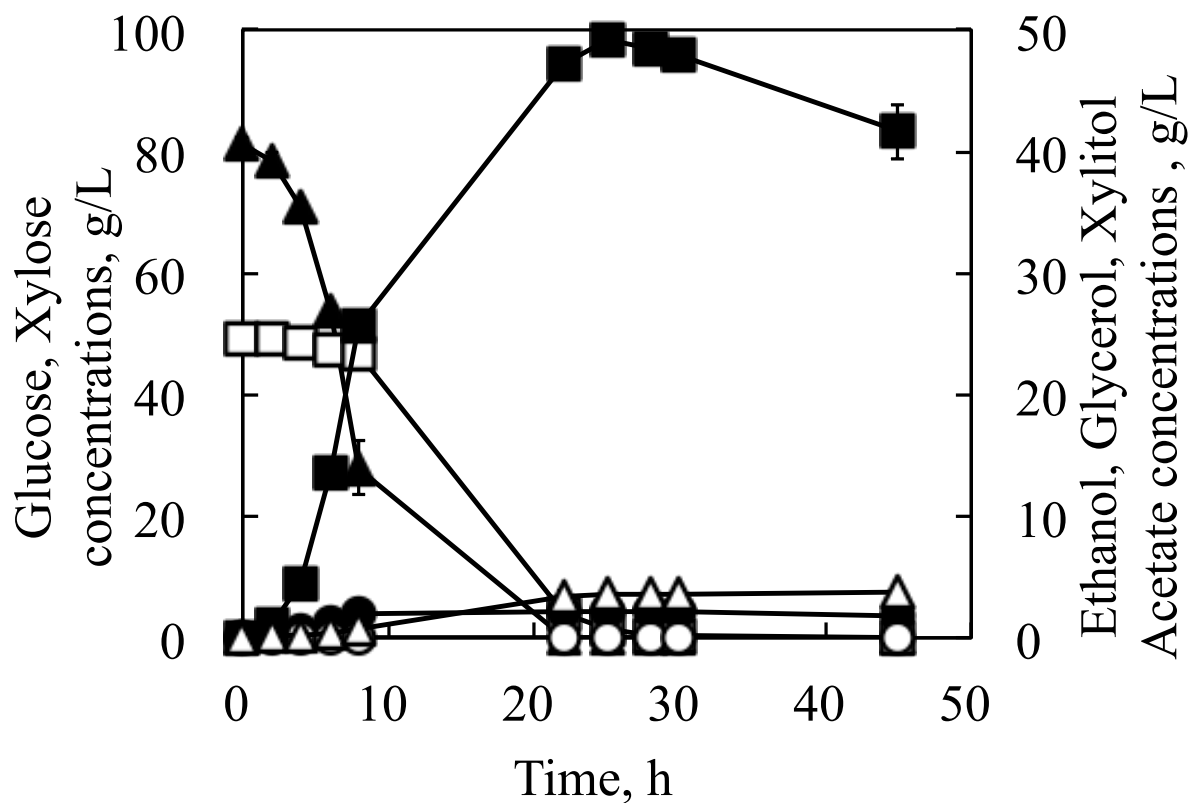circles; Glycerol, closed circles; Acetate, open triangles.

4.4 Discussion

In chapter 3, a kinetic simulation model of the ethanol producing pathway was constructed and sensitivity analysis was conducted in that model. Then, three metabolic bottlenecks were estimated in the pathway. Among them, upregulation of ADH (R26 in Fig. 3-1) was actually carried out, because this manipulation strategy was logically congruous. Simulation analysis revealed that the reaction catalyzed by ADH was a bottleneck, and that overexpression of *ADH1*, which encodes ADH, would enable the self-cloning xylose-using *S. cerevisiae* to increase the ethanol yield. This was verified in the presence of xylose in flask-scale cultures (K7-XYL 12.5 g/L, K7-XYL-ADH1 13.8 g/L), and in the presence of glucose and xylose in 5-L jar fermenter cultures (K7-XYL 44.9 g/L, K7-XYL-ADH1 49.2 g/L). Improvement in ethanol yield by 10% means that variable and fixed costs are reduced by 10%. That would have a dynamic impact on industry, especially in manufacture of a low-priced product such as ethanol. Naturally, lignocellulosic biomass contains both glucose and xylose. The ethanol yield (g ethanol/g sugars) from strain K7-XYL-ADH1 was 0.38 in the presence of glucose and xylose in 5-L jar fermenter culture. By comparison, the ethanol yield from genetically modified yeasts that possessed *Scheffersomyces stipitis* XR and XDH was 0.40 (Matsushika, A. and Sawayama, S., 2010; Casey, E. *et al.,* 2010).

Scheffersomyces stipitis XR can use both NADPH and NADH. However, GRE3 has strict NADPH specificity (Kuhn, A. *et al.,* 2010). *S. stipitis* XDH and SOR1 use only NAD^+ as a cofactor, but self-cloning xylose-using *S. cerevisiae* containing GRE3 cannot supply NAD^+ for the XDH reaction. That is, the metabolic pathways in the self-cloning xylose-using *S. cerevisiae* tend to cause a cofactor imbalance. Creating a self-cloning xylose-using *S. cerevisiae* is difficult (as mentioned above), but would be expected to contribute to the reduction of ethanol production costs. In oxygen-controlled fermentation conditions,

self-cloning xylose-using *S. cerevisiae* showed close to the same ethanol yield as the genetically modified yeast, suggesting that there is a possibility that self-cloning xylose-using *S. cerevisiae* can be used for industrial ethanol production. Strain K7-XYL-ADH1 showed higher ethanol yield than K7-XYL in the presence of glucose and xylose in 5-L jar fermenter culture but not in flask culture. It was guessed that this was because, in flask culture, the dissolved oxygen was low during the xylose consumption phase because most of it had been consumed during the glucose consumption phase, and, due to lack of respiration, NAD^+ regeneration did not occur. Therefore, the NAD^+ supply was not sufficient for the reaction of XDH. The increased oxygen supply in the aerated 5-L jar fermenter might make it possible to regenerate NAD^+ by respiration and thus accelerate the conversion of xylitol to xylulose by XDH, leading to an overall increase in ethanol production. Since only one oxygen concentration was tested in the experiment, ethanol productivity may increase further if the oxygen concentration is optimized.

A kinetic model of ethanol production from xylose was constructed and a sensitivity analysis was conducted to assess the validity of the model and clarify which pathway(s) have most impact on the ethanol productivity. This model identified a bottleneck in the ethanol production pathway. Since the experimental data were consistent with the prediction by simulation, the method was validated. To further improve ethanol productivity, it may be necessary to identify and overcome the new metabolic bottleneck by iteratively applying the same approach to strain K7-XYL-ADH1.

CHAPTER 5

Conclusion

The 21th Conference of the Parties to the United Nations Framework Convention on Climate Change (COP21) was held in December 2015, and the Paris Agreement was adopted with the goal of controlling the global average temperature rise. Furthermore, the Paris Agreement aims to dramatically reduce the emissions of greenhouse gases to the latter half of the 21st century. Even in the Sustainable Development Goals (SDGs) adopted by the United Nations General Assembly in September 2015, it is required to act on climate change. As mentioned above, the necessity of reducing greenhouse gas emissions has been increasing more and more in recent years.

According to the report of the Ministry of Land, Infrastructure and Transport, the transport sector accounts for 18 % of Japan's carbon dioxide emissions in 2016. Cellulosic bioethanol is an effective means to reduce carbon dioxide emissions from transportation fuels. In order to efficiently produce ethanol from cellulosic biomass, it is necessary to utilize xylose as well as glucose.

In this study, self-cloning, that is same meanings as non-genetically modified organism (GMO), *Saccharomyces cerevisiae*, which can utilize xylose as well, was created. On the other hand, it is common to introduce genes of *Scheffersomyces stipitis* to impart xylose utilization ability for long time and this is regarded as GMO, since it is said xylose-using genes of *S. stipitis* is superior to that of *S. cerevisiae* in cofactor specificity. However, unlike the case of producing expensive chemicals such as pharmaceuticals, it is difficult to use GMO when producing inexpensive fuels such as ethanol. This is because containment measures are required when GMO are used, and it leads to increase ethanol production costs. Thus, self-cloning xylose-using *S. cerevisiae* was developed with practical application of xylose-using yeast in this study. Originality of this study is that only genes of *S. cerevisiae* were used to impart xylose utilization capability, and a detailed kinetic model from

94

xylose to ethanol of the self-cloning xylose-using *S. cerevisiae* was constructed. All the

previously reported metabolic models were related to GMO which possesses genes of *S.

stipitis*. Also, the behavior of metabolites is assumed to be in steady state. This study is the

first metabolic model of self-cloning xylose-using *S. cerevisiae*. Furthermore, it was

measured that all the metabolites in the ethanol producing pathway from xylose with time

change, and the behavior of the metabolites in nonstaeady state were incorporated in the

model.

Self-cloning xylose-using *S. cerevisiae* was successfully created in this study. The

bottleneck reaction in the ethanol production pathway of the self-cloning xylose-using *S.

cerevisiae* was estimated by simulation, and further improvement of ethanol productivity was

attempted by eliminating the bottleneck reaction. The results were summarized below.

In chapter 2, xylose-using *S. cerevisiae* was constructed by two methods. One was

endogenous genes utilized *S. cerevisiae*, which possessed *GRE3* and *SOR1* genes from *S.

cerevisiae*. The other was engineered *S. cerevisiae* with *XYL1* and *XYL2* genes from

Scheffersomyces (Pichia) stipitis. The former self-cloning *S. cerevisiae* showed higher

ethanol productivity than the latter genetically modified *S. cerevisiae*. As far as I know, this is

the first result showing that ethanol can be produced successfully from xylose by using only

genes of *S. cerevisiae*.

In chapter 3, in order to further improve ethanol productivity from xylose of

self-cloning *S. cerevisiae*, a kinetic model of the ethanol production pathway from xylose was

constructed. Since the simulation results of the model coincident with the experimental

time-course data, metabolic bottleneck reaction and its solution were estimated by using this

kinetic model. The simulation proposed three solutions, upregulation of XDH (R5 in Fig. 3-1),

downregulation of xylose uptake (R1 in Fig. 3-1), and upregulation of ADH (R26 in Fig. 3-1).

Among the three proposals, upregulation of ADH was experimentally feasible even under the constraint of self-cloning and considered to be logically correct.

Based on the simulation results shown in chapter 3, the upregulation effect of ADH was examined in chapter 4. The effect of improving ethanol productivity was observed when only xylose was present by the upregulation of ADH but no improvement effect on ethanol productivity was observed when both glucose and xylose were present in flask culture. It was presumed that the internal redox balances of the cells changed due to the presence of the glucose. In order to change the internal redox balances, glucose and xylose mixed culturing using a 5-L jar fermenter was carried out with an air sparging at 0.016vvm, and it was confirmed that the ethanol productivity was improved by the upregulation of ADH in the presence of glucose and xylose. Furthermore, the ethanol yield of self-cloning *S. cerevisiae* calculated from the result of 5-L jar fermentation was almost equal to that of genetically modified *S. cerevisiae* with *XYL1* and *XYL2* genes from *S. stipitis*. That is, even self-cloning *S. cerevisiae* can increase ethanol productivity from xylose, and it is possible to produce ethanol from cellulosic biomass without using genetically modified *S. cerevisiae.*

We succeeded in producing self-cloning xylose-using *S. cerevisiae* and improving its ethanol productivity by analysis of intracellular and extracellular metabolites, prediction of bottleneck reaction by metabolic simulation, and elimination of bottleneck reaction by genetic manipulation. Based on this fact, a series of techniques for improving the ethanol productivity of the self-cloning *S. cerevisiae* could be established. In other words, it is thought that the ethanol productivity of the self-cloning *S. cerevisiae* can be further improved by repeating these analyses, predictions and genetic manipulations cycles several times.

Compared to ethanol productivity from glucose of self-cloning *S. cerevisiae*, that from xylose is still low, so it is desirable not to be satisfied with current ethanol productivity

of self-cloning *S. cerevisiae* and to further improve it. I have been focusing on self-cloning *S. cerevisiae* and analyzing it in this study, but I need to analyze genetically modified *S. cerevisiae* as well and to compare the results of both yeasts in the future. Since the coenzyme specificities of the enzymes that dehydrogenate xylitol to xylulose when two yeasts metabolize xylose are different, the redox states in the cells are expected to be different, even though the ethanol productivities of both yeasts are the same. It is generally said that XR of *S. stipitis* encoded by *XYL1,* is superior to XR of *S. cerevisiae* encoded by *GRE3*, in coenzyme utilization. As such difference is estimated, it is considered that grasping how each yeast metabolizes xylose is a useful knowledge to create yeast with better ethanol producing ability from xylose.

Finally, although ethanol production plants from cellulosic biomass are almost technically completed, there are many plants where operation is stopped or capacity utilization rate is low due to poor profitability. The use of self-cloning *S. cerevisiae* unnecessary for diffusion prevention measures can improve the profitability of lignocellulosic ethanol plant and wishes that the findings obtained in this study will help it.

ACKNOLEDGMENT

February 20th, 2019

REFERENCES

Akada, R.: Genetically modified industrial yeast ready for application, J. Biosci. Bioeng., 94, 536-544 (2002).

Akimoto, Y., Nagata, Y., Sakuma, J., Ono, I and Kobayashi, S.: Proposal and evaluation of Adaptive Real-Coded Crossover AREX, Trans. Jpn. Soc. Artif. Intell., **24**, 446-458 (2009).

Amore, R., Wilhelm, M. and Hollenberg, C. P.: The fermentation of xylose-an analysis of the expression of *Bacillus* and *Actinoplanes* xylose isomerase genes in yeast, Appl. Microbilo. Biotechnol., **30**, 351-357 (1989).

Antoniewicz, M. R.: Dynamic metabolic flux analysis – tools for probing transient states of metabolic netoworks, Curr. Opin. Biotechnol., **24**, 973-978 (2013).

Aritomo, K., Hirosawa, I., Hoshida, H., Shiigi, M., Nishizawa, Y., Kashiwagi, S., and Akada, R.: Self-cloning yeast strains containing novel FAS2 mutations produce a high amount of ethyl caproate in japanese sake, Biosci. Biotechnol. Biochem., **68**, 206-214 (2004).

Atkinson, B. and Mavituna, F.: Biochemical engingeering and biotechnology handbook, Stockton, New York, NY, USA (1991).

Almeida, J. R., Modig, T., Petersson, A., Hahn-Hägerdal, B., Lidén, G. and Gorwa-Grauslund, M. F.: Increased tolerance and conversion of inhibitors in lignocellulosic hydrolysates by *Saccharomyces cerevisiae*, J. Chem. Technol. Biotechnol., **82**, 340-349 (2007).

Badger, P. C.: Ethanol from cellulose: a general review, in Trends in New Crops and Nes Uses, J. Janick and A. Whipskey, Eds., 17-21, ASHS Press, Alexandria, Va, USA (2002).

Bailey, J. E.: Toward a science of metabolic engineering, Science, **252**, 1668-1675 (1991).

Bär, J., Naumann, M., Reuter, R. and Kopperschläger, G.: Improved purification of ribulose 5-phosphate 3-epimerase from *Saccharomyces cerevisiae* and characterization of the enzyme, Bioseparation, **6**, 233-41 (1996).

Bengtsson, O., Hahn-Hägerdal, B. and Gorwa-Grauslund, M. F.: Xylose reductase from *Pichia stipitis* with altered coenzyme preference improves ethanolic xylose fermentation by recombinant *Saccharomyces cerevisiae*, Biotechnol. Biofuels, **2**, 9- (2009).

Berdis, A.J., and Cook, P.F.: Overall kinetic mechanism of 6-phosphogluconate dehydrogenase from *Candida utilis*, Biochemistry, **32**, 2036-2040 (1993).

Bertilsson, M., Andersson, J. and Lidén, G.: Modeling simultaneous glucose and xylose uptake in *Saccharomyces cerevisiae* from kinetics and gene expression of sugar transporters, Bioprocess Biosyst. Eng., **31**, 369-377 (2008).

Bothast, R. J., Nichols, N. N. and Dien B. S.: Fermentations with new recombinant organisms, Biotechnol. Prog., **15**, 867-875 (1999).

Boxma, B., Voncken, F., Jannink, S, van Alken, T., Akhmanova, A., van Weelden, S. W., van Hellemond, J. J., Richard, G., Huynen, M., Tielens, A. G., andHackstein, J. H.: The anaerobic chytridiomycete fungus *Piromyces* sp. E2 produce ethanol via pyruvate: formate lyase and an alchol dehydrogenase, E. Mol. Microbiol, **51**, 1389-1399 (2004).

Branson, J.P., Nezic, M., Wallace, J.C. and Attwood, P.V.: Kinetic characterization of yeast pyruvate carboxylase isozyme pyc1, Biochemistry, **41**, 4459-4466 (2002).

Byers, L.D.: Glycerlaldehyde-3-phosphate dehydrogenase from yeast, Methods Enzymol., **89**, 326-335 (1982).

Casey, E., Sedlak, M., Ho, N. W. Y. and Mosier, N. S.: Effect of acetic acid and pH on the cofermentation of glucose and xylose to ethanol by a genetically engineered strain of *Saccharomyces cerevisiae*, FEMS Yeast Res., **10**, 385-393 (2010).

Carroll, A. and Somerville, C.: Cellulosic biofuels, Annu. Rev. Plant Biol., **60**, 165-182 (2009).

Chartchalerm, I. N. A., Tanawut, T., Hikamporn, K., Ponpitak, P. and Virapong, P.: Appropriate technology for the bioconversion of Water Hyacinth (*Eichhornia crassipes*) to liquid ethanol: future prospects for community strengthening and sustainable development, EXCLI J., **6**, 167-176 (2007).

Chassagnole, C., Noisommit-Rizzi, N., Schmid, J.W., Mauch, K. and Reuss, M.: Dynamic modeling of the central carbon metabolism of *Escherichia coli*, Biotechnol. Bioeng., **79**, 53-73 (2002).

Chen, X., Alonso, A. P., Allen, D. K., Reed, J. L. and Shachar-Hill, Y.: Synergy between (13)C-metabolic flus analysis and flux balance analysis for understanding metabolic adaptation to anaerobiosis in *E. coli*, Metab. Eng., **13**, 38-48 (2011).

Chiang, L. C., Gong, C. S., Chen, L. F. and Tsao, G. T.: D-Xylulose fermentation to ethanol by *Saccharomyces cerevisiae*, Appl. Environment. Microbiol., **139**, 152-160 (1981).

Cleland, W. W.: The kinetics of enzyme-catalyzed reactions with two or more substrates or products: I. Nomenclature and rate equations, Biochim. Biophys. Acta, **67**, 104-137 (1963).

Coughlan, M.: The properties of fungal and bacterial cellulases with comment of their production and application, Biotechnol. Genet. Eng. Rev., **3**, 39-110 (1985).

Cristina Ravanal, M., Flores, M., Perez, E., Aroca, F. and Cardemil, E.: *Saccharomyces cerevisiae* phosphoenolpyruvate carboxykinase: relevance of arginine 70 for catalysis, Biochimie, **86**, 357-362 (2004).

Dahabieh, M. S., Husnik, J. I. and van Vuuren, H. J. J.: Functional enhancement of sake yeast strains to minimize the production of ethyl carbamate in sake wine, J. Appl. Microbiol, **109**, 963-973 (2010).

Deanda, K., Zhang, M., Eddy C. and Picataggio, S.: Development of an arabinose-fermenting *Zymomonas mobilis* strain bay metabolic pathway engineering, Appl. Environ. Microbiol., **62**, 4465-4470 (1996).

Dien, B. S., Cotta, M. A. and Jefferies, T. W.: Bacteria engineered for fuel ethanol production: current status, Appl. Microbiol. Biotechnol., **57-58**, 258-266 (2003).

Eriksson, K. E., Blanchette, R. A. and Ander, P.: Microbial and Enzymatic degradation of wood and wood components, Springer-Verlag, Verlin (1990).

Ebringerova, A., Hromadkova, Z. and Heinze, T.: Hemicellulose, Adv. in Poly. Sci., **186**, 1-67 (2005).

Ebringerova, A.: Structural diversity and application potential of hemicelluloses, Macromol. Symp., **232**, 1-12 (2006).

Eliasson, A., Hofmeyr, J.-H.S., Pedler, S. and Hahn-Hägerdal, B.: The xylose reductase/xylitol dehydrogenase/xylulokinase ratio affects product formation in recombinant xylose-utilizing *Saccharomyces cerevisiae*, Enzyme Microb. Technol., **29**, 288-297 (2001).

Falk, M. C., Chassy, B. M., Harlande, S. K., Hoban, IV, T. J., McGloughlin, M. N. and Akhlaghi, A. R.: Food biotechnology: benefits and concerns, J. Nutr., **132**, 1384-1390 (2002).

Fischer, S., Procopio, S. and Becker, T.: Self-cloning brewing yeast: a new dimension in beverage production, Eur. Food Res. Technol., **237**, 851-863 (2013).

Frenkel, E.P. and Kitchens, R.L.: Acetyl-CoA synthetase from baker's yeast (*Saccharomyces cerevisiae*), Methods Enzymol., **71**, 317-324 (1981).

Galbe, M. and Zacchi, G.: A review of the production of ethanol from sohttwood, Appl. Microbiol. Biotechnol., **59**, 618-628 (2002).

Gárdnyi, M. and Hahn-Hägerdal, B.: The *Streptomyces rubiginosus* xylose isomerase is

misfolded when expressed in *Saccharomyces cerevisiae*, Enzyme Microb. Technol., **32**, 252-259 (2003).

Gear, C. W.: Numerical Initial Value Problem in ordinary Differential Equations, Prentice-Hall, Upper Saddle River (1971).

Giets, D., St Jean, A., Woods, R. A. and Schiestl, S. H.: Improved method for high efficiency transformation of intact yeast cells, Nucleic Acids Res., **20**, 1425 (1992).

Grotkjaer, T., Christakopoulos, P., Nielsen, J. and Olsson L.: Comparative metabolic network analysis of two xylose fermenting recombinant *Saccharomyces cerevisiae* strains, Metab. Eng., **7** 437-444 (2005).

Guranowski, A., Gunther Sillero, M.A. and Sillero, A.: Adenosine 5'-tetraphosphate and adenosine 5'-pentaphosphate are synthesized by yeast acetyl coenzyme A synthetase, J. Bacteriol., **176**, 2986-2990 (1994).

Hahn-Hägerdal, B., Jeppsson, H., Olsson, L. and Mohagheghi, A.: An interlaboratory comparison of performance of ethanol-producing micro-organisms in a xylose-rich acid hydrolysate, Appl. Microbiol. Biotechnol., **42**, 62-71 (1994).

Hahn-Hägerdal, B., Karhumaa, K., Fonseca, C., Spencer-Martins, I. and Gorwa-Grauslund, M.: Towards industrial pentose-fermenting yeast strains, Appl. Microbiol. Biotechnol., **74**, 937-953 (2007).

Harhangi, H. R., Akhmanova, A. S., Emmens, R., van der Drift, C., Laat W. T. A. M., van Dijken, J. P., Jetten, M. S. M., Pronk, J. T. and Op den Camp, H. J. M.: Xylose metabolism in the anaerobic fungus *Piromyces* sp. strain E2 follows the bacterial pathway, Arch. Micobiol., **180**, 134-14- (2003).

Hespell, R. B., Wyckoff, H., Dien, B. S. and Bothast, R. J.: Stabilization of pet operon plasmids and ethanol production in *Escherichia coli* strains lacking lactate dehydrogenase

and pyruvate formate-lyase activities, Appl. Environ. Microbiol., **62**, 4594-4597 (1996).

Himmel, M. E., Ding, S. Y., Johnson, D. K., Adney, W. S., Nimlos, M. R., Brady, J. W. and Foust, T. D.: Biomass recalcitrance: engineering plants and enzymes for biofuels production, Science, **315**, 804-807 (2007).

Hino, A.: Safety assessment and public concerns for genetically modified food products; the Japanese experience, Toxicol. Pathol., **30**, 126-128 (2002).

Hirosawa, I., Aritomo, K., Hoshida, H., Kashiwagi, W., Nishizawa, Y. and Akada, R.: Construction of a self-cloning sake yeast that overexpresses alcohol acetyltransferase gene by a two-step gene replacement protocol, Appl. Microbiol. Biogechnol., **65**, 68-73 (2004).

Ho, N., Stevis, P., Rosenfeld S., Huang, J. and Tsao, G.: Expression of the *E. coli* isomerase gene by a yeast promoter, Biotechnol. Bioengi. Sympo., **13**, 245-250 (1983).

Ho, N. W., Chen, X. and Brainard, A. P.: Genetically engineered *Saccharomyces* yeast capable of effective cofermentation of glucose and xylose, Appl. Environ. Microbiol., **64**, 1852-1859 (1998).

Hofmann, E. and Kopperschlager, G.: Phosphofructokinase from yeast, Methods Enzymol., **90 (Pt E)**, 49-60 (1982).

Holme, I. B., Wendt, T. and Holm, P.B.: Intragenesis and cisgenesis as alternatives to transgenic crop development, Plant Biotechnol. J., **11**, 395-407 (2013).

Hsu, T. A., Ladisch, M. R. and Tsao, G. T.: Alcohol from cellulose, Chem. Technol., **10**, 315-319 (1980).

Hynne, F., Danø, S. and Sørensen, P. G.: Full-scale model of glycolysis in *Saccharomyces cerevisiae*, Biophysical Chemistry, **94**, 121-163 (2001).

Iijima, K., and Ogata, T.: Construction and evaluation of self-cloning bottom-fermenting yeast with high SSU1 expression, J. Appl. Microbiol., **109**, 1906-1913 (2010).

Ingram, L. O., Conway, T., Clark, D. P., Sewell, G. W. and Preston J. F.: Genetic engineering of ethanol production in *Escherichia coli*, Appl. Environ. Microbiol., **53**, 2420-2425 (1987).

Ishida-Fujii, K., Goto, S., Sugiyama, H., Takagi, Y., Saiki, T. and Takagi, M.: Breeding of flocculent industrial alcohol yeast strains by self-cloning of the flocculation gene FLO1 and repeated-batch fermentation by transformants, J. Gen. Appl. Microbiol., **44**, 347-353 (1998).

Jeffries, T. W.: Utilization of xylose by bacteria, yeasts, and fungi, Adv. Biochem. Eng. Biotechnol., **27**, 1-32 (1983).

Jeppsson, M., Bengtsson, O., Franke, K., Lee, H., Hahn-Hägerdal, B. and Gorwa-Grauslund, M. F.: The expression of a *Pichia stipitis* xylose reductase mutant with higher K (M) for NADPH increased ethanol production from xylose in recombinant *Saccharomyces cerevisiae*, Biotechnol. Bioeng., **93**, 665-673 (2006).

Jin, Y., Jones, S., Shi, N and Jeffries, T. W.: Molecular cloning of *XYL3* (D-Xylulokinase) from *Pichia stipitis* and characterization of its physiological function, Appl. Environment. Microbiol., **68**, 1232-1239 (2002).

Jo, J. H., Park, Y. C., Jin, Y. S. and Seo, J. H.: Construction of efficient xylose-fermenting *Saccharomyces cerevisiae* through a synthetic isozyme system of xylose reductase from *Scheffersomyces stipitis*, Bioresour. Technol., **241**, 88-94 (2017).

Jonas, D. A., Elmadfa, I., Engel, K. –H., Heller, K. J., Kozianowski, G., König, A., Müller, D., Narbonne, J. F., Wackernagel, W., and Kleiner, J.: Safety considerations of DNA in food, Ann. Nurt. Metab., **45**, 235-254 (2001).

Joseleau, J. P., Comatat, J. and Ruel, K.: Chemical structure of xylans and their interaction in the plant cell walls, Xylans and xylanases, 1-15, Elsevier, Amsterdam, (1992).

Karhumaa, K., Fromanger, R., Hahn-Hägerdal, B. and Gorwa-Grauslund, M. F.: High activity of xylose reductase and xylitol dehydrogenase improves xylose fermentation by recombinant *Saccharomyces cerevisiae*, Appl. Microbiol. Biotechnol., **73**, 1039-1046 (2007)

Karhumaa, K., Sanchez R. G., Hahn-Hägerdal, B. and Gorwa-Grauslund, M. F.: Comparison of the xylose reductase-xylitol dehydrogenase and xylose isomerase pathways for xylose fermentation by recombinant *Saccharomyces cerevisiae*, Microb. Cell Fact., **6**, 5- (2007).

Kasai, Y., Oshima, K., Ikeda, F., Abe, J., Yoshimitsu, Y. and Harayama.: Construction of as self-cloning system in the unicellular green alga *Pseudochoricystis ellipsoidea*, Biotechnol. Biofuels, **8**, 94-105 (2015).

Kauffman, J. K., Prakash, P. and Edwatds, J. S.: Advances in flux balance analysis, Curr. Opin. Biotechnol., **14**, 491-496 (2003).

Kim, S. R., Ha S. J., Kong, I. I. and Jin, Y. S.: High expression of XYL2 coding for xylitol dehydrogenase is necessary for efficient xylose fermentation by engineered *Saccharomyces cerevisiae*, Metab. Eng., **14**, 336-343 (2012).

Kiyonari, S., Iimori, M., Matsuoka, K., Watanabe, S., Morikawa-Ichinose, T., Miura, D., Niimi, S., Saeki, H., Tokunaga, E., Oki, E. and other 4 authors: The 1,2-diaminocyclohexane carrier ligand in oxaliplatin induces p53-dependent transcriptional repression of factors involved in thymidylate biosynthesis, Mol. Cancer Ther., **14**, 2332-2342 (2015).

Konishi, J., Fukuda, A., Mutaguchi, K. and Uemura, T.: Xylose fermentation by *Saccharomyces cerevisiae* using endogenous xylose-assimilating genes, Biotechnol. Lett., **37**, 1623-1630 (2015).

Kötter, P. and Ciriacy, M.: Xylose fermentation by *Saccharomyces cerevisiae*, Appl. Microbiol. Biotechnol., **38**, 776-783 (1993).

Krietsch, W.K.G.: Triosephosphate isomerase from yeast, Methods Enzymol., **41B**, 434-438 (1975).

Kuhn, A., van Zyl, C., van Tonder, A., and Prior, B. A.: Purification and partial characterization of an aldo-keto reductase from *Saccharomyces cerevisiae*, Appl. Environ. Microbiol., **61**, 1580-1585 (1995).

Kummar, P., Barrett, D. M., Delwiche, M. J. and Stroeve, P.: Methods for pretreatment of lignocellulosic biomass for efficient hydrolysis and biofuel production, Ind. Eng. Chem. Res., **48**, 3713-3729 (2009).

Kuriya, Y., Tanaka, S., Kobayashi, G., Hanai, T. and Okamoto, M.: Development of an analytical pipeline for optimizing substrate feeding and eliminating metabolic bottlenecks, Chem-Bio. Informatics J., **11**, 1-23 (2011).

Kuyper, M., Harhangi, H. R., Stave, A. K., Winkler, A. A., Jetten, M. S. M., de Laat, W. T. A. M., den Hidder, J. J. J., Op den Camp, H. J. M. van Dijken, J. P. and Pronk J. T.: High-level functional expression of a fungal xylose isomerase: the key to efficient ethanolic fermentation of xylose by *Saccharomyces cerevisiae*, FEMS Yeast Res., **4**, 69-78 (2003).

Kuyper, M., Winkler, A. A., van Dijken, J. P. and Pronk, J. T.: Minimal metabolic engineering of *Saccharomyces cerevisiae* for efficient anaerobic xylose fermentation: a proof of principle, FEMS Yeast Res., **4**, 655-664 (2004).

Kusunoki, K. and Ogata, T.: Construction of self-cloning bottom-fermenting yeast with low vicinal diketone production by the homo-ingegration of ILV5, Yeast, **29**, 435-442 (2012).

Larroy, C., Fernández, M. R., González, E., Parés, X. and Biosca, J. A.: Characterization of the *Saccharomyces cerevisiae* YMR318C (ADH6) gene product as a broad specificity NADPH-dependent alcohol dehydrogenase, Biochem. J., **361(Pt 1)**, 163-172 (2002).

Larsson-Raźnikiewicz, M. and Arvidsson, L.: Inhibition of phosphoglycerate kinase and product homologues, Eur. J. Biochem., **22**, 506-512 (1971).

Lau, M. W., Gunawan, C., Balan, V. and Dale, B. E.: Comparing the fermentation performance of *Escherichia coli* KO11, Saccharomyces cerevisiae 424A(LNH-ST) and *Zymomonas mobilis* AX101 for cellulosic ethanol production, Biotechnol. Biofuel, **3**, 11 (2010).

Lee, W. J., Kim, M. D., Ryu, Y. W., Bisson, L. F., and Seo, J. H.: Kinetic studies on glucose and xylose transport in *Saccharomyces cerevisiae*, Appl. Microbiol. Biotechnol., **60,** 186-191 (2002).

Leskovac, V., Trivić, S. and Peričin, D.: The three zinc-containing alcohol dehydrogenase from baker's yeast, *Saccharomyces cerevisiae*, FEMS Yeast Res., **2**, 481-494 (2002).

Limtong, S., Sumpradit, T., Kitpreechavanich, V., Tuntirungkij, M., Seki, T. and Yoshida, T.: Effect of acetic acid on growth and ethanol fermentation of xylose fermenting yeast and *Saccharomyces cerevisiae*, Kasetsart J., **34**, 64-73 (2000).

Lusser, M. and Davies, H. V.: Comparative Regulatory approaches for groups of new plant breeding techniques, N. Biotechnol., **30**, 437-46 (2013).

Lynd, L. R.: Overview and evaluation of fuel ethanol from cellulosic biomass: technology, economics, the environment and policy, Ann. Rev. Energy Environ., **21**, 403-465 (1996).

Mahadevan, R., Edwards, J. S. and Doyle, F. J.III: Dynamic flux balance analysis of diauxic growth in *Escherichia coli*, Biophys. J., **83**, 1331-1340 (2002).

Martin, H. G., Kumar V. S., Weaver, D., Ghosh, A., Chubukov V., Mukhopadhyay, A., Arkin, A. and Keasling, J. D.: A method to constrain genome-scale models with ^{13}C labeling data, PLos Comput. Biol., **11**, e1004363 (2015).

Matsushika, A., Watanabe, S., Kodaki, T., Makino, K., Inoue, H., Murakami, K., Takimura, O. and Sawayama, S.: Expression of protein engineered NADP$^+$-dependent xylitol dehydrogenase increases ethanol production from xylose in recombinant *Saccharomyces cerevisiae* Appl. Microbiol. Biotechnol., **81**, 243-255 (2008).

Matsushika, A. and Sawayama, S.: Effect of initial cell concentration on ethanol production by flocculent *Saccharomyces cerevisiae* with xylose-fermenting ability, Appl. Biochem. Biotechnol., **162**, 1952-1960 (2010).

Matsushika, A., Nagashima, A., Goshima, T. and Hoshino, T.: Fermentation of xylose causes inefficient metabolic state due to carabon/energy starvation and reduced glycolytic flux in recombinant industrial *Saccharomyces cerevisiae*, PloS ONE, **8**, e69005 (2013).

Moes, C. J., Pretorius, I. S. and van Zyl, W. H.: Cloning and expression of *Clostridium thermosulfurogenes* D-xylose isomerase gene (*xylA*) in *Saccharomyces cerevisiae*, Biotechnol. Lett., **18**, 269-274 (1996).

Mohagheghi A., Evans, K., Chou, Y. C. and Zhang, M.: Cofermentation of glucose, xylose, and arabinose by genomic DNA-integrated xylose/arabinose fermenting strain of *Zymomonas mobilis* AX101, Appl. Biochem. Biotechnol., **98-100**, 885-898 (2002).

Moysés, D. N., Reis, V.C., de Almeida, J. R., de Moraes, L. M. and Torres F. A.: Xylose fermentation by *Saccharomyces cerevisiae*: Challenges and Prospects, Int. J. Mol. Sci., **17**, 207-215 (2016).

Narendranath, N. V., Thomas, K. C. and Ingledew, W. M.: Effects of acetic acid and lactic acid on the growth of *Saccharomyces cerevisiae* in a minimal medium, J. Ind. Microbiol. Biotechnol., **26**, 171-177 (2001).

Nanchen, A., Fuhrer, T. and Sauer, U.: Determination of metabolic flux ratios from ^{13}C-experiments and gas chromatography-mass spectrometry data: protocol and principles, Methods Mol. Biol., **358**, 177-197 (2007).

Noltmann, E.A.: Aldose-ketose isomerases. The Enzymes, 3rd Ed. (Boyer, P. D. , ed.), Academic Press, New York. 6, 271-354 (1972).

Norbeck, J., Påhlman, A.K., Akhtar, N., Blomberg, A. and Adler, L.: Purification and characterization of two isoenzymes of DL-glycerol-3-phosphatase from *Saccharomyces cerevisiae*, J. Biol. Chem., **271**, 13875-13881 (1996).

Ogata, T., Kobayashi, M. and Bibson, B. R.: Pilot-scale brewing using self-cloning bottom-fermenting yeast with high SSU expression, J. Inst. Brew., **119**, 17-22 (2013).

Orth, J. D., Thiele, I. and Palsson, B. Ø.: What is flux balance analysis?, Nat. Biotechnol., **28**, 245-248 (2010).

Pahlman, I.L., Larsson, C., Averet, N., Bunoust, O., Boubekeur, S., Gustafsson, L. and Rigoulet, M.: Kinetic Regulation of the Mitochondrial Glycerol-3-phosphate Dehydrogenase by the External NADH Dehydrogenase in *Saccharomyces cerevisiae*, J. Biol. Chem., **277**, 27991-27995 (2002).

Palsson, B. Ø.: Systems Biology: Properties of Reconstructed Networks, Cambridge University Press (2006).

Panagiotou, G., Christakopoulos, P., Grotkajaer, T. and Olsson, L.: Engineering of the redox imbalance of *Fusarium oxysporum* enables anaerobic growth on xylose, Metab. Eng., **8**, 474-482 (2006).

Parachin, N. S., Bergdahl, B., van Niel, E. W. and Gorwa-Grauslund, M.F.: Kinetic modelling reveals current limitations in the production of ethanol from xylose by recombinant *Saccharomyces cerevisiae*, Metab. Eng., **13**, 508-517 (2011).

Partow, S., Siewers, V., Bjørn, S., Nielsen, J. and Maury, J.: Characterization of different promoters for designing a new expression vector in *Saccharomyces cerevisiae*, Yeast, **27**, 955-64 (2010).

Perez, E. and Cardemil, E.: *Saccharomyces cerevisiae* phosphoenolpyruvate carboxykinase: the relevance of Glu299 and Leu460 for nucleotide binding, Protein J., **29**, 299-305 (2010).

Petschacher, B. and Nidetzky, B.: Altering the coenzyme preference of xylose reductase to favor utilization of NADH enhances ethanol yield from xylose in a metabolically engineered strain of *Saccharomyces cerevisiae*, Microb. Cell Fact., **7**, 9- (2008).

Pitkansen J.P., Aristidou, A., Salusjarvi, L., Ruohonen, L. and Penttila, M.: Metabolic flux analysis of xylose metabolism in recombinant *Saccharomyces cerevisiae* using continuous culture, Metab. Eng., **5**, 16-31 (2003).

Racker, E.: Transketolase. The Enzymes 2nd Ed.(Boyer, P. D., Lardy, H. & Myrback, K., eds), Academic Press, New York. 5, 397-406 (1961).

Rendina, A.R., Hermes, J.D. and Cleland, W.W.: Use of multiple isotope effects to study the mechanism of 6-phosphogluconate dehydrogenase, Biochemistry, **23**, 6257-6262 (1984).

Richard, P., Toivari, M.H. and Penttila, M.: Evidence that the gene *YLR070c* of *Saccharomyces cerevisiae* encodes a xylitol dehydrogenase, FEBS Lett., **457**, 135-138 (1999).

Richard, P., Toivari, M.H. and Penttila, M.: The role of xylulokinase in *Saccharomyces cerevisiae* xylulose catabolism, FEMS Microbiol. Lett., **190**, 39-43 (2000).

Rizzi, M., Baltes, M., Theobald, U. and Reuss, M.: In vivo analysis of metabolic dynamics in *Saccharomyces cerevisiae*: II. Mathematical model, Biotechnol. Bioeng., **55**, 592-608 (1997).

Rodriguez-Pena, J. M., Cid, V. J., Arroyo, J. and Nombela, C.: The YGR194c (XKS1) gene encodes the xylulokinase from the budding yeast *Saccharomyces cerevisiae*, FEMS Microbiol. Lett., **162**, 155-160 (1998).

Runquist, D., Hahn-Hägerdal, B. and Bettiga, M.: Increased ethanol productivity in xylose-utilizing *Saccharomyces cerevisiae* via a randomly mutagenized xylose reductase, Appl. Environment. Microbiol., **76**, 7796-7802 (2010).

Saini, A., Aggarwal N. K., Sharma, A. and Yadav, A.: Prospects for irradiation in cellulosic ethanol production, Biotechnol. Res. Int., **2015**, Article ID 157139 13pages (2015).

Saloheimo, A., Rauta, J., Stasyk, O. V., Sibirny, A. A., Penttila, M. and Ruohonen, L.: Xylose transport studies with xylose-utilizing *Saccharomyces cerevisiae* strains expressing heterologous and homologous permeases, Appl. Microbiol. Biotechnol., **74**, 1041-1052 (2007).

Sarthy, A. V., McConaughy, B. I., Lobo, Z., Sundsttrom, J. A., Furlong, C. E. and Hall B. D.: Expression of the Escherichia coli xylose isomerase gene in Saccharomyces cerevisiae, Appl. Environ. Microbiol., **53**, 1996-2000 (1987).

Sarthy, A. V., Schopp, C. and Idler, K. B.: Cloning and sequence determination of the gene encoding sorbitol dehydorogenase from *Saccharomyces cerevisiae*, Gene, **140**, 121-126 (1994).

Sauer, U., Lasko, D. R., Fiaux, J., Hochuli, M., Glaser, R., Szyperski, T., Wuthrich, K. and Bailey, J. E.: Metabolic flux ratio analysis of genetic an environmental modulations of *Escherichia coli* central carbon metabolism, J. Bacteriol., **181**, 6679-6688 (1999).

Scheidel, A. and Sorman, A. H.: Energy transition and the global land rush: ultimate drivers and persistent consequences, Global Environ. Chang., **22**, 588-595 (2012).

Schenk, G., Duggleby, R.G. and Nixon, P.F.: Properties and functions of the thiamine diphosphate dependent enzyme transketolase, Int. J. Biochem. Cell Biol., **30**, 1297-1318 (1998).

Schilter, B. and Constable, A.: Regulatory control of genetically modified (GM) foods: likely developments, Toxicol. Lett., **127**, 341-349 (2002).

Schomburg, I., Chang, A., Placzek, S., Söhngen, C., Rother, M., Munaretto, C., Stelzer, M., Grote, A., Scheer, M. and Schomburg, D.: BRENDA in 2013: integrated reactions, kinetic data, enzyme function data, improved disease classification: new options and content in BRENDA, Nucleic Acid Res., **41**, D764-772 (2013).

Seegmiller, J.E.: Triphosphopyridine nucleotide-linked aldehyde dehydrogenase from yeast, J. Biol. Chem., **201**, 629-637 (1953).

Sepulveda, C., Poch, A., Espinoza, R. and Cardemil, E.: Electrostatic interactions play a significant role in the affinity of *Saccharomyces cerevisiae* phosphoenolpyruvate carboxykinase for Mn2+, Biochimie, **92**, 814-819 (2010).

Sergienko, E.A. and Jordan, F.: Catalytic acid-base groups in yeast pyruvate decarboxylase. 3. a steady-state kinetic model consistent with the behavior of both wild-type and variant enzymes at all relevant pH values, Biochemstry, **40**, 7382-7403 (2001).

Sevostyanova, I.A., Selivanov, V.A., Yurshev, V.A., Solovjeva, O.N., Zabrodskaya, S.V. and Kochetov, G.A.: Cooperative binding of substrates to transketolase from *Saccharomyces cerevisiae*, Biochemistry-Moscow, **74**, 789-792 (2009).

Skoog, K and Hahn-Hägerdal, B.: Xylose fermentation, Enzyme Microb. Technol., **10**, 66-80 (1988).

Skoog, K. and Hahn-Hägerdal, B.: Effect of oxygenation on xylose fermentation by Pichia Stipitis, Appl. Environ. Microbiol., **56**, 3389-3394 (1990).

Sprenger, G.A., Schorken, U., Sprenger, G. and Sahm, H.: Transketolase A of *Escherichia coli* K12. Purification and properties of the enzyme from recombinant strains, Eur. J. Biochem, **230**, 525-532 (1995).

Stephanopoulos, G. and Vallino, J. J.: Network rigidity and metabolic engineering in metabolite overproduction, Science, **252**, 1675-1681 (1991).

Stephanopoulos, G., Aristidou, A. A. and Nielsen, J.: Metabolic engineering: principles and methodologies, Academic Press (1998).

Stephanopoulos, G.: Challenges in engineering microbes for biofuels production, Science, **315**, 801-804 (2007).

Sonderegger, M. Jeppsson, M. Hahn-Hägerdal, B. and Sauer, U.: Molecular basis for anaerobic growth of *Saccharomyces cerevisiae* on xylose, investigated by global gene expression and metabolic flux analysis, Appl. Environment. Microbiol., **70**, 2307-2317 (2004).

Swings, J. and DeLey, J.: The biology of Zymomonas mobilis, Bacteriol. Rev., **41,** 1-46 (1977).

Takagi, H., Matsui, F., Kawaguchi, A., Wu, H., Shimoi, H. and Kubo, Y.: Construction and analysis of self-cloning sake yeasts that accumulate proline, J. Biosci. Bioeng., **103**, 377-380 (2007).

Teusink, B., Diderich, J. A., Westerhoff, H. V., van Dam, K. and Walsh, M. C.: Intracellular glucose concentration in derepressed yeast cells consuming glucose is high enough to reduce the glucose transport rate by 50%, J. Bacteriol., **180**, 556-562 (1998).

Teusink, B., Passarge, J., Reijenga, C. A., Esgalhado, E., van der Weijden, C. C.,

Schepper, M., Walsh, M. C., Bakker, B. M., van Dam, K, Westerhoff, H. V. and Snoep, J. L.: Can yeast glycolysis be understood in terms of in vitro kinetics of the constituent enzymes? Testing biochemistry, Eur. J. Biochem., **267**, 5313-5329 (2000).

Toivari, M. H., Salusjärvi, L., Ruohonen, L. and Penttilä, M.: Endogenous xylose patyway in *Saccharomyces cerevisiae*, Appl. Environ. Microbiol., **70**, 3681-3686 (2004).

Toivola, A., Yarrow, D., van den Bosch, E., van Dijken, J. P. and Scheffers, W. A.: Alcoholic fermentation of d-xylose by yeasts, Appl. Environ. Microbiol., **47**, 1221-1223 (1984).

Träff, K. L., Jönsson, L. J. and Hahn-Hägerdal, B.: Putative xylose and arabinose reductases in *Saccharomyces cerevisiae*, Yeast, **19**, 1233-1241 (2002).

Tsolas, O. and Horecker, B.L.: Transaldolase. The Enzymes, 3rd Ed. (Boyer, P. D. , ed.), Academic Press, New York. 7, 259-280 (1972).

Ueng, P. P., Hunter, C. A., Gong, C. S. and Tsao, G. T.: D-Xylulose fermentation in yeasts, Biotechnol. Lett., **6**, 315-320 (1981).

Vallino, J. J. and Stephanopoulos, G.: Metabolic flux distributions in *Corynebacterium glutamicum* during growth and lysine overproduction, Biotechnol. Bioeng., **41**, 633-646 (1993).

van den Berg, M.A., de Jong-Gubbels, P., Kortland, C.J., van Dijken, J.P., Pronk, J.T. and Steensma, H.Y.: The two acetyl-coenzyme A synthetases of *Saccharomyces cerevisiae* differ with respect to kinetic properties and transcriptional regulation, J. Biol. Chem, **271**, 28953-28959 (1996).

van Urk, H., Mak, P. R., Scheffers, W. A. and van Dijken, J. P.: Metabolic responses of *Saccharomyces cerevisiae* CBS 8066 and Candida utilis CBS 621 upon transition from glucose limitation to glucose excess, Yeast, **4**, 283-291 (1988).

van Vleet, J.H. and Jeffries, T. W.: Yeast metabolic engineering for hemicellulosic ethanol production, Curr. Opin. Biotechnol., **20**, 300-306 (2009).

von Sivers, M. and Zacchi, G.: A techno-economical comparison of three processes for the production of ethanol from pine, Biores. Technol., **51**, 43-52 (1995).

von Sivers, M. and Zacchi, G.: Ethanol from lignocellulosics: a review of the economy, Biores. Technol., **56**, 131-140 (1996).

Wahlbom, C. F., Eliasson, A. and Hahn-Hägerdal, B.: Intracellular fluxes in a recombinant xylose-utilizing *Saccharomyces cerevisiae* cultivated anaerobically at different dilute rates and feed concentrations, Biotechnol. Bioeng., **72**, 289-296 (2001).

Walfridsson, M., Bao, X., Anderlund, M., Lilius G., Bulow, L. and Hahn-Hägerdal, B.: Ethanolic fermentation of xylose with *Saccharomyces cerevisiae* harboring the *Thermus thermophilus xylA* gene, which expresses an active xylose (glucose) isomerase, Appl. Environment. Mirobiol., **62**, 4648-4651 (1996).

Wang P. Y. and Schneider, H.: Growth of yeasts on D-xylulose, Can. J. Microbilo., **26**, 1165-1168 (1980).

Wang, X., Mann, C.J., Bai, Y., Ni, L. and Weiner, H.: Molecular cloning, characterization, and potential roles of cytosolic and mitochondrial aldehyde dehydrogenases in ethanol metabolism in *Saccharomyces cerevisiae*, J. Bacteriol., **180**, 822-830 (1998).

Wang, Z. Y., He, X. P. and Zhang, B. R.: Over-expression of GSH1 gene and disruption of PEP4 gene in self-cloning industrial brewer's yeast, Int. J. Food Microbiol, **119**, 192-199 (2007).

Wang, Z. Y., He, X. P., Liu, N. and Zhang, B. R.: Construction of self-cloning industrial brewing yeast with high-glutathione and low-diacetyl production, Int. J. Food Sci., **43**, 989-994 (2008).

Wang, Z. Y., Wang, J. J., Liu, X. F., He, X. P. and Zhang, B. R.: Recombinant industrial brewing yeast strains with ADH2 interruption using self-cloning GSH1+CUP1 cassette, FEMS Yeast Res., **9**, 574-581 (2009).

Wasylenko, T. M. and Stephanopoulos, G.: Metabolomic and ^{13}C-metabolic flux analysis of a xylose-consuming *Saccharomyces cerevisiae* strain expressing xylose isomerase, Biotechnol. Bioeng., **112**, 470-483 (2015).

Watanabe, S., Abu Saleh, A., Pack, S. P., Annaluru, N., Kodaki, T. and Makino, K: Ethanol production from xylose by recombinant *Saccharomyces cerevisiae* expressing protein-engineered NADH-preferring xylose reductase from *Pichia stipitis*, Microbiology, **153**, 3044-3054 (2007).

Wiechert, W.: ^{13}C metabolic flux analysis, Metab. Eng., **3**, 265-283 (2001).

Wiegel, J. and Ljungdahl, L. G.: The importance of thermophilic bacteria in biotechnology, Crit. Rev. Biotechnol., **3**, 39-108 (1986).

Wingren, A., Galbe, M. and Zacchi, G.: Techno-economic evaluation of producing ethanol from softwood: comparison of SSF and SHF and identification of bottlenecks, Biotechnol. Prog., **19**, 1109-1117 (2003).

Wu J. F. and Ljungdahl, L. G.: Ethanol production from sugars derived from plant biomass by a novel fungus, Nature, **321**, 887-888 (1986).

Yurshev, V.A., Sevostyanova, I.A., Solovjeva, O.N., Zabrodskaya, S.V. and Kochetov, G.A.: Nonequivalence of transketolase active centers with respect to acceptor substrate binding, Biochem. Biophys. Res. Commun., **361**, 1044-1047 (2007).

Zamboni, N., Fendt, S. M., Ruhl, M. and Sauer, U.: (^{13})C-based metabolic flux analysis, Nat. Protocols, **4**, 878-892 (2009).

Zeng, Q. K., Du, H. L., Wang, J. F., Wei, D. Q., Wang, X. N., Li, Y. X. and Lin, Y.: Reversal of coenzyme specificity and improvement of catalytic efficiency of Pichia stipitis xylose reductase by rational site-directed mutagenesis, Biotechnol. Lett., **31**, 1025-1029 (2009).

Zhang, M., Eddy, C., Deanda, K., Finkelstein, M. and Picataggio, S.: Metabolic engineering of a pentose metabolism pathway in ethanologenic *Zymomonas mobilis*, Science, **267**, 240-243 (1995).